UNIVERSITY OF CALIFORNIA
RIVERSIDE

Deciphering the Molecular Mechanism of Hyperglycemia-Mediated Tumorigenesis

A Dissertation submitted in partial satisfaction
of the requirements for the degree of

Doctor of Philosophy

in

Biochemistry and Molecular Biology

by

Qi Zhou

September 2023

Dissertation Committee:
Dr. Xuan Liu, Chairperson
Dr. Sihem Cheloufi
Dr. Declan McCole

The Dissertation of Qi Zhou is approved:

Committee Chairperson

University of California, Riverside

Acknowledgements

I am deeply grateful to all those who have supported and guided me throughout my PhD journey. Their steadfast encouragement and assistance have been instrumental in shaping my academic growth.

First and foremost, I express my heartfelt appreciation to my advisor, Dr. Xuan Liu. Her mentorship and support over the years have been invaluable. Her guidance in my research and provision of necessary resources have been crucial to the success of my work. Her inspiration has ignited me the passion to pursue science wholeheartedly.

I extend my sincere thanks to my dissertation committee members, Dr. Sihem Cheloufi and Dr. Declan McCole, for their unwavering help and insightful suggestions during our annual meeting. Their support motivated me to push the boundaries of my research and continually strive for excellence. I am equally grateful to my oral committee members, Dr. Meng Chen and Dr. David A Eastmond, for their valuable guidance and advice for my research.

My deepest gratitude goes out to the members of Dr. Xuan Liu's lab. To Dr. Dongmei Bai, I am indebted for her contribution of the RNA-Seq experiment, which laid the foundation for this project. To Dr. Jacob Schrier, thank you for your exceptional assistance in bioinformatic analysis and for being a constant source of innovative ideas and emotional support, especially during the challenging final stages of my PhD. To Dr. Carina Edmondson, your presence both in and out of the lab has been a constant source of comfort and encouragement. Your unwavering support has made this journey more manageable. To Dr. Thomas Benedict, thank you for your prompt help in fixing lab

equipment and for brightening my days with your humor. The camaraderie and technical support from all the members of Dr. Liu's lab have been an invaluable pillar of strength throughout my graduate life.

I would also like to extend my gratitude to my neighbors, Dr. Sihem Cheloufi and Dr. Jernej Murn labs, and all their past and current lab members. Their prompt and robust technical support for my research project has been invaluable.

Beyond the campus, I owe a debt of gratitude to those who have supported and loved me unconditionally. To my parents, Guoping Zhou and Ping Xu, your unwavering love and support have been my driving force to pursue a doctoral degree. To Mr. Ted Marwitz and Mrs. Liza Marwitz, thank you for embracing me as part of your family and providing me a home away from home. Your care and kindness have been a constant source of strength. To Dr. & Mr. Dong Wu and Mrs. Wu, your motivation and encouragement have been pivotal in propelling me to complete my PhD study. Dr. Dong Wu, your mentorship has redefined my perspective and instilled in me the courage to dream big and strive for greatness.

In closing, my heartfelt appreciation goes out to everyone who has played a role in my academic and personal development. Without your unwavering support, I could not have accomplished this milestone in my life.

ABSTRACT OF THE DISSERTATION

Deciphering the Molecular Mechanism of Hyperglycemia-Mediated Tumorigenesis

by

Qi Zhou

Doctor of Philosophy, Graduate Program in Biochemistry and Molecular Biology
University of California, Riverside, September 2023
Dr. Xuan Liu, Chairperson

Cancer is the second leading cause of global mortality. Accumulating evidence strongly suggests that aberrant alterations in signaling cascades can lead to uncontrolled cell growth, driving the progression of this disease. While the promotion of cancer cell growth by hyperglycemia has been extensively studied, the comprehensive mechanism underlying this relationship remains incompletely elucidated. In the current study, we present findings that high glucose levels (HG) indeed bolster DNA synthesis and cell cycle progression, fostering tumor cell growth, as revealed by genome-wide analyses. Moreover, our investigation identified E2F family as the central transcription factor responsible for the adaptive response induced by HG. The use of the pan-E2F inhibitor HLM006474 and shRNA-mediated E2F1 depletion, effectively counteracted HG-triggered DNA synthesis and cell growth. Furthermore, we establish that HG amplifies Rb1 phosphorylation, directly contributing to the activation of E2F1. Inhibition of Rb1 phosphorylation using the CDK2/4/6 inhibitor compound PF-3600 substantially mitigates the E2F1-mediated transcriptional activation of downstream DNA replication genes. Notably, among the E2F1 target genes induced by HG, RRM2 plays an essential role in

the nucleotide synthesis by generating essential dNTPs required for DNA replication. Our investigation reveals that HG promotes intracellular dNTP levels in an E2F1-RRM2-dependent manner, closely associated with increased DNA synthesis and subsequent cancer cell growth. The RNR inhibitor Triapine effectively impedes RRM2-mediated elevation of intracellular dATP and dGTP, and DNA synthesis. To gain more insights into the metabolic alterations occurring in HG-treated cancer cells, we carried out the untargeted metabolomic profiling. This analysis not only reaffirms the activation of glycolysis in HG-treated cells, as evidenced by the elevated levels of lactic acid, but also illustrates noteworthy enhancements in the levels of sucrose and fructose in the polyol pathway. These findings provide another facet of how cancer cells utilize excess glucose to fuel their proliferation. Collectively, our findings decipher the oncogenic signaling and metabolic connections between hyperglycemia and cancer cell proliferation, mediated through the Rb1/E2F and polyol pathways. This study provides a detailed molecular mechanism that sheds light on how hyperglycemia directs tumor cells to enhanced cell cycle progression and cell proliferation.

Table of Contents **Page**

List of Figures **Page**

List of Tables **Page**

Chapter 1

Introduction

1.1 Cancer Metabolism

In the past decade, there has been a notable emergence of metabolic reprogramming as a significant hallmark of cancer (Hanahan & Weinberg, 2011). Throughout the progression and development of cancer, transformed cells exhibit a flexible adaptation to specific metabolic alterations, thereby favoring tumor growth (Vander Heiden & DeBerardinis, 2017). These metabolic changes are comprised of intricate networks of metabolic pathways that can be categorized into three distinct fields: catabolism, anabolism and redox homeostasis (Hsieh et al., 2015). Catabolism involves a multitude of metabolic processes to break down macromolecules into small units, accompanied by the generation of ATP energy and reductive power, such as NADPH. Conversely, anabolism encompasses a set of metabolic pathways of rebuilding of small units into macromolecules, requiring energy for these reactions. The equilibrium between catabolism and anabolism is determined by nutrient availability and the cellular state. Unlike quiescent cells, cancer cells grow rapidly by intricately integrating these metabolic pathways, resulting in heightened energy demands to fuel proliferation. In particular, glucose and glutamine serve as the primary substrates taken up by tumor cells to meet their proliferation demands. The intermediates generated during the catabolism of glucose and glutamine can be employed for the biosynthesis of macromolecules. Furthermore, by ensuring adequate levels of NADH/$FADH_2$ within cells, cellular redox capacity is effectively controlled, thereby guaranteeing the ATP production in the mitochondria (Pavlova & Thompson, 2016).

1.1a Warburg Effect

In 1956, Otto Warburg and his research team disclosed a groundbreaking discovery in cancer cell metabolism, known as the "Warburg effect" (House et al., 1956; Warburg, 1956). In their study, they revealed that cancer cells exhibit a preference for cellular respiration through glycolysis, even under aerobic conditions, instead of the oxidative phosphorylation pathway (Alfarouk et al., 2014). This distinct metabolic characteristic arises from the compromised mitochondria respiration in cancer cells, leading to an increased reliance on the less efficient aerobic glycolysis (House et al., 1956; Warburg, 1956).

The Warburg effect also demonstrates that substantial amounts of lactic acid are generated in the final stage of glycolysis and can be extruded into extracellular space, resulting in a consistent acidification of the tumor microenvironment (TME). This acidosis within the TME yields various advantages for tumor cell aggressiveness and malignant progression. One advantageous outcome is the initiation of extracellular matrix (ECM) degradation, promoting tumor metastasis. Concurrently, this acidic milieu modulates both cell apoptosis and proliferation, fostering clonal evolution and selection by triggering gene mutations and chromosomal instability. Furthermore, the acidic environment interferes with the immune response, rendering cancer cells more resistant to chemotherapy and radiation (Böhme & Bosserhoff, 2016; Justus et al., 2013). In medical application, researchers and clinicians have harnessed the Warburg effect for a diagnostic technique called positron emission tomography (PET), utilizing the glucose analogue tracer ^{18}fluorodeoxyglucose (FdG). By mapping the course of glucose

metabolism, this approach enables non-invasive visualization of tumor grading, metastasis, and monitoring of tumor progression within living organisms (Gambhir, 2002; Hawkins & Phelps, 1988; Weber et al., 1999).

1.1b Glucose Metabolism

Glucose metabolic pathways encompass a series of carbohydrate-related processes. These encompass not only glycolysis, pentose phosphate pathway and gluconeogenesis, but also contain the processes of glycogenolysis and glycogenesis, alongside fructose and galactose metabolism (Nakrani et al., 2021). Polysaccharides undergo digestion into monosaccharides by enzymes in the gut, after which they are absorbed into the bloodstream and transported to various tissues (Sanders, 2016). Among the different monosaccharides, glucose stands out due to its significantly larger presence in the diet compared to fructose and galactose (Sanders, 2016). It enters the cytoplasm via membranous glucose transporters (GLUTs) and is subsequently phosphorylated by hexokinase (HK) into glucose-6-phosphate (G6P), which serves as a metabolic hub for the interconversion of all the previously mentioned glucose-associated metabolic pathways. This underscores the vital role blood glucose levels play in the regulation of glucose metabolism in human body.

The regulation of glucose homeostasis is primarily governed by two well-defined hormones: insulin and glucagon (Kitabchi, 1975; Röder et al., 2016). However, recent advances have brought forth other non-hormonal regulators and mechanisms that also participate in controlling glucose metabolism. Simultaneously, glucose metabolism

engages in a dynamic interaction with these regulators, influencing cell proliferation- a topic further explored in the subsequent discussion.

1.2 Cell Signaling Regulation of Glucose Metabolism

1.2a PI3K/Akt Signaling

In addition to serving as a source of energy for ATP generation, glucose plays a pivotal role as a carbon source for biomass synthesis, which involves lipid, nucleotides, and non-essential amino acids (NEAA) (Zhu & Thompson, 2019). In the context of cancer cells, an escalated flux of glucose is often observed, meeting the demands of cellular growth and proliferation through the upregulation of signaling pathways associated with biomass synthesis. The phosphoinositide 3-kinase (PI3K) signaling pathway serves as a master controller, linking glucose metabolism with growth regulation (DeBerardinis et al., 2008; Vander Heiden et al., 2009). Activation of the PI3K/Akt pathway brings about downstream metabolic consequences, including anaerobic glycolysis (Franke et al., 2003).

Cancer cells express high levels of GLUT1 to facilitate the glucose intake at the cell membrane. Akt phosphorylation prompts glucose uptake by either inducing the transcriptional activation of GLUT1 or maintaining its cell surface presence, contingent upon cell types and contexts (Barata et al., 2004; Hoxhaj & Manning, 2020; Wieman et al., 2007). Furthermore, phosphorylated Akt can regulate the gene expression and enzymatic activity of glycolytic rate-limiting enzymes, such as HK and phosphofructokinase-1 (PFK1), through both prolonged transcriptional effects and acute

post-translational modifications (DeBerardinis et al., 2008; Hoxhaj & Manning, 2020; Rathmell et al., 2003).

Tumor cells harboring somatic mutations in PI3K/Akt pathway often exhibit a gain of function or hyperactivity manner, resulting in a continuous glucose uptake to fulfill the increased demands of cellular metabolism (Keppler-Noreuil et al., 2016; Martini et al., 2014). A recent study introduced a novel insight into PI3K-mediated glycolytic regulation involving aldolase A in an Akt-independent manner through association with cytoskeletal dynamics (Hoxhaj & Manning, 2020; Hu et al., 2016). Upon stimulation by growth factors and insulin, aldolase A is released from filamentous actin, subsequently becoming more actively engaged in glycolysis.

1.2b mTOR Signaling

The mechanistic target of rapamycin (mTOR) is recognized as a central regulator of cell proliferation and metabolism. It couples growth factors and nutrients signals to biomass synthesis through the direct phosphorylation of downstream substrates, such as S6K (a target of mTOR Complex 1, mTORC1) and Akt (a target of mTOR Complex 2, mTORC2) (Mossmann et al., 2018). In general, mTOR engages in activating the glycolytic pathway by targeting GLUTs and glycolytic enzymes like HK2, PFK and enolase. Both GLUT1 and HK2 can be transcriptionally regulated by MYC and HIF1, which are downstream substrates of mTORC1 and mTORC2 (Mossmann et al., 2018). In its phosphorylated form, G6P, HK2 captures glucose in the cytoplasm, a pivotal step in the occurrence and interconnection of glucose metabolism. mTORC1/4EBP1 axis also

increases HK2 expression at the translational level in prostate cancer cells (L. Wang et al., 2014). In addition, the long noncoding RNA MALAT1 was found to be involved in mTORC1/4EBP1-mediated translational upregulation of the metabolic transcription factor TCF7L2 by interacting with its 5'-UTR. Consequently, TCF7L2 can activate the downstream gene expressions of glycolytic enzymes and inhibit the transcription of gluconeogenic enzymes (Malakar et al., 2019). mTORC2 enhances HK2 phosphorylation ability by facilitating more direct access to ATP produced from mitochondria in an Akt/mTORC2-dependent manner (Betz et al., 2013). Pyruvate kinase muscle isoform 2 (PKM2) is exclusively overexpressed in malignant tumor cells. It is also a target of both HIF1 and MYC proteins but modulated by distinct molecular mechanisms. HIF1 boosts the transcriptional level of PKM2 upon mTORC1 activation, whereas MYC maintains the distinct splicing isoform of PKM2 through targeting the splice factor (Sun et al., 2011). Conversely, PKM2 can also impact mTORC1 activity by phosphorylating its inhibitor AKT1S1 (He et al., 2016).

1.2c AMP-activated Protein Kinase (AMPK)

It is well recognized that AMPK serves as an energy sensor, becoming activated when intracellular energy and glucose levels decline (S.-C. Lin & Hardie, 2018). Functioning as a heterotrimeric protein complex, AMPK consists of one catalytic subunit (α) and two regulatory subunits (β & γ) (Carling, 2004). The activity of AMPK is tightly regulated by the phosphorylation of Thr172 located in the α catalytic subunit (Oakhill et al., 2011). The tumor suppressor LKB1 and the Ca^{2+}/calmodulin-dependent kinase

CaMKK2 are confirmed upstream activators of Thr172 (S.-C. Lin & Hardie, 2018). Under conditions where cells experience a higher AMP/ATP or ADP/ATP ratio, especially the former, Thr172 can be phosphorylated to initiate downstream pathways that sustain cellular energy demands. Traditionally, AMPK activation due to glucose depletion has been attributed to ATP/energy loss. However, Zhang et al. discovered an unexpected revelation: there is no change in the AMP/ATP and ADP/ATP ratios when AMPK is activated in response to glucose starvation (C.-S. Zhang et al., 2017). Indeed, this activation stems from reduced levels of fructose-1,6-bisphosphate (FBP) due to diminished glycolytic activity. The unoccupied aldolase enzyme, due to the absence of FBP, is more inclined to trigger the formation of the lysosomal complex, thus inducing AMPK activation (C.-S. Zhang et al., 2017). Cell-free reconstitution assays also confirmed that the addition of FBP disrupted the formation of lysosomal complex (C.-S. Zhang et al., 2017). This innovative discovery provides a new perspective on the AMP/ADP-independent mechanism of AMPK activation.

1.3 Regulation of Oncogenes and Tumor Suppressors in Glucose Metabolism

1.3a RAS Family

The RAS family comprises KRAS, NRAS and HRAS isoforms, and point mutations are prevalent across various cancer types, notably colorectal and non-small-cell lung cancers (Kerk et al., 2021; Mo et al., 2018). The oncogene KRAS has been established as a signature linked to enhanced aerobic glycolysis in multiple cell types (Kawada et al., 2017). In $KRAS^{G12D}$ -induced mouse models of pancreatic and colorectal

cancer, KRAS mutants bolster glucose uptake by elevating GLUT1 expression on the cell surface (Kawada et al., 2017; Ying et al., 2012). In addition, the expression levels of the rate-limiting enzymes like HK, PFK1 and lactate dehydrogenase (LDH) are upregulated in KRAS mutant cells. Also, lactate is rapidly exported from the cytoplasm through monocarboxylate transporters (MCTs) in a KRAS-dependent manner, maintaining intracellular redox balance (Kerk et al., 2021).

Numerous studies have showcased the effectiveness of the glycolysis inhibitor 3-bromopyruvate (3-BrPA) in halting tumor growth driven by KRAS mutant (Kawada et al., 2017; Patra et al., 2013; Ying et al., 2012; Yun et al., 2009). Beyond regulating glycolysis alone, the inducible KRAS-mutant pancreatic mouse model demonstrates the ability to metabolically rewire glycolysis towards the hexokinase biosynthesis pathway (HBP) for protein glycosylation and pentose phosphate pathway (PPP) to facilitate ribonucleotide synthesis (Kawada et al., 2017; Ying et al., 2012). In the non-small cell lung cancer (NSCLC) mouse model, homozygous $KRAS^{G12D/G12D}$ undergoes a glycolytic shift into the TCA cycle and augments glutathione biosynthesis, a critical intracellular antioxidant metabolite (Kerr & Martins, 2018). Collectively, the roles of KRAS signaling in glucose metabolism are geared towards promoting tumor cells' dependence on aerobic glycolysis to sustain their growth and viability.

1.3b MYC

The MYC proto-oncoproteins, including c-MYC, MYCN and MYCL, have been extensively investigated in cancer disease. Typically functioning as transcription factors,

they bind to approximately 10-15% of all promoter regions across the genome. Due to their influence on transcription and their ability to access a surplus of promoters, MYC dysregulation can aberrantly heighten the transcriptional levels of specific genes involved in glucose metabolism. This hypothesis has been tested and verified *in vivo* through ^{13}C-Glucose labeling in various cancer types (Le et al., 2012; Murphy et al., 2013; Yuneva et al., 2012).

In anerobic glycolysis, MYC is capable of transactivating glucose transporters and crucial glycolytic enzymes, including HK, PFK-muscle type and enolase (Dejure & Eilers, 2017; Wahlström & Arsenian Henriksson, 2015). It also enhances the levels of LDH and MCT1 to uphold intracellular NAD^+/NADH and lactate equilibrium (Dejure & Eilers, 2017). Apart from direct transcriptional activation, MYC can indirectly promote the expression of a distinct isoform of PKM2 through its regulatory control over hnRNP splicing factors (David et al., 2010). Moreover, MYC can indirectly inhibit the glycolysis-negative regulator, thioredoxin-interacting protein (TXNIP), by disrupting the transcriptional control of Mondo A in triple-negative breast cancer (Shen et al., 2015). Mondo A, a transcriptional factor, exerts its influence over glucose availability and utilization.

The hexosamine biosynthetic pathway (HBP) is highly activated in cancer, and O-GlcNAc transferase (OGT) plays a pivotal role in adding UDP-N-acetylglucosamine (UDP-Glc-NAc) to substrates' serine/threonine residues. HSP90, a transcriptional target of MYC, can stabilize OGT protein, which in turn stabilizes MYC protein by modifying on its Serine 58 residue, establishing a regulatory loop (Itkonen et al., 2013; Sodi et al.,

2015). This loop sustains the positive impact of MYC on the glucose uptake and aerobic activity in cancer cells.

Interestingly, glucose availability can influence MYC protein levels, with multiple studies indicating reductions during glucose depletion. Scientists found that limited glucose availability can lead to MYC protein degradation through proteasome degradation and calpain-mediated proteolysis, giving rise to a truncated by-product: cytosolic MYC-Nick (Dejure & Eilers, 2017). This truncated form lacks the functional domain required for nuclear translocation, leading to a transcriptionally independent function of α-tubulin acetylation. This, in turn, impacts cytoplasmic architecture and cell differentiation (Conacci-Sorrell et al., 2010). Strikingly, a particular study reported that glucose starvation could paradoxically elevate MYC protein levels in specific cancer cell types via the dephosphorylation of PI3K/Akt signaling pathway (S. Wu et al., 2015). In case of ER stress, such as that induced by glucose starvation, MYC protein can be translated via Internal Ribosome Entry Site (IRES) in multiple myeloma cells (Dejure & Eilers, 2017).

1.3c p53

p53, renowned as the guardian of the genome, has emerged as a critical regulator of cancer metabolism. Wild-type p53 is recognized for its ability to counteract the Warburg effect, thereby promoting oxidative phosphorylation (OXPHOS) (Gomes et al., 2018; Itahana & Itahana, 2018; Kung & Murphy, 2016). This regulation stems from both direct and indirect transcriptional repressions of GLUTs (Kawauchi et al., 2008;

Schwartzenberg-Bar-Yoseph et al., 2004). Additionally, the hotspot gain-of-function (GOF) p53 mutants, R175H and R273H, can facilitate the translocation of GLUT1 to the plasma membrane in a transcriptional-independent manner (C. Zhang et al., 2013). Furthermore, p53 influences several key negative regulators of glycolysis, including the regulation of TP-53 induced glycolysis and apoptosis regulator (TIGAR). Acting as a direct transcriptional target of p53, TIGAR functions as a phosphatase that, upon activation, dephosphorylates the allosteric regulator fructose-2,6-biphosphate (F-2,6-BP), consequently reducing PFK1 activity. This, in turn, leads to a decrease in the production of glycolytic intermediate fructose-1,6-bisphosphate (F-1,6-BP) (Berkers et al., 2013; Gomes et al., 2018a; Itahana & Itahana, 2018; Kung & Murphy, 2016).

In addition to its individual functions, p53 also engages in crosstalk with other signaling pathways, such as c-MYC, HIF1, LKB1/AMPK and PI3K/AKT (Gomes et al., 2018b). For instance, p53 can repress the expressions of IGFBP3 and PTEN3, which subsequently exert a negative regulatory influence on the activity of PI3K/AKT pathway (Y. Liang et al., 2013).

1.3d Hypoxia-inducible factor 1 (HIF1)

Hypoxia-inducible factors (HIFs) constitutes a cluster of transcription factors that emerge in response to oxygen depletion, encompassing three family members: HIF1, HIF2 and HIF3. HIF1, extensively studied, exhibits ubiquitous expression in cells (Dang et al., 2008). It comprises an alpha subunit encoded by HIF1A gene and a beta subunit encoded by the aryl hydrocarbon receptor nuclear translocator (ARNT), forming a

heterodimer. In normoxic conditions, HIF1 remains at minimal levels due to rapid von Hippel-Lindau protein-mediated ubiquitin-proteosome degradation (A. S. Lee, 2014). However, under hypoxic conditions, HIF1 activates glycolysis by increasing expression levels of nearly all related genes, such as GLUT1 and HK (Dang et al., 2008; Pezzuto & Carico, 2018). As a result, quantities of glycolytic intermediates, including the end-product pyruvate, increase. Pyruvate functions as a switch determining whether it continues into TCA cycle/oxidative phosphorylation in the presence of oxygen or undergoes fermentation into lactate without oxygen. Intriguingly, HIF1 can activate the transcription of pyruvate dehydrogenase kinase 1 (PDK1), which subsequently inactivates pyruvate dehydrogenase (PDH) though phosphorylation, hindering the progression of the TCA cycle. This mechanism enables cells to maintain ATP levels and counteract toxic ROS accumulation despite insufficient O_2 levels (Kim et al., 2006).

Furthermore, HIF1 serves a downstream target of mTORC1 and the tumor suppressor LKB1, a negative regulator of mTOR signaling (Shaw et al., 2004). Interestingly, LKB1 has been discovered to dedicate itself to HIF1-dependent metabolic reprogramming (Faubert et al., 2014; Shackelford et al., 2009). Precisely, the loss of LKB1 strengthens HIF1 protein levels through the commitment of mTORC1 and ROS. Nevertheless, it remains unclear whether mTORC1 and ROS function individually or in tandem (Faubert et al., 2014). Moreover, in pancreatic cancer, HIF1 protein stability has been shown to be enhanced through its physical interaction with MUC1, a type I transmembrane protein (Chaika et al., 2012; Shukla et al., 2017). This intermolecular communication empowers HIF1 to be more effectively recruited to the promoters of

glycolysis associated genes, thus activating transcription. This stabilization mechanism also sheds light on overcoming gemcitabine resistance in pancreatic cancer patients, as tumor cells adeptly adapt to the environment by securing their energy source for survival (Shukla et al., 2017).

1.4 Glucose Metabolism and Cell Cycle

Apart from their role in catalyzing glycolytic steps in anaerobic respiration, glycolytic enzymes also exert their nonmetabolic functions by regulating cell cycle progression. The control of cell cycle involves managing checkpoints and orchestrating the sequential activation of cyclin-dependent kinases (CDKs). Leveraging the intricate connection between glucose metabolism and cell cycle holds significant potential for the development of metabolism-associated therapeutic approaches for cancer treatment.

The enzyme PKM2 is widely recognized for its involvement in the Warburg effect. However, its glycolytic-independent kinase activity has recently come to light within cell nuclei. Cyclin D1, encoded by the gene CCND1, forms a critical partnership with CDK4, constituting a complex essential for the G1/S transition (Icard et al., 2019). Scientific research suggests that PKM2 can translocate into the cell nucleus to directly regulate CCND1 expression. This nuclear localization of PKM2 is facilitated by acetylation carried out by the acetyltransferase p300, targeting the K433 residue. This modification prevents its interaction with the allosteric activator FBP, leading to the accumulation of PKM2 in the nucleus (Lv et al., 2013). Inside the nuclei, PKM2 continues to function as a protein kinase, phosphorylating histone H3 at Thr33. This

phosphorylation event prompts the dissociation of histone deacetylase 3 (HDAC3) from the CCND1 promoter, consequently promoting the transcription of CCND1. These actions have been confirmed to be pivotal for cell cycle progression, cell proliferation, and tumor advancement *in vivo* (Yang et al., 2012). Additionally, the interaction between PKM2 and the phosphatase Cdc25A stabilizes PKM2's nuclear function. Cdc25A's dephosphorylation of PKM2 at Ser37 enhances PKM2-dependent transcriptional activity, encompassing glycolytic genes and Cdc25 itself (J. Liang et al., 2016).

Conversely, the cyclin-dependent kinase complex can influence PKM2's enzymatic activity, forging a connection between the cell cycle and metabolism. For instance, the cyclin D3/CDK6 protein complex phosphorylates PKM2 and PFK1, effectively inhibiting their functions. As a result, the glycolytic pathway is suppressed, compelling cells to divert towards the PPP to produce more antioxidant NADPH. This adaptation ensures cellular survival while averting apoptosis (H. Wang et al., 2017).

Aldolase, another enzyme, exhibits dual localization in both the cytoplasm and nucleus (Mamczur et al., 2010, 2013). Similarly, the nuclear localization of aldolase correlates with cell cycle progression and proliferation in lung cancer cells, as evidenced by increased expression of the proliferation marker Ki-67 (Mamczur et al., 2013). Triosephosphate isomerase (TPI), responsible for the interconverting dihydroxyacetone phosphate and glyceraldehyde 3-phosphate, undergoes CDK2-mediated phosphorylation upon etoposide treatment in Hela cells. This phosphorylation impairs TPI's catalytic function, compromising anaerobic glycolysis and rendering cells more susceptible to apoptosis (W.-H. Lee et al., 2010).

1.5 Diabetes and Cancer

Diabetes constitutes a cluster of metabolic disorders triggered by the dysregulation of glucose metabolism, resulting in elevated blood glucose levels or hyperglycemia. It has rapidly emerged as a prevalent ailment, transcending age, gender, and ethnicity worldwide. By 2045, the estimated number of cases is projected to surge to 693 million (Cho et al., 2018). Among the main diabetes types, namely type 1 (T1DM), type 2 (T2DM) and gestational diabetes, this discussion predominantly focuses on the first two (CDC, 2021b). T1DM, an autoimmune disease, entails a deficiency in insulin production and secretion within the pancreatic beta cells. This insufficiency in serum insulin precipitates a failure in maintaining the glucose homeostasis in body. Managing this condition necessitates a lifelong regimen of insulin injections and vigilant monitoring of blood sugar levels (CDC, 2021a). Primarily associated with children, teenagers, and young adults, T1DM is colloquially known as juvenile diabetes (CDC, 2021a). Despite its impact, it only accounts for 5-10% of all diabetes cases and is less prevalent than T2DM (Daneman, 2006). In contrast, T2DM, which constitutes approximately 90% of diabetes cases, manifests predominantly in adulthood. It is characterized by the occurrence of insulin resistance at early stage and compromised pancreatic beta cell function in the final stage. Consequently, cells fail to appropriately respond to insulin, leading to an inability to maintain glucose within the normal physiological range (Chatterjee et al., 2017). This condition's etiology is multifaceted, arising from both genetic anomalies and environmental factors such as obesity, unhealthy dietary habits, and a sedentary lifestyle (DeFronzo et al., 2015). To thwart the onset of microvascular

and macrovascular complications, individuals diagnosed with T2DM must diligently monitor their blood glucose levels (DeFronzo et al., 2015).

Both T1DM and T2DM have been associated with elevated risks of neoplasm occurrence and mortality. Numerous epidemiological studies have indicated that T1DM is linked to an increased risk of stomach, cervical and endometrial cancers (Szablewski, 2014). However, when combined with the results of multiple cohort studies, the findings have been mixed and inconsistent (Gordon-Dseagu et al., 2013). This discrepancy could arise from variations in study methodologies, diagnostic criteria for T1DM, and inconsistent parameters employed to assess outcomes (Gordon-Dseagu et al., 2013). In the case of T2DM, it exhibits a stronger correlation with cancer due to its shared common risk factors, including obesity, aging and smoking (Table 1) (Bjornsdottir et al., 2020; M. Wang et al., 2020). Liver, pancreatic and endometrial cancers exhibit a risk more than two-fold higher in the T2DM population, with diabetes being deemed an independent risk factor for these occurrences (Szablewski, 2014; M. Wang et al., 2020). The relative risk is slightly lower, around 1.2 to 1.5-fold, for colorectal, breast and bladder cancers (Szablewski, 2014). However, conflicting outcomes have been reported in bladder cancer studies (M. Wang et al., 2020). These inconsistent study results might stem from potential factors such as early detection bias and reverse causation.

1.5a Biological links between diabetes and cancers

Broadly, diabetes can impact tumorigenesis through three principle mechanisms: hyperinsulinemia, hyperglycemia, and chronic inflammation (Giovannucci et al., 2010).

Each of these factors possesses the potential to independently initiate and promote tumorigenesis, while also exhibiting the capacity for interaction.

The signaling of insulin and insulin-like growth factors (IGFs) has gained widespread recognition for its pivotal role in the mitogenesis and proliferation of cancer cells. Upon binding to their respective receptors, insulin/IGFs stimulate receptor phosphorylation and associated adaptor proteins, thereby initiating downstream effects through ongoing protein phosphorylation or recruitment/dissociation of related proteins (Gallagher & LeRoith, 2010). In addition, insulin-like growth factor-binding proteins (IGFBPs) interact with insulin/IGFs to curtail their bioactivities in cancer progression. Notably, certain IGFBPs can bind to IGF1, attenuating its function. Research also indicates that insulin can transcriptionally downregulate IGFBP1 levels in both *in vitro* and *in vivo* settings (Ooi et al., 1992; Powell et al., 1991). Moreover, IGFBP1 expression has been noted to rise in the serum of both type 1 and type 2 diabetic patients (Y.-W. Lin et al., 2021). Consequently, the suppressive influence of IGFBP1 on IGF1 protein function is negated, allowing for the activation of the IGF1 signaling pathway.

Hyperglycemia, a long-standing biological link between diabetes and cancers, stems from cancer cells' elevated reliance on glycolysis, known as the Warburg effect. Conceptually, hyperglycemia supplies cancer cells with an abundance of glucose, fueling proliferation through consistent ATP generation (Szablewski, 2014). Distinguishing the isolated effect of hyperglycemia from that of hyperinsulinemia *in vivo*, particularly among T2DM patients, remains challenging (Szablewski, 2014). Addressing this issue, researchers employed chemical compounds to disable insulin-producing pancreatic beta

cells and establish hyperglycemic animal models. Surprisingly, rats with type 1 diabetes induced by alloxan displayed tumor regression, suggesting a significant reliance of malignancy on insulin stimulation (Heuson & Legros, 1972). Similarly, another study recently revealed no substantial difference in tumor growth between xenograft mice with or without hyperglycemia, utilizing a model induced by a compound called STZ, which functions analogously to alloxan (D. Wu et al., 2018).

However, a high glucose microenvironment can attenuate cancer cells' sensitivity to chemotherapy (Gerards et al., 2017). This inhibitory effect is linked to the interference of apoptotic pathways, including PUMA and ceramide synthesis (Gerards et al., 2017). In cancer, dysregulated glucose metabolism accompanies an elevation in chronic inflammatory makers like IL-1β, IL-6 and TNF-α, which can trigger an unchecked proinflammatory response (S.-C. Chang & Yang, 2016). Consequently, the persistent state of inflammation can create a microenvironment conducive to tumor advancement and progression.

1.6 E2F Family Regulation Throughout Cell Cycle

The E2F family comprises eight distinct members, denoted as E2F1-8, with E2F3 giving rise to two distinct isoforms through alternative transcription starting sites (TSS) (Kent & Leone, 2019). These individual E2Fs exhibit unique expression patterns across the cell cycle. During the G1/S phase transition, E2F1, E2F2 and E2F3A experience peak expression levels, whereas E2F7 and E2F8 reach their peaks during the later S phase. E2F4, E2F5 and E2F6 maintain a constant expression throughout the cell cycle. In

general, E2F proteins can be classified into three types based on their transcriptional effects: activators (E2F1, E2F2, E2F3A & E2F3B), repressors (E2F4, E2F5 and E2F6), and atypical repressors (E2F7 and E2F8).

Throughout the cell cycle, individual E2F members collaborate in a coordinated manner. In quiescent and differentiated (G0) cells, repressors E2F4 and E2F5 form inhibitory protein complexes with pocket proteins (RB, p107 and p130). These complexes bind to the promoters of E2F targets, effectively suppressing transcriptional activities. Upon receiving mitogenic signals, pocket proteins become phosphorylated by associated CCN/CDKs. As a result, E2F4 and E2F5 dissociate from the promoters during the early G1 phase. As phosphorylation activity peaks in mid-to-late G1, activators E2F1, E2F2 and E2F3 take the place of E2F4 and E2F5, initiating the transcription of E2F targets. As cells progress to the S phase, atypical repressors, namely E2F7 or E2F8, position themselves on the promoters of E2F targets, particularly those of E2F1, E2F2 and E2F3, to quell their transcriptional activities. Upon reaching the G2 phase, the E2F4 protein relocates to the nucleus, reestablishing inhibitory protein complex with pocket proteins as previously described, thus suppressing the transcription of E2F targets. E2F4 maintains its presence on the promoters of E2F targets until cells are once again promoted by new mitogenic signals (Fig. 1) (Kent & Leone, 2019).

1.6a Regulation of E2F1 Expression and Activity

E2F1 has garnered extensive attention among all the members of E2F protein family. A prominent mechanism governing E2F1 activity is the CDK/Rb/E2F1 axis.

Pocket proteins, including Rb1, p107 and p130, form direct interactions with E2F1 on the promoters of the DNA segments, effectively curbing E2F1's capacity for transcriptional regulation. Upon receiving specific stimuli, CCN/CDK complexes phosphorylate Rb1, leading to its dissociation from E2F1 on the promoters. Freed from Rb's inhibitory effect, E2F1 partners with its counterpart protein DP, thereby instigating the transcriptional activation of genes pertinent to cell cycle progression (Henley & Dick, 2012; Kent & Leone, 2019).

Furthermore, E2F1 protein level are subject to tight control through a regulatory loop mediated by miRNA. In specific, p73, an E2F1 target, suppresses miR-205 expression, while miR-205 subsequently downregulates the translational level of E2F1 protein (Alla et al., 2012; Dar et al., 2011). E2F1 stability was previously found to be maintained by protein acetylation, involving acetylation by the p300/CBP-associated factor P/CAF and deacetylation by Rb1-associated deacetylase. The lysine residues involved in this process are conserved among E2F1-3 (Martínez-Balbás et al., 2000).

More recently, an array of post-translational modifications of E2F1, including phosphorylation, methylation, ubiquitination and ADP-ribosylation, have been unveiled and recognized to occur in a coordinated fashion. The kinase CDK8 can phosphorylate E2F1 at Ser375, impacting its downstream transactivation capacity. However, this phosphorylation does not affect E2F1's binding affinity on promoters or its dimerization ability with DP (J. Zhao et al., 2013). Our lab has also identified another kinase, TAF1, involved in the phosphorylation of Ser 375, and this has been verified both *in vitro* and *in vivo*. The F-box domain in Cyclin F (CCNF) can mediate E2F1 ubiquitination via its

interaction with the N-terminal cyclin binding motif of E2F1. This regulatory event occurs in late S and G2 phase, dampening the transcriptional expressions of E2F1 targets to prevent inappropriate DNA replication (Clijsters et al., 2019).

Poly (ADP-ribosyl)ation involves intracellular PARP1, which stabilizes E2F1 by reinforcing its interaction with BIN1, an Rb1-independent E2F1 repressor (Kumari et al., 2015). These post-translational modifications also exhibit interplay, regulating E2F1's function. Methylation of E2F1 at Lys185 can enhance the NEDDylation on the same residue, further promoting protein degradation while concurrently inhibiting acetylation and phosphorylation of residues at distant positions (Kontaki et al., 2010; Loftus et al., 2012).

1.6b E2F1 and Cancer

E2F1 primarily functions as a transcription factor that governs the G1/S transition in cells, a pivotal phase tightly linked to uncontrolled cell proliferation in tumors. Earlier evidence demonstrated that $E2F1^{-/-}$ mice experienced more keratinocytes death following UV radiation exposure, a phenomenon that could be reversed through E2F1 re-expression (Wikonkal et al., 2003). Clinical studies have similarly revealed that diminished E2F1 expression levels were associated with favorable prognosis among breast cancer patients (Vuaroqueaux et al., 2007). In estrogen-stimulated breast cancer, E2F1 expression levels are elevated in patient samples. Concurrently, its promoter displayed a higher association with H3R17me2, a modification necessary for the coactivator-associated arginine methyltransferase CARM1 (Frietze et al., 2008).

Furthermore, E2F1 protein exhibits a physical interaction with the coactivator ATCR at its N-terminal domain, an interaction that takes place simultaneously on the promoters of E2F1 target genes. As a result, ACTR facilitates E2F1 in transactivating downstream target genes to promote the G1/S transition (Louie et al., 2004). Notably, in prostate cancer, NUSAP1 is considered a pivotal prognostic marker and deeply involved in the invasion, migration and metastasis of tumor cells (Gordon et al., 2017). E2F1's role extends to direct binding on its two conserved CCAAT motifs, regulating transcriptional level (Gulzar et al., 2013).

Analyzing microarray data from patient samples diagnosed with bladder cancer revealed E2F1 as a master regulator in tumor progression and aggressiveness. In particular, downstream targets modulated by E2F1/EZH2 and E2F1/SUZ12 are closely associated with chemotherapy resistance and unfavorable cancer aggressiveness (S.-R. Lee et al., 2015). Moreover, the loss and inactivation of Rb1 tumor suppressor gives rise to distinct E2F1 cistrome patterns and binding specificities, providing insights into E2F1's diverse functions linking to various Rb1 statuses (McNair et al., 2018).

1.6c E2F1 and Cancer Metabolism

Metabolic reprogramming stands out as a significant hallmark in cancer disease, and E2F1, functioning as a transcription factor, wields influence over cancer metabolism by regulating the transcriptional activity of genes linked to metabolic pathways. An established metabolic signature observed in many cancer cells is the Warburg effect. E2F1 has been demonstrated to amplify glycolysis in the cytoplasm while suppressing

glucose oxidation in the mitochondrion. To bring about this metabolic shift, E2F1 fosters the expressions of 6-phosphofructo-2-kinase/fructose-2,6-bisphosphatase (PFKB) and pyruvate dehydrogenase kinase (PDK) (Fernández de Mattos et al., 2002; L.-Y. Wang et al., 2016). Among the PDK family members, both PDK1 and PDK3 emerge as direct transcriptional targets of E2F1. E2F1 collaborates with the histone lysine demethylase KDM4A on the promoters of these two genes to modulate their transcriptional activity (L.-Y. Wang et al., 2016).

In instances where E2F1 is acutely lost in Hela cells, mitochondrial topoisomerase I (TOP1MT) witnesses an increase, promoting mitochondrial biogenesis and increase of ATP levels (Goto et al., 2006). Conversely, perturbations in mitochondrial function can exert an impact on E2F1 activity. For instance, deficiency in the electron transport chain (ETC) deficiency and inhibition of ATP synthase significantly affect E2F1's transcriptional network, leading to a marked impediment in cell cycle progression (Gemin et al., 2005; Mori et al., 2016).

Studies have also indicated that E2F1's commitment in anabolic metabolism to fulfill the heightened demand for macromolecules required for proliferation. In nucleotide synthesis, E2F1 operates through the regulation of thymidine kinase (TK) and dihydrofolate reductase (DHFR) expressions (Y. Li et al., 1994; Slansky et al., 1993). In de novo lipid synthesis, researchers have revealed the key role of Sonic hedgehog/E2F1/fatty acid synthase (FAS) axis in medulloblastoma (Bhatia et al., 2011). Furthermore, E2F1, in conjugation with E2F2, functions to suppress the expression of the gene encoding carnitine palmitoytransferase 2 (CPT2), an enzyme essential for fatty acid

oxidation and closely associated with nonalcoholic fatty acid liver disease (NAFLD)-related hepatocellular carcinoma (González-Romero et al., 2021).

In prostate cancer, the Rb1 loss can engender an E2F1-dependent mode of metabolic reprogramming, particularly concerning redox metabolism. As a result, the augmented synthesis of anti-oxidant glutathione shields tumor cells from reactive oxygen species (ROS) during chemotherapy (Mandigo et al., 2021). Moreover, studies suggest that E2F1 potentially engages in crosstalk with other signaling pathways (PI3K/Akt, mTORC1 & HIF1) intricately involved in cancer metabolism.

1.7 Ribonucleotide Reductase (RNR)

Ribonucleotide reductase (RNR) assumes the role of reducing the 2' carbon of ribonucleoside diphosphate (NDP) to generate the corresponding deoxyribonucleoside diphosphate (dNDP), a rate-limiting step in the *de novo* pathway. Following this, dNDPs undergo phosphorylation by nucleoside diphosphate kinase (NDPK) to yield dNTPs (Kunz & Kohalmi, 1991). In mammals, RNR operates as a tetrameric holoenzyme composed of two α and two β subunits. The α subunit houses one catalytic site and two distinct allosteric sites. The β subunit harbors a di-nuclear iron center (Fe-O-Fe) and a protein tyrosyl radical (Y-O•) that is crucial for catalytic functionality. The RNA α subunit is encoded by RRM1 gene, while the β subunit is encoded by two distinct genes, RRM2 and p53R2. RRM2 remains consistently expressed in cells, whereas p53R2 is induced exclusively upon DNA damage (A. L. Chabes et al., 2003).

Several distinct mechanisms tightly control RNR activity to uphold intracellular dNTP levels. One such mechanism involves intrinsic allosteric modulation by ATP/dATP. The allosteric A site on the α subunit regulates enzyme activity by binding different levels of NTP/dNTP. A higher ratio of ATP/dATP leads to a more active form of RNR and vice versa (Fairman et al., 2011). Another major regulatory mechanism is through the cell cycle stage-specific control of RNR protein levels to maintain RNR activity during S phase (A. Chabes & Thelander, 2000; Engström et al., 1985; Eriksson et al., 1984). RRM1 reaches peak levels during S phase and remains steady throughout the cell cycle due to its extended half-life (Engström et al., 1985). On the other hand, RRM2 is abundant during S phase but undergoes degradation upon exit from S phase. In G2 phase, Cyclin F facilitates RRM2 degradation through SCF (Skp1-Cul1-F-box protein) ubiquitination to ensure balanced dNTP pools and genome stability (D'Angiolella et al., 2012). Additionally, some studies have implicated that subcellular localization of RNR might act as a regulatory mechanism, although it remains a subject of controversy.

1.7a RRM1

Multiple studies have suggested a dual role for RRM1 in tumorigenesis: acting as a tumor suppressor during initiation yet contributing to chemoresistance. The RRM1 gene is located on chromosome 11p, proximate to three other tumor suppressors (WT1, HBB & D11S860). This genomic region has also been identified as undergoing loss of heterozygosity in non-small-cell lung cancer (NSCLC) patients, with much of the literature on RRM1 focusing NSCLC (Bepler & Garcia-Blanco, 1994). Elevated RRM1

expression level is found to be a predictor for longer survival and delayed disease relapse among lung cancer patients (Bepler et al., 2016). Interestingly, RRM1 expression correlates positively with PTEN level, resulting in suppressed tumor migration, invasion and metastasis (Bepler et al., 2016; Gautam et al., 2003). In the context of early-stage NSCLC, co-expressions of RRM1 and excision repair cross-complementation group 1 (ERCC1) protein emerge as a favorable survival determinant post-surgery (Zheng et al., 2007).

Gemcitabine, a commonly used DNA damage agent in chemotherapy regimens, has its clinical outcomes associated with RRM1 expression. A meta-analysis has indicated that RRM1 expression levels in NSCLC patients correlated with a significantly higher response rate to gemcitabine treatment (Gong et al., 2012). Recently, a novel insight emerged regarding RRM1 phosphorylation at Ser 559 by CDK2/Cyclin A, enhancing RNR activity to ensure adequate dNTPs production for DNA replication in S/G2 phase. This mechanism plays a crucial role in maintaining genome integrity in response to DNA damage (Shu et al., 2020).

1.7b RRM2 and RRM2B

The proto-oncogene role of RRM2 in cancer has been extensively investigated. Remarkably, RRM2 ranked among the top 10% of the most overexpressed genes in 73 out of 168 individual cancer analyses (Aye et al., 2015). The TCGA database also highlights elevated RRM2 expression in breast, ovarian and uterine cancers (Fig. 2A) (Aye et al., 2015). Its expression is relatively lower in benign skin lesions compared to

melanoma tumor sections (Aird et al., 2013). Among breast and epithelia ovarian cancer patients, RRM2 expression correlates with tumor grades, indicating its involvement in supporting rapid cell proliferation in high-grade tumors (Aird et al., 2014; Ma et al., 2003).

Recent efforts have been made to unravel the mechanisms through which RRM2 exhibits its oncogenic properties in cancers. Overexpression of RRM2 in human cancer cells has been shown to reduce thrombospondin 1 (TSP-1) while increasing VEGF production, implying RRM2's role in angiogenesis (K. Zhang et al., 2009). Another study revealed that dysregulation of RRM2 can introduce mutagenesis during DNA replication, contributing to lung cancer carcinogenesis in transgenic mice (Xu et al., 2008). Emerging evidence also confirms RRM2's significance as a predictor of chemotherapeutic response. Interference with RRM2 sensitizes cancer cells to DNA-damaging agents like cisplatin and gemcitabine, a finding confirmed *in vitro* and animal models (Duxbury et al., 2004; Z. P. Lin et al., 2004). Similar findings have recently emerged in ovarian and pancreatic cancers, where high RRM2 expression is associated with poor responses to gemcitabine, reduced overall survival (OS) and disease free survival (DFS) as well (Fig. 2B) (Ferrandina et al., 2010).

In addition, the regulatory mechanism of long intergenic non-coding RNA-Nucleotide Metabolism Regulator (lincNMR) on RRM2 activity has been reported. lincNMR directly binds to RRM2 promoters and modulates its transcriptional expression through interaction with an RNA binding protein YBX1. This interaction ensures

sufficient dNTP production for DNA replication, thus supporting cell growth (Gandhi et al., 2020).

RRM2B represents another variant of β subunit, specifically induced by the transcription factor p53, earning it the alternative name p532B. Unlike RRM2, RRM2B demonstrates specific expression in cells upon DNA damage, playing an indispensable role in DNA repair by providing the necessary dNTP materials. Several studies have confirmed that exposure to various types of DNA damage, such as including UV irradiation, γ-irradiation and chemotherapeutic agents, triggers elevated DNA synthesis through RNR activation via increased RRM2B expression, as opposed to RRM2 (Devlin et al., 2008; Yamaguchi et al., 2001; Zhou et al., 2003). Upon DNA damage, p53 activates RRM2B transcriptionally, allowing it to collaborate with RRM1 in forming the holoenzyme that carries out its function. Accordingly, impaired transcriptional activation of RRM2B is observed in p53-mutant cells, leading to the inability to bind with RRM1 and form the RNR complex (Zhou et al., 2003). These findings underscore the critical role of RRM2B in DNA synthesis, particularly in the repair of damaged DNA to ensure cell survival and viability.

Additionally, studies have highlighted the physical interaction between RRM2B and MEK2 at its amino acids 161-206, which serves to suppress the MAPK signaling cascade (Piao et al., 2009). Moreover, RRM2B's in negatively modulating tumor cells invasion and anchorage-dependent cell growth has been identified, with these effects being rescued upon MEK2 knockdown (Piao et al., 2009). Decitabine, a hypomethylating agent that targets DNA methyltransferase (DNMT1), is commonly used in treating

myelodysplastic syndromes and acute myeloid leukemia. RRM2B has been shown to be undergo transcriptional induction by decitabine in cell lines. Interestingly, this induction is independent of hypomethylation, as the RRM2B promoter is already significantly hypomethylated before decitabine treatment. Notably, patients displaying successful RRM2B induction post-treatment were significantly associated with a good clinical response, evident in bone marrow complete or partial remission (Link et al., 2008).

Furthermore, post-translational modification has been reported in the case of RRM2B. To facilitate a prompt response to DNA damage, the ataxia telangiectasia mutated (ATM) kinase phosphorylates RRM2B rapidly at Ser72 in cells, thereby stabilizing it. Conversely, the unphosphorylated residue interacts with MDM2 to promote the proteasomal-mediated protein degradation of RRM2B (L. Chang et al., 2008).

1.8 References

Aird, K. M., Li, H., Xin, F., Konstantinopoulos, P. A., & Zhang, R. (2014). Identification of ribonucleotide reductase M2 as a potential target for pro-senescence therapy in epithelial ovarian cancer. *Cell Cycle*, *13*(2), 199–207. https://doi.org/10.4161/cc.26953

Aird, K. M., Zhang, G., Li, H., Tu, Z., Bitler, B. G., Garipov, A., Wu, H., Wei, Z., Wagner, S. N., Herlyn, M., & Zhang, R. (2013). Suppression of nucleotide metabolism underlies the establishment and maintenance of oncogene-induced senescence. *Cell Reports*, *3*(4), 1252–1265. https://doi.org/10.1016/j.celrep.2013.03.004

Alfarouk, K. O., Verduzco, D., Rauch, C., Muddathir, A. K., Adil, H. H. B., Elhassan, G. O., Ibrahim, M. E., David Polo Orozco, J., Cardone, R. A., Reshkin, S. J., & Harguindey, S. (2014). Glycolysis, tumor metabolism, cancer growth and dissemination. A new pH-based etiopathogenic perspective and therapeutic approach to an old cancer question. *Oncoscience*, *1*(12), 777–802.

Alla, V., Kowtharapu, B. S., Engelmann, D., Emmrich, S., Schmitz, U., Steder, M., & Pützer, B. M. (2012). E2F1 confers anticancer drug resistance by targeting ABC transporter family members and Bcl-2 via the p73/DNp73-miR-205 circuitry. *Cell Cycle*, *11*(16), 3067–3078. https://doi.org/10.4161/cc.21476

Aye, Y., Li, M., Long, M. J. C., & Weiss, R. S. (2015). Ribonucleotide reductase and cancer: Biological mechanisms and targeted therapies. *Oncogene*, *34*(16), 2011–2021. https://doi.org/10.1038/onc.2014.155

Barata, J. T., Silva, A., Brandao, J. G., Nadler, L. M., Cardoso, A. A., & Boussiotis, V. A. (2004). Activation of PI3K is indispensable for interleukin 7-mediated viability, proliferation, glucose use, and growth of T cell acute lymphoblastic leukemia cells. *The Journal of Experimental Medicine*, *200*(5), 659–669. https://doi.org/10.1084/jem.20040789

Bepler, G., & Garcia-Blanco, M. A. (1994). Three tumor-suppressor regions on chromosome 11p identified by high-resolution deletion mapping in human non-small-cell lung cancer. *Proceedings of the National Academy of Sciences*, *91*(12), 5513–5517. https://doi.org/10.1073/pnas.91.12.5513

Bepler, G., Sharma, S., Cantor, A., Gautam, A., Haura, E., Simon, G., Sharma, A., Sommers, E., & Robinson, L. (2016). RRM1 and PTEN As Prognostic Parameters for Overall and Disease-Free Survival in Patients With Non–Small-Cell Lung Cancer. *Journal of Clinical Oncology*. https://doi.org/10.1200/JCO.2004.12.002

Berkers, C. R., Maddocks, O. D. K., Cheung, E. C., Mor, I., & Vousden, K. H. (2013). Metabolic Regulation by p53 Family Members. *Cell Metabolism*, *18*(5), 617–633. https://doi.org/10.1016/j.cmet.2013.06.019

Betz, C., Stracka, D., Prescianotto-Baschong, C., Frieden, M., Demaurex, N., & Hall, M. N. (2013). MTOR complex 2-Akt signaling at mitochondria-associated endoplasmic reticulum membranes (MAM) regulates mitochondrial physiology. *Proceedings of the National Academy of Sciences*, *110*(31), 12526–12534. https://doi.org/10.1073/pnas.1302455110

Bhatia, B., Hsieh, M., Kenney, A. M., & Nahlé, Z. (2011). Mitogenic Sonic hedgehog signaling drives E2F1-dependent lipogenesis in progenitor cells and medulloblastoma. *Oncogene*, *30*(4), 410–422. https://doi.org/10.1038/onc.2010.454

Bjornsdottir, H. H., Rawshani, A., Rawshani, A., Franzén, S., Svensson, A.-M., Sattar, N., & Gudbjörnsdottir, S. (2020). A national observation study of cancer incidence and mortality risks in type 2 diabetes compared to the background population over time. *Scientific Reports*, *10*(1), Article 1. https://doi.org/10.1038/s41598-020-73668-y

Böhme, I., & Bosserhoff, A. K. (2016). Acidic tumor microenvironment in human melanoma. *Pigment Cell & Melanoma Research*, *29*(5), 508–523. https://doi.org/10.1111/pcmr.12495

Carling, D. (2004). The AMP-activated protein kinase cascade – a unifying system for energy control. *Trends in Biochemical Sciences*, *29*(1), 18–24. https://doi.org/10.1016/j.tibs.2003.11.005

CDC. (2021a, March 25). *What Is Type 1 Diabetes?* Centers for Disease Control and Prevention. https://www.cdc.gov/diabetes/basics/what-is-type-1-diabetes.html

CDC. (2021b, November 16). *What is Diabetes?* Centers for Disease Control and Prevention. https://www.cdc.gov/diabetes/basics/diabetes.html

Chabes, A. L., Pfleger, C. M., Kirschner, M. W., & Thelander, L. (2003). Mouse ribonucleotide reductase R2 protein: A new target for anaphase-promoting complex-Cdh1-mediated proteolysis. *Proceedings of the National Academy of Sciences*, *100*(7), 3925–3929. https://doi.org/10.1073/pnas.0330774100

Chabes, A., & Thelander, L. (2000). Controlled protein degradation regulates ribonucleotide reductase activity in proliferating mammalian cells during the normal cell cycle and in response to DNA damage and replication blocks. *The Journal of Biological Chemistry*, *275*(23), 17747–17753. https://doi.org/10.1074/jbc.M000799200

Chaika, N. V., Gebregiworgis, T., Lewallen, M. E., Purohit, V., Radhakrishnan, P., Liu, X., Zhang, B., Mehla, K., Brown, R. B., Caffrey, T., Yu, F., Johnson, K. R., Powers, R., Hollingsworth, M. A., & Singh, P. K. (2012). MUC1 mucin stabilizes and activates hypoxia-inducible factor 1 alpha to regulate metabolism in pancreatic cancer. *Proceedings of the National Academy of Sciences*, *109*(34), 13787–13792. https://doi.org/10.1073/pnas.1203339109

Chang, L., Zhou, B., Hu, S., Guo, R., Liu, X., Jones, S. N., & Yen, Y. (2008). ATM-mediated serine 72 phosphorylation stabilizes ribonucleotide reductase small subunit p53R2 protein against MDM2 to DNA damage. *Proceedings of the National Academy of Sciences*, *105*(47), 18519–18524. https://doi.org/10.1073/pnas.0803313105

Chang, S.-C., & Yang, W.-C. V. (2016). Hyperglycemia, tumorigenesis, and chronic inflammation. *Critical Reviews in Oncology/Hematology*, *108*, 146–153. https://doi.org/10.1016/j.critrevonc.2016.11.003

Chatterjee, S., Khunti, K., & Davies, M. J. (2017). Type 2 diabetes. *The Lancet*, *389*(10085), 2239–2251. https://doi.org/10.1016/S0140-6736(17)30058-2

Cho, N. H., Shaw, J. E., Karuranga, S., Huang, Y., Fernandes, J. D. da R., Ohlrogge, A. W., & Malanda, B. (2018). IDF Diabetes Atlas: Global estimates of diabetes prevalence for 2017 and projections for 2045. *Diabetes Research and Clinical Practice*, *138*, 271–281. https://doi.org/10.1016/j.diabres.2018.02.023

Clijsters, L., Hoencamp, C., Calis, J. J. A., Marzio, A., Handgraaf, S. M., Cuitino, M. C., Rosenberg, B. R., Leone, G., & Pagano, M. (2019). Cyclin F Controls Cell-Cycle Transcriptional Outputs by Directing the Degradation of the Three Activator E2Fs. *Molecular Cell*, *74*(6), 1264-1277.e7. https://doi.org/10.1016/j.molcel.2019.04.010

Conacci-Sorrell, M., Ngouenet, C., & Eisenman, R. N. (2010). Myc-Nick: A Cytoplasmic Cleavage Product of Myc that Promotes α-Tubulin Acetylation and Cell Differentiation. *Cell*, *142*(3), 480–493. https://doi.org/10.1016/j.cell.2010.06.037

Daneman, D. (2006). Type 1 diabetes. *The Lancet*, *367*(9513), 847–858. https://doi.org/10.1016/S0140-6736(06)68341-4

Dang, C. V., Kim, J., Gao, P., & Yustein, J. (2008). The interplay between MYC and HIF in cancer. *Nature Reviews Cancer*, *8*(1), 51–56. https://doi.org/10.1038/nrc2274

D'Angiolella, V., Donato, V., Forrester, F. M., Jeong, Y.-T., Pellacani, C., Kudo, Y., Saraf, A., Florens, L., Washburn, M. P., & Pagano, M. (2012). Cyclin F-Mediated Degradation of Ribonucleotide Reductase M2 Controls Genome Integrity and DNA Repair. *Cell*, *149*(5), 1023–1034. https://doi.org/10.1016/j.cell.2012.03.043

Dar, A. A., Majid, S., Semir, D. de, Nosrati, M., Bezrookove, V., & Kashani-Sabet, M. (2011). MiRNA-205 Suppresses Melanoma Cell Proliferation and Induces Senescence via Regulation of E2F1 Protein. *Journal of Biological Chemistry*, *286*(19), 16606–16614. https://doi.org/10.1074/jbc.M111.227611

David, C. J., Chen, M., Assanah, M., Canoll, P., & Manley, J. L. (2010). HnRNP proteins controlled by c-Myc deregulate pyruvate kinase mRNA splicing in cancer. *Nature*, *463*(7279), 364–368. https://doi.org/10.1038/nature08697

DeBerardinis, R. J., Lum, J. J., Hatzivassiliou, G., & Thompson, C. B. (2008). The Biology of Cancer: Metabolic Reprogramming Fuels Cell Growth and Proliferation. *Cell Metabolism*, *7*(1), 11–20. https://doi.org/10.1016/j.cmet.2007.10.002

DeFronzo, R. A., Ferrannini, E., Groop, L., Henry, R. R., Herman, W. H., Holst, J. J., Hu, F. B., Kahn, C. R., Raz, I., Shulman, G. I., Simonson, D. C., Testa, M. A., & Weiss, R. (2015). Type 2 diabetes mellitus. *Nature Reviews Disease Primers*, *1*(1), 1–22. https://doi.org/10.1038/nrdp.2015.19

Dejure, F. R., & Eilers, M. (2017). MYC and tumor metabolism: Chicken and egg. *The EMBO Journal*, *36*(23), 3409–3420. https://doi.org/10.15252/embj.201796438

Devlin, H.-L., Mack, P. C., Burich, R. A., Gumerlock, P. H., Kung, H.-J., Mudryj, M., & deVere White, R. W. (2008). Impairment of the DNA Repair and Growth Arrest Pathways by p53R2 Silencing Enhances DNA Damage–Induced Apoptosis in a p53-Dependent Manner in Prostate

Cancer Cells. *Molecular Cancer Research*, *6*(5), 808–818. https://doi.org/10.1158/1541-7786.MCR-07-2027

Duxbury, M. S., Ito, H., Zinner, M. J., Ashley, S. W., & Whang, E. E. (2004). RNA interference targeting the M2 subunit of ribonucleotide reductase enhances pancreatic adenocarcinoma chemosensitivity to gemcitabine. *Oncogene*, *23*(8), Article 8. https://doi.org/10.1038/sj.onc.1207272

Engström, Y., Eriksson, S., Jildevik, I., Skog, S., Thelander, L., & Tribukait, B. (1985). Cell cycle-dependent expression of mammalian ribonucleotide reductase. Differential regulation of the two subunits. *Journal of Biological Chemistry*, *260*(16), 9114–9116.

Eriksson, S., Gräslund, A., Skog, S., Thelander, L., & Tribukait, B. (1984). Cell cycle-dependent regulation of mammalian ribonucleotide reductase. The S phase-correlated increase in subunit M2 is regulated by de novo protein synthesis. *Journal of Biological Chemistry*, *259*(19), 11695–11700.

Fairman, J. W., Wijerathna, S. R., Ahmad, Md. F., Xu, H., Nakano, R., Jha, S., Prendergast, J., Welin, M., Flodin, S., Roos, A., Nordlund, P., Li, Z., Walz, T., & Dealwis, C. G. (2011). STRUCTURAL BASIS FOR ALLOSTERIC REGULATION OF HUMAN RIBONUCLEOTIDE REDUCTASE BY NUCLEOTIDE-INDUCED OLIGOMERIZATION. *Nature Structural & Molecular Biology*, *18*(3), 316–322. https://doi.org/10.1038/nsmb.2007

Faubert, B., Vincent, E. E., Griss, T., Samborska, B., Izreig, S., Svensson, R. U., Mamer, O. A., Avizonis, D., Shackelford, D. B., Shaw, R. J., & Jones, R. G. (2014). Loss of the tumor suppressor LKB1 promotes metabolic reprogramming of cancer cells via HIF-1α. *Proceedings of the National Academy of Sciences*, *111*(7), 2554–2559. https://doi.org/10.1073/pnas.1312570111

Fernández de Mattos, S., Lam, E. W.-F., & Tauler, A. (2002). An E2F-binding site mediates the activation of the proliferative isoform of 6-phosphofructo-2-kinase/fructose-2,6-bisphosphatase by phosphatidylinositol 3-kinase. *The Biochemical Journal*, *368*(Pt 1), 283–291. https://doi.org/10.1042/BJ20020622

Ferrandina, G., Mey, V., Nannizzi, S., Ricciardi, S., Petrillo, M., Ferlini, C., Danesi, R., Scambia, G., & Del Tacca, M. (2010). Expression of nucleoside transporters, deoxycitidine kinase, ribonucleotide reductase regulatory subunits, and gemcitabine catabolic enzymes in primary ovarian cancer. *Cancer Chemotherapy and Pharmacology*, *65*(4), 679–686. https://doi.org/10.1007/s00280-009-1073-y

Franke, T. F., Hornik, C. P., Segev, L., Shostak, G. A., & Sugimoto, C. (2003). PI3K/Akt and apoptosis: Size matters. *Oncogene*, *22*(56), Article 56. https://doi.org/10.1038/sj.onc.1207115

Frietze, S., Lupien, M., Silver, P. A., & Brown, M. (2008). CARM1 Regulates Estrogen-Stimulated Breast Cancer Growth through Up-regulation of E2F1. *Cancer Research*, *68*(1), 301–306. https://doi.org/10.1158/0008-5472.CAN-07-1983

Gallagher, E. J., & LeRoith, D. (2010). The proliferating role of insulin and insulin-like growth factors in cancer. *Trends in Endocrinology & Metabolism*, *21*(10), 610–618. https://doi.org/10.1016/j.tem.2010.06.007

Gambhir, S. S. (2002). Molecular imaging of cancer with positron emission tomography. *Nature Reviews Cancer*, *2*(9), Article 9. https://doi.org/10.1038/nrc882

Gandhi, M., Groß, M., Holler, J. M., Coggins, S. A., Patil, N., Leupold, J. H., Munschauer, M., Schenone, M., Hartigan, C. R., Allgayer, H., Kim, B., & Diederichs, S. (2020). The lncRNA lincNMR regulates nucleotide metabolism via a YBX1—RRM2 axis in cancer. *Nature Communications*, *11*(1), 3214. https://doi.org/10.1038/s41467-020-17007-9

Gautam, A., Li, Z.-R., & Bepler, G. (2003). RRM1-induced metastasis suppression through PTEN-regulated pathways. *Oncogene*, *22*(14), Article 14. https://doi.org/10.1038/sj.onc.1206232

Gemin, A., Sweet, S., Preston, T. J., & Singh, G. (2005). Regulation of the cell cycle in response to inhibition of mitochondrial generated energy. *Biochemical and Biophysical Research Communications*, *332*(4), 1122–1132. https://doi.org/10.1016/j.bbrc.2005.05.061

Gerards, M. C., van der Velden, D. L., Baars, J. W., Brandjes, D. P. M., Hoekstra, J. B. L., Vriesendorp, T. M., & Gerdes, V. E. A. (2017). Impact of hyperglycemia on the efficacy of chemotherapy—A systematic review of preclinical studies. *Critical Reviews in Oncology/Hematology*, *113*, 235–241. https://doi.org/10.1016/j.critrevonc.2017.03.007

Giovannucci, E., Harlan, D. M., Archer, M. C., Bergenstal, R. M., Gapstur, S. M., Habel, L. A., Pollak, M., Regensteiner, J. G., & Yee, D. (2010). Diabetes and Cancer: A Consensus Report. *CA: A Cancer Journal for Clinicians*, *60*(4), 207–221. https://doi.org/10.3322/caac.20078

Gomes, A. S., Ramos, H., Soares, J., & Saraiva, L. (2018). p53 and glucose metabolism: An orchestra to be directed in cancer therapy. *Pharmacological Research*, *131*, 75–86. https://doi.org/10.1016/j.phrs.2018.03.015

Gong, W., Zhang, X., Wu, J., Chen, L., Li, L., Sun, J., Lv, Y., Wei, X., Du, Y., Jin, H., & Dong, J. (2012). RRM1 expression and clinical outcome of gemcitabine-containing chemotherapy for advanced non-small-cell lung cancer: A meta-analysis. *Lung Cancer*, *75*(3), 374–380. https://doi.org/10.1016/j.lungcan.2011.08.003

González-Romero, F., Mestre, D., Aurrekoetxea, I., O'Rourke, C. J., Andersen, J. B., Woodhoo, A., Tamayo-Caro, M., Varela-Rey, M., Palomo-Irigoyen, M., Gómez-Santos, B., de Urturi, D. S., Núñez-García, M., García-Rodríguez, J. L., Fernández-Ares, L., Buqué, X., Iglesias-Ara, A., Bernales, I., De Juan, V. G., Delgado, T. C., … Aspichueta, P. (2021). E2F1 and E2F2-Mediated Repression of CPT2 Establishes a Lipid-Rich Tumor-Promoting Environment. *Cancer Research*, *81*(11), 2874–2887. https://doi.org/10.1158/0008-5472.CAN-20-2052

Gordon, C. A., Gong, X., Ganesh, D., & Brooks, J. D. (2017). NUSAP1 promotes invasion and metastasis of prostate cancer. *Oncotarget*, *8*(18), 29935–29950. https://doi.org/10.18632/oncotarget.15604

Gordon-Dseagu, V. L. Z., Shelton, N., & Mindell, J. S. (2013). Epidemiological evidence of a relationship between type-1 diabetes mellitus and cancer: A review of the existing literature. *International Journal of Cancer*, *132*(3), 501–508. https://doi.org/10.1002/ijc.27703

Goto, Y., Hayashi, R., Kang, D., & Yoshida, K. (2006). Acute loss of transcription factor E2F1 induces mitochondrial biogenesis in Hela cells. *Journal of Cellular Physiology*, *209*(3), 923–934. https://doi.org/10.1002/jcp.20802

Gulzar, Z. G., McKenney, J. K., & Brooks, J. D. (2013). Increased expression of NuSAP in recurrent prostate cancer is mediated by E2F1. *Oncogene*, *32*(1), Article 1. https://doi.org/10.1038/onc.2012.27

Hanahan, D., & Weinberg, R. A. (2011). Hallmarks of Cancer: The Next Generation. *Cell*, *144*(5), 646–674. https://doi.org/10.1016/j.cell.2011.02.013

Hawkins, R. A., & Phelps, M. E. (1988). PET in clinical oncology. *Cancer Metastasis Reviews*, *7*(2), 119–142. https://doi.org/10.1007/bf00046482

He, C.-L., Bian, Y.-Y., Xue, Y., Liu, Z.-X., Zhou, K.-Q., Yao, C.-F., Lin, Y., Zou, H.-F., Luo, F.-X., Qu, Y.-Y., Zhao, J.-Y., Ye, M.-L., Zhao, S.-M., & Xu, W. (2016). Pyruvate Kinase M2 Activates mTORC1 by Phosphorylating AKT1S1. *Scientific Reports*, *6*(1), 21524. https://doi.org/10.1038/srep21524

Henley, S. A., & Dick, F. A. (2012). The retinoblastoma family of proteins and their regulatory functions in the mammalian cell division cycle. *Cell Division*, *7*(1), 10. https://doi.org/10.1186/1747-1028-7-10

Heuson, J. C., & Legros, N. (1972). Influence of insulin deprivation on growth of the 7,12-dimethylbenz(a)anthracene-induced mammary carcinoma in rats subjected to alloxan diabetes and food restriction. *Cancer Research*, *32*(2), 226–232.

House, S. W., Warburg, O., Burk, D., & Schade, A. L. (1956). On Respiratory Impairment in Cancer Cells. *Science*, *124*(3215), 267–272. JSTOR.

Hoxhaj, G., & Manning, B. D. (2020). The PI3K–AKT network at the interface of oncogenic signalling and cancer metabolism. *Nature Reviews Cancer*, *20*(2), 74–88. https://doi.org/10.1038/s41568-019-0216-7

Hsieh, A. L., Walton, Z. E., Altman, B. J., Stine, Z. E., & Dang, C. V. (2015). MYC and metabolism on the path to cancer. *Seminars in Cell & Developmental Biology*, *43*, 11–21. https://doi.org/10.1016/j.semcdb.2015.08.003

Hu, H., Juvekar, A., Lyssiotis, C. A., Lien, E. C., Albeck, J. G., Oh, D., Varma, G., Hung, Y. P., Ullas, S., Lauring, J., Seth, P., Lundquist, M. R., Tolan, D. R., Grant, A. K., Needleman, D. J., Asara, J. M., Cantley, L. C., & Wulf, G. M. (2016). Phosphoinositide 3-Kinase Regulates Glycolysis through Mobilization of Aldolase from the Actin Cytoskeleton. *Cell*, *164*(3), 433–446. https://doi.org/10.1016/j.cell.2015.12.042

Icard, P., Fournel, L., Wu, Z., Alifano, M., & Lincet, H. (2019). Interconnection between Metabolism and Cell Cycle in Cancer. *Trends in Biochemical Sciences*, *44*(6), 490–501. https://doi.org/10.1016/j.tibs.2018.12.007

Itahana, Y., & Itahana, K. (2018). Emerging Roles of p53 Family Members in Glucose Metabolism. *International Journal of Molecular Sciences*, *19*(3), 776. https://doi.org/10.3390/ijms19030776

Itkonen, H. M., Minner, S., Guldvik, I. J., Sandmann, M. J., Tsourlakis, M. C., Berge, V., Svindland, A., Schlomm, T., & Mills, I. G. (2013). O-GlcNAc Transferase Integrates Metabolic Pathways to Regulate the Stability of c-MYC in Human Prostate Cancer Cells. *Cancer Research*, *73*(16), 5277–5287. https://doi.org/10.1158/0008-5472.CAN-13-0549

Justus, C. R., Dong, L., & Yang, L. V. (2013). Acidic tumor microenvironment and pH-sensing G protein-coupled receptors. *Frontiers in Physiology*, *4*. https://doi.org/10.3389/fphys.2013.00354

Kawada, K., Toda, K., & Sakai, Y. (2017). Targeting metabolic reprogramming in KRAS-driven cancers. *International Journal of Clinical Oncology*, *22*(4), 651–659. https://doi.org/10.1007/s10147-017-1156-4

Kawauchi, K., Araki, K., Tobiume, K., & Tanaka, N. (2008). P53 regulates glucose metabolism through an IKK-NF-κB pathway and inhibits cell transformation. *Nature Cell Biology*, *10*(5), Article 5. https://doi.org/10.1038/ncb1724

Kent, L. N., & Leone, G. (2019). The broken cycle: E2F dysfunction in cancer. *Nature Reviews Cancer*, *19*(6), 326–338. https://doi.org/10.1038/s41568-019-0143-7

Keppler-Noreuil, K. M., Parker, V. E. R., Darling, T. N., & Martinez-Agosto, J. A. (2016). Somatic overgrowth disorders of the PI3K/AKT/mTOR pathway & therapeutic strategies. *American Journal of Medical Genetics Part C: Seminars in Medical Genetics*, *172*(4), 402–421. https://doi.org/10.1002/ajmg.c.31531

Kerk, S. A., Papagiannakopoulos, T., Shah, Y. M., & Lyssiotis, C. A. (2021). Metabolic networks in mutant KRAS-driven tumours: Tissue specificities and the microenvironment. *Nature Reviews Cancer*, *21*(8), 510–525. https://doi.org/10.1038/s41568-021-00375-9

Kerr, E. M., & Martins, C. P. (2018). Metabolic rewiring in mutant Kras lung cancer. *The FEBS Journal*, *285*(1), 28–41. https://doi.org/10.1111/febs.14125

Kim, J., Tchernyshyov, I., Semenza, G. L., & Dang, C. V. (2006). HIF-1-mediated expression of pyruvate dehydrogenase kinase: A metabolic switch required for cellular adaptation to hypoxia. *Cell Metabolism*, *3*(3), 177–185. https://doi.org/10.1016/j.cmet.2006.02.002

Kitabchi, A. E. (1975). Hormonal control of glucose metabolism. *Otolaryngologic Clinics of North America*, *8*(2), 335–344.

Kumari, A., Iwasaki, T., Pyndiah, S., Cassimere, E. K., Palani, C. D., & Sakamuro, D. (2015). Regulation of E2F1-induced apoptosis by poly(ADP-ribosyl)ation. *Cell Death & Differentiation*, *22*(2), Article 2. https://doi.org/10.1038/cdd.2014.146

Kung, C.-P., & Murphy, M. E. (2016). The role of the p53 tumor suppressor in metabolism and diabetes. *The Journal of Endocrinology*, *231*(2), R61–R75. https://doi.org/10.1530/JOE-16-0324

Kunz, B. A., & Kohalmi, S. E. (1991). Modulation of Mutagenesis by Deoxyribonucleotide Levels. *Annual Review of Genetics*, *25*(1), 339–359. https://doi.org/10.1146/annurev.ge.25.120191.002011

Le, A., Lane, A. N., Hamaker, M., Bose, S., Gouw, A., Barbi, J., Tsukamoto, T., Rojas, C. J., Slusher, B. S., Zhang, H., Zimmerman, L. J., Liebler, D. C., Slebos, R. J. C., Lorkiewicz, P. K., Higashi, R. M., Fan, T. W. M., & Dang, C. V. (2012). Glucose-independent glutamine metabolism via TCA cycling for proliferation and survival in B cells. *Cell Metabolism*, *15*(1), 110–121. https://doi.org/10.1016/j.cmet.2011.12.009

Lee, A. S. (2014). Glucose-regulated proteins in cancer: Molecular mechanisms and therapeutic potential. *Nature Reviews Cancer*, *14*(4), Article 4. https://doi.org/10.1038/nrc3701

Lee, S.-R., Roh, Y.-G., Kim, S.-K., Lee, J.-S., Seol, S.-Y., Lee, H.-H., Kim, W.-T., Kim, W.-J., Heo, J., Cha, H.-J., Kang, T.-H., Chung, J. W., Chu, I.-S., & Leem, S.-H. (2015). Activation of EZH2 and SUZ12 Regulated by E2F1 Predicts the Disease Progression and Aggressive Characteristics of Bladder Cancer. *Clinical Cancer Research*, *21*(23), 5391–5403. https://doi.org/10.1158/1078-0432.CCR-14-2680

Lee, W.-H., Choi, J.-S., Byun, M.-R., Koo, K., Shin, S., Lee, S.-K., & Surh, Y.-J. (2010). Functional inactivation of triosephosphate isomerase through phosphorylation during etoposide-induced apoptosis in HeLa cells: Potential role of Cdk2. *Toxicology*, *278*(2), 224–228. https://doi.org/10.1016/j.tox.2010.02.005

Li, C., Tang, Z., Zhang, W., Ye, Z., & Liu, F. (2021). GEPIA2021: Integrating multiple deconvolution-based analysis into GEPIA. *Nucleic Acids Research*, *49*(W1), W242–W246. https://doi.org/10.1093/nar/gkab418

Li, Y., Slansky, J. E., Myers, D. J., Drinkwater, N. R., Kaelin, W. G., & Farnham, P. J. (1994). Cloning, chromosomal location, and characterization of mouse E2F1. *Molecular and Cellular Biology*, *14*(3), 1861–1869.

Liang, J., Cao, R., Zhang, Y., Xia, Y., Zheng, Y., Li, X., Wang, L., Yang, W., & Lu, Z. (2016). PKM2 dephosphorylation by Cdc25A promotes the Warburg effect and tumorigenesis. *Nature Communications*, *7*(1), 12431. https://doi.org/10.1038/ncomms12431

Liang, Y., Liu, J., & Feng, Z. (2013). The regulation of cellular metabolism by tumor suppressor p53. *Cell & Bioscience*, *3*(1), 9. https://doi.org/10.1186/2045-3701-3-9

Lin, S.-C., & Hardie, D. G. (2018). AMPK: Sensing Glucose as well as Cellular Energy Status. *Cell Metabolism*, *27*(2), 299–313. https://doi.org/10.1016/j.cmet.2017.10.009

Lin, Y.-W., Weng, X.-F., Huang, B.-L., Guo, H.-P., Xu, Y.-W., & Peng, Y.-H. (2021). IGFBP-1 in cancer: Expression, molecular mechanisms, and potential clinical implications. *American Journal of Translational Research*, *13*(3), 813–832.

Lin, Z. P., Belcourt, M. F., Cory, J. G., & Sartorelli, A. C. (2004). Stable Suppression of the R2 Subunit of Ribonucleotide Reductase by R2-targeted Short Interference RNA Sensitizes p53(–/–) HCT-116 Colon Cancer Cells to DNA-damaging Agents and Ribonucleotide Reductase Inhibitors. *Journal of Biological Chemistry*, *279*(26), 27030–27038. https://doi.org/10.1074/jbc.M402056200

Link, P. A., Baer, M. R., James, S. R., Jones, D. A., & Karpf, A. R. (2008). P53-Inducible Ribonucleotide Reductase (p53R2/RRM2B) Is a DNA Hypomethylation–Independent Decitabine Gene Target That Correlates with Clinical Response in Myelodysplastic Syndrome/Acute Myelogenous Leukemia. *Cancer Research*, *68*(22), 9358–9366. https://doi.org/10.1158/0008-5472.CAN-08-1860

Louie, M. C., Zou, J. X., Rabinovich, A., & Chen, H.-W. (2004). ACTR/AIB1 functions as an E2F1 coactivator to promote breast cancer cell proliferation and antiestrogen resistance. *Molecular and Cellular Biology*, *24*(12), 5157–5171. https://doi.org/10.1128/MCB.24.12.5157-5171.2004

Lv, L., Xu, Y.-P., Zhao, D., Li, F.-L., Wang, W., Sasaki, N., Jiang, Y., Zhou, X., Li, T.-T., Guan, K.-L., Lei, Q.-Y., & Xiong, Y. (2013). Mitogenic and Oncogenic Stimulation of K433 Acetylation Promotes PKM2 Protein Kinase Activity and Nuclear Localization. *Molecular Cell*, *52*(3), 340–352. https://doi.org/10.1016/j.molcel.2013.09.004

Ma, X.-J., Salunga, R., Tuggle, J. T., Gaudet, J., Enright, E., McQuary, P., Payette, T., Pistone, M., Stecker, K., Zhang, B. M., Zhou, Y.-X., Varnholt, H., Smith, B., Gadd, M., Chatfield, E., Kessler, J., Baer, T. M., Erlander, M. G., & Sgroi, D. C. (2003). Gene expression profiles of human breast cancer progression. *Proceedings of the National Academy of Sciences of the United States of America*, *100*(10), 5974–5979. https://doi.org/10.1073/pnas.0931261100

Malakar, P., Stein, I., Saragovi, A., Winkler, R., Stern-Ginossar, N., Berger, M., Pikarsky, E., & Karni, R. (2019). Long Noncoding RNA MALAT1 Regulates Cancer Glucose Metabolism by Enhancing mTOR-Mediated Translation of TCF7L2. *Cancer Research*, *79*(10), 2480–2493. https://doi.org/10.1158/0008-5472.CAN-18-1432

Mamczur, P., Gamian, A., Kolodziej, J., Dziegiel, P., & Rakus, D. (2013). Nuclear localization of aldolase A correlates with cell proliferation. *Biochimica et Biophysica Acta (BBA) - Molecular Cell Research*, *1833*(12), 2812–2822. https://doi.org/10.1016/j.bbamcr.2013.07.013

Mamczur, P., Mazurek, J., & Rakus, D. (2010). Ubiquitous presence of gluconeogenic regulatory enzyme, fructose-1,6-bisphosphatase, within layers of rat retina. *Cell and Tissue Research*, *341*(2), 213–221. https://doi.org/10.1007/s00441-010-1008-2

Mandigo, A. C., Yuan, W., Xu, K., Gallagher, P., Pang, A., Guan, Y. F., Shafi, A. A., Thangavel, C., Sheehan, B., Bogdan, D., Paschalis, A., McCann, J. J., Laufer, T. S., Gordon, N., Vasilevskaya, I. A., Dylgjeri, E., Chand, S. N., Schiewer, M. J., Domingo-Domenech, J., … Knudsen, K. E. (2021). RB/E2F1 as a Master Regulator of Cancer Cell Metabolism in Advanced Disease. *Cancer Discovery*, *11*(9), 2334–2353. https://doi.org/10.1158/2159-8290.CD-20-1114

Martínez-Balbás, M. A., Bauer, U. M., Nielsen, S. J., Brehm, A., & Kouzarides, T. (2000). Regulation of E2F1 activity by acetylation. *The EMBO Journal*, *19*(4), 662–671. https://doi.org/10.1093/emboj/19.4.662

Martini, M., Santis, M. C. D., Braccini, L., Gulluni, F., & Hirsch, E. (2014). PI3K/AKT signaling pathway and cancer: An updated review. *Annals of Medicine*, *46*(6), 372–383. https://doi.org/10.3109/07853890.2014.912836

McNair, C., Xu, K., Mandigo, A. C., Benelli, M., Leiby, B., Rodrigues, D., Lindberg, J., Gronberg, H., Crespo, M., Laere, B. D., Dirix, L., Visakorpi, T., Li, F., Feng, F. Y., Bono, J. de,

Demichelis, F., Rubin, M. A., Brown, M., & Knudsen, K. E. (2018). Differential impact of RB status on E2F1 reprogramming in human cancer. *The Journal of Clinical Investigation*, *128*(1), 341–358. https://doi.org/10.1172/JCI93566

Mo, S. P., Coulson, J. M., & Prior, I. A. (2018). RAS variant signalling. *Biochemical Society Transactions*, *46*(5), 1325–1332. https://doi.org/10.1042/BST20180173

Mori, K., Uchida, T., Fukumura, M., Tamiya, S., Higurashi, M., Sakai, H., Ishikawa, F., & Shibanuma, M. (2016). Linkage of E2F1 transcriptional network and cell proliferation with respiratory chain activity in breast cancer cells. *Cancer Science*, *107*(7), 963–971. https://doi.org/10.1111/cas.12953

Mossmann, D., Park, S., & Hall, M. N. (2018). MTOR signalling and cellular metabolism are mutual determinants in cancer. *Nature Reviews Cancer*, *18*(12), 744–757. https://doi.org/10.1038/s41568-018-0074-8

Murphy, T. A., Dang, C. V., & Young, J. D. (2013). Isotopically nonstationary 13C flux analysis of Myc-induced metabolic reprogramming in B-cells. *Metabolic Engineering*, *15*, 206–217. https://doi.org/10.1016/j.ymben.2012.07.008

Nakrani, M. N., Wineland, R. H., & Anjum, F. (2021). Physiology, Glucose Metabolism. In *StatPearls [Internet]*. StatPearls Publishing. https://www.ncbi.nlm.nih.gov/books/NBK560599/

Oakhill, J. S., Steel, R., Chen, Z.-P., Scott, J. W., Ling, N., Tam, S., & Kemp, B. E. (2011). AMPK Is a Direct Adenylate Charge-Regulated Protein Kinase. *Science*, *332*(6036), 1433–1435. https://doi.org/10.1126/science.1200094

Ooi, G. T., Tseng, L. Y., Tran, M. Q., & Rechler, M. M. (1992). Insulin rapidly decreases insulin-like growth factor-binding protein-1 gene transcription in streptozotocin-diabetic rats. *Molecular Endocrinology*, *6*(12), 2219–2228. https://doi.org/10.1210/mend.6.12.1283442

Patra, K. C., Wang, Q., Bhaskar, P. T., Miller, L., Wang, Z., Wheaton, W., Chandel, N., Laakso, M., Muller, W. J., Allen, E. L., Jha, A. K., Smolen, G. A., Clasquin, M. F., Robey, B., & Hay, N. (2013). Hexokinase 2 is required for tumor initiation and maintenance and its systemic deletion is therapeutic in mouse models of cancer. *Cancer Cell*, *24*(2), 213–228. https://doi.org/10.1016/j.ccr.2013.06.014

Pavlova, N. N., & Thompson, C. B. (2016). The Emerging Hallmarks of Cancer Metabolism. *Cell Metabolism*, *23*(1), 27–47. https://doi.org/10.1016/j.cmet.2015.12.006

Pezzuto, A., & Carico, E. (2018). Role of HIF-1 in Cancer Progression: Novel Insights. A Review. *Current Molecular Medicine*, *18*(6), 343–351. https://doi.org/10.2174/1566524018666181109121849

Piao, C., Jin, M., Kim, H. B., Lee, S. M., Amatya, P. N., Hyun, J.-W., Chang, I.-Y., & You, H. J. (2009). Ribonucleotide reductase small subunit p53R2 suppresses MEK–ERK activity by binding to ERK kinase 2. *Oncogene*, *28*(21), Article 21. https://doi.org/10.1038/onc.2009.84

Powell, D. R., Suwanichkul, A., Cubbage, M. L., DePaolis, L. A., Snuggs, M. B., & Lee, P. D. (1991). Insulin inhibits transcription of the human gene for insulin-like growth factor-binding protein-1. *Journal of Biological Chemistry*, *266*(28), 18868–18876. https://doi.org/10.1016/S0021-9258(18)55144-9

Rathmell, J. C., Fox, C. J., Plas, D. R., Hammerman, P. S., Cinalli, R. M., & Thompson, C. B. (2003). Akt-Directed Glucose Metabolism Can Prevent Bax Conformation Change and Promote Growth Factor-Independent Survival. *Molecular and Cellular Biology*, *23*(20), 7315–7328. https://doi.org/10.1128/MCB.23.20.7315-7328.2003

Röder, P. V., Wu, B., Liu, Y., & Han, W. (2016). Pancreatic regulation of glucose homeostasis. *Experimental & Molecular Medicine*, *48*(3), e219. https://doi.org/10.1038/emm.2016.6

Sanders, L. M. (2016). Carbohydrate: Digestion, Absorption and Metabolism. In B. Caballero, P. M. Finglas, & F. Toldrá (Eds.), *Encyclopedia of Food and Health* (pp. 643–650). Academic Press. https://doi.org/10.1016/B978-0-12-384947-2.00114-8

Schwartzenberg-Bar-Yoseph, F., Armoni, M., & Karnieli, E. (2004). The Tumor Suppressor p53 Down-Regulates Glucose Transporters GLUT1 and GLUT4 Gene Expression. *Cancer Research*, *64*(7), 2627–2633. https://doi.org/10.1158/0008-5472.CAN-03-0846

Shackelford, D. B., Vasquez, D. S., Corbeil, J., Wu, S., Leblanc, M., Wu, C.-L., Vera, D. R., & Shaw, R. J. (2009). MTOR and HIF-1α-mediated tumor metabolism in an LKB1 mouse model of Peutz-Jeghers syndrome. *Proceedings of the National Academy of Sciences*, *106*(27), 11137–11142. https://doi.org/10.1073/pnas.0900465106

Shaw, R. J., Bardeesy, N., Manning, B. D., Lopez, L., Kosmatka, M., DePinho, R. A., & Cantley, L. C. (2004). The LKB1 tumor suppressor negatively regulates mTOR signaling. *Cancer Cell*, *6*(1), 91–99. https://doi.org/10.1016/j.ccr.2004.06.007

Shen, L., O'Shea, J. M., Kaadige, M. R., Cunha, S., Wilde, B. R., Cohen, A. L., Welm, A. L., & Ayer, D. E. (2015). Metabolic reprogramming in triple-negative breast cancer through Myc suppression of TXNIP. *Proceedings of the National Academy of Sciences of the United States of America*, *112*(17), 5425–5430. https://doi.org/10.1073/pnas.1501555112

Shu, Z., Li, Z., Huang, H., Chen, Y., Fan, J., Yu, L., Wu, Z., Tian, L., Qi, Q., Peng, S., Wei, C., Xie, Z., Li, X., Feng, Q., Sheng, H., Li, G., Wei, D., Shan, C., & Chen, G. (2020). Cell-cycle-dependent phosphorylation of RRM1 ensures efficient DNA replication and regulates cancer vulnerability to ATR inhibition. *Oncogene*, *39*(35), 5721–5733. https://doi.org/10.1038/s41388-020-01403-y

Shukla, S. K., Purohit, V., Mehla, K., Gunda, V., Chaika, N. V., Vernucci, E., King, R. J., Abrego, J., Goode, G. D., Dasgupta, A., Illies, A. L., Gebregiworgis, T., Dai, B., Augustine, J. J., Murthy, D., Attri, K. S., Mashadova, O., Grandgenett, P. M., Powers, R., … Singh, P. K. (2017). MUC1 and HIF-1alpha Signaling Crosstalk Induces Anabolic Glucose Metabolism to Impart Gemcitabine Resistance to Pancreatic Cancer. *Cancer Cell*, *32*(1), 71-87.e7. https://doi.org/10.1016/j.ccell.2017.06.004

Slansky, J. E., Li, Y., Kaelin, W. G., & Farnham, P. J. (1993). A protein synthesis-dependent increase in E2F1 mRNA correlates with growth regulation of the dihydrofolate reductase promoter. *Molecular and Cellular Biology*, *13*(3), 1610–1618.

Sodi, V. L., Khaku, S., Krutilina, R., Schwab, L. P., Vocadlo, D. J., Seagroves, T. N., & Reginato, M. J. (2015). MTOR/MYC Axis Regulates O-GlcNAc Transferase (OGT) Expression and O-GlcNAcylation in Breast Cancer. *Molecular Cancer Research : MCR*, *13*(5), 923–933. https://doi.org/10.1158/1541-7786.MCR-14-0536

Sun, Q., Chen, X., Ma, J., Peng, H., Wang, F., Zha, X., Wang, Y., Jing, Y., Yang, H., Chen, R., Chang, L., Zhang, Y., Goto, J., Onda, H., Chen, T., Wang, M.-R., Lu, Y., You, H., Kwiatkowski, D., & Zhang, H. (2011). Mammalian target of rapamycin up-regulation of pyruvate kinase isoenzyme type M2 is critical for aerobic glycolysis and tumor growth. *Proceedings of the National Academy of Sciences*, *108*(10), 4129–4134. https://doi.org/10.1073/pnas.1014769108

Szablewski, L. (2014). Diabetes mellitus: Influences on cancer risk. *Diabetes/Metabolism Research and Reviews*, *30*(7), 543–553. https://doi.org/10.1002/dmrr.2573

Vander Heiden, M. G., Cantley, L. C., & Thompson, C. B. (2009). Understanding the Warburg Effect: The Metabolic Requirements of Cell Proliferation. *Science (New York, N.Y.)*, *324*(5930), 1029–1033. https://doi.org/10.1126/science.1160809

Vander Heiden, M. G., & DeBerardinis, R. J. (2017). Understanding the Intersections between Metabolism and Cancer Biology. *Cell*, *168*(4), 657–669. https://doi.org/10.1016/j.cell.2016.12.039

Vuaroqueaux, V., Urban, P., Labuhn, M., Delorenzi, M., Wirapati, P., Benz, C. C., Flury, R., Dieterich, H., Spyratos, F., Eppenberger, U., & Eppenberger-Castori, S. (2007). Low E2F1 transcript levels are a strong determinant of favorable breast cancer outcome. *Breast Cancer Research*, *9*(3), R33. https://doi.org/10.1186/bcr1681

Wahlström, T., & Arsenian Henriksson, M. (2015). Impact of MYC in regulation of tumor cell metabolism. *Biochimica et Biophysica Acta (BBA) - Gene Regulatory Mechanisms*, *1849*(5), 563–569. https://doi.org/10.1016/j.bbagrm.2014.07.004

Wang, H., Nicolay, B. N., Chick, J. M., Gao, X., Geng, Y., Ren, H., Gao, H., Yang, G., Williams, J. A., Suski, J. M., Keibler, M. A., Sicinska, E., Gerdemann, U., Haining, W. N., Roberts, T. M., Polyak, K., Gygi, S. P., Dyson, N. J., & Sicinski, P. (2017). The metabolic function of cyclin D3–CDK6 kinase in cancer cell survival. *Nature*, *546*(7658), Article 7658. https://doi.org/10.1038/nature22797

Wang, L., Xiong, H., Wu, F., Zhang, Y., Wang, J., Zhao, L., Guo, X., Chang, L.-J., Zhang, Y., You, M. J., Koochekpour, S., Saleem, M., Huang, H., Lu, J., & Deng, Y. (2014). Hexokinase 2-Mediated Warburg Effect Is Required for PTEN- and p53-Deficiency-Driven Prostate Cancer Growth. *Cell Reports*, *8*(5), 1461–1474. https://doi.org/10.1016/j.celrep.2014.07.053

Wang, L.-Y., Hung, C.-L., Chen, Y.-R., Yang, J. C., Wang, J., Campbell, M., Izumiya, Y., Chen, H.-W., Wang, W.-C., Ann, D. K., & Kung, H.-J. (2016). KDM4A Coactivates E2F1 to Regulate the PDK-Dependent Metabolic Switch between Mitochondrial Oxidation and Glycolysis. *Cell Reports*, *16*(11), 3016–3027. https://doi.org/10.1016/j.celrep.2016.08.018

Wang, M., Yang, Y., & Liao, Z. (2020). Diabetes and cancer: Epidemiological and biological links. *World Journal of Diabetes*, *11*(6), 227–238. https://doi.org/10.4239/wjd.v11.i6.227
Warburg, O. (1956). On the Origin of Cancer Cells. *Science*, *123*(3191), 309–314. JSTOR.

Weber, W. A., Avril, N., & Schwaiger, M. (1999). Relevance of positron emission tomography (PET) in oncology. *Strahlentherapie Und Onkologie: Organ Der Deutschen Rontgengesellschaft ... [et Al]*, *175*(8), 356–373. https://doi.org/10.1007/s000660050022

Wieman, H. L., Wofford, J. A., & Rathmell, J. C. (2007). Cytokine Stimulation Promotes Glucose Uptake via Phosphatidylinositol-3 Kinase/Akt Regulation of Glut1 Activity and Trafficking. *Molecular Biology of the Cell*, *18*(4), 1437–1446. https://doi.org/10.1091/mbc.E06-07-0593

Wikonkal, N. M., Remenyik, E., Knezevic, D., Zhang, W., Liu, M., Zhao, H., Berton, T. R., Johnson, D. G., & Brash, D. E. (2003). Inactivating E2f1 reverts apoptosis resistance and cancer sensitivity in Trp53-deficient mice. *Nature Cell Biology*, *5*(7), Article 7. https://doi.org/10.1038/ncb1001

Wu, D., Hu, D., Chen, H., Shi, G., Fetahu, I. S., Wu, F., Rabidou, K., Fang, R., Tan, L., Xu, S., Liu, H., Argueta, C., Zhang, L., Mao, F., Yan, G., Chen, J., Dong, Z., Lv, R., Xu, Y., … Shi, Y. G. (2018). Glucose-regulated phosphorylation of TET2 by AMPK reveals a pathway linking diabetes to cancer. *Nature*, *559*(7715), 637–641. https://doi.org/10.1038/s41586-018-0350-5

Wu, S., Yin, X., Fang, X., Zheng, J., Li, L., Liu, X., & Chu, L. (2015). C-MYC responds to glucose deprivation in a cell-type-dependent manner. *Cell Death Discovery*, *1*, 15057. https://doi.org/10.1038/cddiscovery.2015.57

Xu, X., Page, J. L., Surtees, J. A., Liu, H., Lagedrost, S., Lu, Y., Bronson, R., Alani, E., Nikitin, A. Y., & Weiss, R. S. (2008). Broad Overexpression of Ribonucleotide Reductase Genes in Mice Specifically Induces Lung Neoplasms. *Cancer Research*, *68*(8), 2652–2660. https://doi.org/10.1158/0008-5472.CAN-07-5873

Yamaguchi, T., Matsuda, K., Sagiya, Y., Iwadate, M., Fujino, M. A., Nakamura, Y., & Arakawa, H. (2001). P53R2-dependent Pathway for DNA Synthesis in a p53-regulated Cell Cycle Checkpoint1. *Cancer Research*, *61*(22), 8256–8262.

Yang, W., Xia, Y., Hawke, D., Li, X., Liang, J., Xing, D., Aldape, K., Hunter, T., Alfred Yung, W. K., & Lu, Z. (2012). PKM2 phosphorylates histone H3 and promotes gene transcription and tumorigenesis. *Cell*, *150*(4), 685–696. https://doi.org/10.1016/j.cell.2012.07.018

Ying, H., Kimmelman, A. C., Lyssiotis, C. A., Hua, S., Chu, G. C., Fletcher-Sananikone, E., Locasale, J. W., Son, J., Zhang, H., Coloff, J. L., Yan, H., Wang, W., Chen, S., Viale, A., Zheng, H., Paik, J., Lim, C., Guimaraes, A. R., Martin, E. S., … DePinho, R. A. (2012). Oncogenic Kras Maintains Pancreatic Tumors through Regulation of Anabolic Glucose Metabolism. *Cell*, *149*(3), 656–670. https://doi.org/10.1016/j.cell.2012.01.058

Yun, J., Rago, C., Cheong, I., Pagliarini, R., Angenendt, P., Rajagopalan, H., Schmidt, K., Willson, J. K. V., Markowitz, S., Zhou, S., Diaz, L. A., Velculescu, V. E., Lengauer, C., Kinzler, K. W., Vogelstein, B., & Papadopoulos, N. (2009). Glucose Deprivation Contributes to the Development of KRAS Pathway Mutations in Tumor Cells. *Science*, *325*(5947), 1555–1559. https://doi.org/10.1126/science.1174229

Yuneva, M. O., Fan, T. W. M., Allen, T. D., Higashi, R. M., Ferraris, D. V., Tsukamoto, T., Matés, J. M., Alonso, F. J., Wang, C., Seo, Y., Chen, X., & Bishop, J. M. (2012). The Metabolic Profile of Tumors Depends on both the Responsible Genetic Lesion and Tissue Type. *Cell Metabolism*, *15*(2), 157–170. https://doi.org/10.1016/j.cmet.2011.12.015

Zhang, C., Liu, J., Liang, Y., Wu, R., Zhao, Y., Hong, X., Lin, M., Yu, H., Liu, L., Levine, A. J., Hu, W., & Feng, Z. (2013). Tumour-associated mutant p53 drives the Warburg effect. *Nature Communications*, *4*(1), Article 1. https://doi.org/10.1038/ncomms3935

Zhang, C.-S., Hawley, S. A., Zong, Y., Li, M., Wang, Z., Gray, A., Ma, T., Cui, J., Feng, J.-W., Zhu, M., Wu, Y.-Q., Li, T. Y., Ye, Z., Lin, S.-Y., Yin, H., Piao, H.-L., Hardie, D. G., & Lin, S.-C. (2017). Fructose-1,6-bisphosphate and aldolase mediate glucose sensing by AMPK. *Nature*, *548*(7665), Article 7665. https://doi.org/10.1038/nature23275

Zhang, K., Hu, S., Wu, J., Chen, L., Lu, J., Wang, X., Liu, X., Zhou, B., & Yen, Y. (2009). Overexpression of RRM2 decreases thrombspondin-1 and increases VEGF production in human cancer cells in vitro and in vivo: Implication of RRM2 in angiogenesis. *Molecular Cancer*, *8*, 11. https://doi.org/10.1186/1476-4598-8-11

Zhao, J., Ramos, R., & Demma, M. (2013). CDK8 regulates E2F1 transcriptional activity through S375 phosphorylation. *Oncogene*, *32*(30), Article 30. https://doi.org/10.1038/onc.2012.364

Zheng, Z., Chen, T., Li, X., Haura, E., Sharma, A., & Bepler, G. (2007). DNA Synthesis and Repair Genes RRM1 and ERCC1 in Lung Cancer. *New England Journal of Medicine*, *356*(8), 800–808. https://doi.org/10.1056/NEJMoa065411

Zhou, B., Liu, X., Mo, X., Xue, L., Darwish, D., Qiu, W., Shih, J., Hwu, E. B., Luh, F., & Yen, Y. (2003). The Human Ribonucleotide Reductase Subunit hRRM2 Complements p53R2 in Response to UV-Induced DNA Repair in Cells with Mutant p531. *Cancer Research*, *63*(20), 6583–6594.

Zhu, J., & Thompson, C. B. (2019). Metabolic regulation of cell growth and proliferation. *Nature Reviews Molecular Cell Biology*, *20*(7), 436–450. https://doi.org/10.1038/s41580-019-0123-5

1.9 Figures and Tables

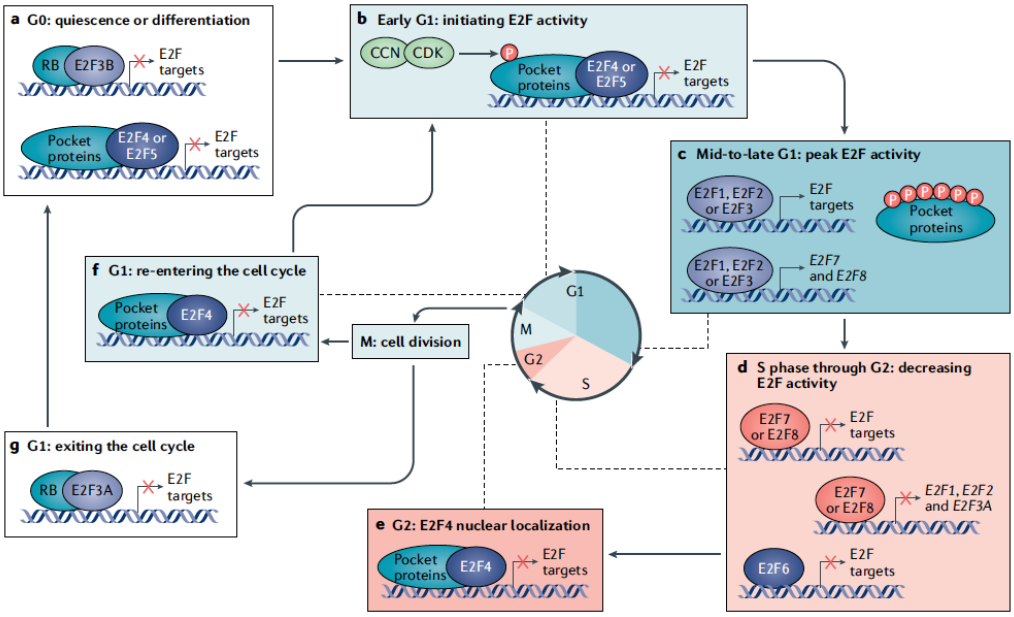

Figure 1.1 Model of E2F regulation and activity throughout the cell cycle. Data obtained from Kent & Leone, 2019.

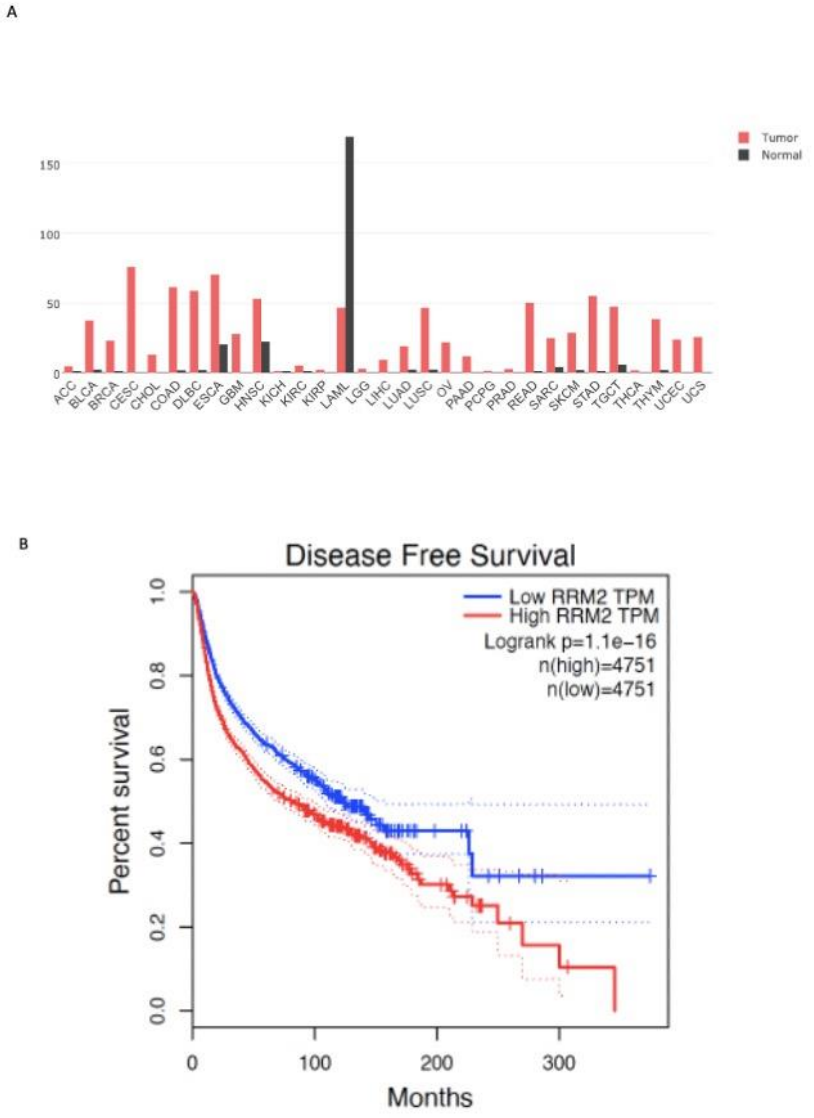

Figure 1.2 RRM2 is overexpressed in multiple cancer types and correlated with decreased disease free survival. (A) RRM2 gene expression profile across multiple tumor samples and paired normal tissues. The height of bar represents the median expression in the the tumor type or normal tissue. (B) Kaplan-Meier curve displays the disease free survivial for cancer patients with either low RRM2 or high RRM2 mRNA expression levels. All samples are collected from TCGA/GTEx datasets and analytic data were generated from GEPIA 2021 (C. Li et al., 2021).

Table1.1 Hazard ratios for cancer incidence using the entire cohort and then restricting diabetes patients to those with < 1 year since diagnosis (mean duration 4 months). HRs are relative to age, sex and county-matched controls in each case. Model adjusted for sex, education, income and marital status. (Data adapted from Bjornsdottir et al., 2020)

	All diabetes	Newly diagnosed (<1 year)	
Most common cancers			
All cancer	1.10 (1.09-1.12)	All cancer	1.22 (1.17- 1.27)
Breast	1.05 (1.01- 1.09)	Breast	1.12 (1.02- 1.23)
Lung	1.01 (0.97- 1.05)	Lung	1.18 (1.04- 1.34)
Prostate	0.82 (0.80- 0.83)	Prostate	0.80 (0.70- 0.90)
Colorectal	1.20 (1.16- 1.23)	Colorectal	1.30 (1.18- 1.43)
Most associated cancers			
Liver	3.31 (3.07- 3.58)	Liver	2.36 (1.74- 3.20)
Pancreas	2.19 (2.06- 2.32)	Pancreas	2.72 (2.28- 3.25)
Corpus uteri	1.78 (1.68- 1.88)	Corpus uteri	1.68 (1.44- 1.96)
Gallbladder	1.32 (1.13- 1.54)	Gallbladder	1.55 (1.02- 2.37)
Kidney	1.45 (1.36- 1.54)	Kidney	1.78 (1.45- 2.19)
Penis	1.56 (1.27- 1.91)	Penis	1.96 (0.77- 4.99)
Stomach	1.21 (1.13- 1.30)	Stomach	1.37 (1.06- 1.77)
Bladder	1.20 (1.15- 1.25)	Bladder	1.15 (0.96- 1.37)
Colorectal	1.20 (1.16- 1.23)	Colorectal	1.30 (1.18- 1.43)

Chapter 2

Hyperglycemia promotes DNA synthesis and cell growth through Rb1/E2F signaling in cancer cells

Chapter 2 is intended to contribute to a publication.

2.1 Abstract

While epidemiological studies have shed light on the association between hyperglycemia and an escalated cancer risk, our comprehension of the underlying molecular mechanism remains limited. This study serves to address this gap by unveiling a mechanism through which high glucose levels (HG) drive DNA replication, consequently fueling tumor cell proliferation, as substantiated by comprehensive genome-wide analyses. Notably, we identify E2F-mediated transcriptomic alteration as a pivotal switch orchestrating the cells' adaptive response to HG. Crucially, inhibition E2F effectively annuls the HG-induced DNA synthesis and cellular growth, reinforcing the important role of E2F in this cascade. E2F1, a thoroughly studied member of the E2F family, also exhibits a curbing effect on the HG-induced activation of DNA synthesis and cellular proliferation. Furthermore, we illustrate that HG enhances the phosphorylation of Rb1, contributing to the E2F1 activation. Intriguingly, within the cohort of E2F1 target genes spurred by HG, RRM2 emerges as a significant participant in nucleotide synthesis, enabling the generation of the indispensable dNTP essential for DNA replication. Noteworthy, our study reveals that HG fosters elevated intracellular dNTP levels in an E2F1-RRM2-dependent manner, aligning with augmented DNA synthesis and the resultant growth of cancer cells. Collectively, our findings decipher a Rb1-E2F1-RRM2 dependent nexus connecting hyperglycemia with cancer cell proliferation, thus elucidating the molecular blueprint by which hyperglycemia propels tumor cells towards increased DNA synthesis.

2.2 Introduction

Cancer stands as the second leading cause of global mortality, contributing to 1 out of 6 deaths (WHO, 2022). It is distinguished by uncontrolled cell proliferation, with sustained proliferative signaling pathways serving as a timeless and quintessential hallmark (Hanahan, 2022; Hanahan & Weinberg, 2000, 2011). An integrated analysis conducted by The Cancer Genome Atlas (TCGA) has validated the presence of 10 canonical signaling pathways scanning various cancer types. These encompass cell cycle, Hippo signaling, Myc signaling, Notch signaling, Nrf2 signaling, PI3K signaling, MAPK signaling, TGF-β signaling, p53 and β-catenin/Wnt signaling (Sanchez-Vega et al., 2018). These curated pathways can function autonomously or manifest cross-interactions in tumor cells in response to dynamic extrinsic and/or intrinsic cues (Sanchez-Vega et al., 2018). In numerous instances, transcription factors (TFs) emerge as pivotal mediators for modified proliferative signaling pathways through transcriptional regulation. Ultimately, these altered signaling cascades culminate in the process of DNA replication and cell cycle progression, fostering excessive cell proliferation.

Diabetes mellitus comprises a cluster of metabolic disorders brought about by the dysregulation of glucose metabolism, resulting in hyperglycemia. It is categorized into two primary types: type 1 (T1DM) and type 2 (T2DM), both of which have been associated with increased risks of neoplasm occurrence and mortality (Gordon-Dseagu et al., 2013; Szablewski, 2014; Wang et al., 2020). Glucose serves as an important source of nutrients for cell survival, particularly for the rapidly proliferating tumor cells (Palm & Thompson, 2017). In fact, the elevation of fasting plasma glucose level has emerged as a

leading risk factor for increased cancer burden in the past decade (Tran et al., 2022). Notably, hyperglycemia has gained widespread recognition as a critical biological link between diabetes and oncogenesis, primarily due to the Warburg effect: a phenomenon wherein tumor cells exhibit a higher reliance on glycolysis to continuously generate ATP energy molecules (Giovannucci et al., 2010c, 2010a; Szablewski, 2014; Warburg, 1956). Furthermore, hyperglycemia can exert an inhibitory impact on the response of cancer cells to chemotherapy by the interference of apoptotic pathways (Gerards et al., 2017). Beyond its direct effect on the cancer cells, elevated glucose levels can sustain an uncontrolled and persistent chronic inflammatory milieu, fostering a tumor-favorable microenvironment conducive to tumor development and metastasis (S.-C. Chang & Yang, 2016). While the influence of hyperglycemia on cancer cells has been a subject of study, a comprehensive understanding of the molecular pathway through which hyperglycemia triggers cancer growth still remains elusive.

To comprehensively explore and elucidate the underlying molecular mechanism in this process, we employed a systemic approach through high throughput RNA-seq analysis. Our data revealed that the pivotal role of the core transcriptional regulator, the E2F family, in steering cancer cells towards DNA synthesis and cell proliferation under elevated glucose conditions. Moreover, we established that heightened glucose levels trigger the phosphorylation of Rb1, resulting in the activation of E2F1 and the consequent transcriptional activation of downstream DNA replication genes. Interestingly, among the E2F1 target genes induced by elevated glucose, RRM2 was identified as a participant in nucleotide synthesis, generating essential dNTPs crucial for DNA replication. Our

findings strongly suggested that hyperglycemia instigates an RRM2-dependent elevation of intracellular dNTP levels, closely associated with DNA synthesis and the ensuing growth of cancer cells. Collectively, our study uncovers a novel molecular mechanism by which elevated glucose levels enhance cell growth and sheds light on the significance of the Rb1/E2F cell cycle signaling axis in individuals grappling with the dual challenge of tumors and diabetes.

2.3 Results

2.3a Elevated glucose levels prompt DNA synthesis and cell growth in cancer cells

To elucidate the molecular mechanism underlying cell proliferation induced by HG, we performed an RNA-Seq analysis in HG-treated colon cancer cell line HCT116. In the context of HG condition, the differential expression analysis revealed a total of 1705 mRNA transcripts that were upregulated, while 1316 downregulated mRNA transcripts. Specifically, 1150 genes exhibited an increase in expression with a significant fold change (FC) greater than 1.5, and 975 genes showed a significant 50% reduction in expression in cells treated with HG (Fig. 1A). Furthermore, employing Gene Set Enrichment Analysis (GSEA), we identified the top two enriched RACTOME pathways as cell cycle checkpoints and DNA synthesis in response to HG treatment (Fig. 1B, 1C). Notably, this trend was also consistent when performing Gene Ontology (GO) analysis on the upregulated genes in HG-treated cells, revealing significant enrichment in DNA replication (Fig. S1A). These genes of interest are indicated on the volcano plot (Fig. 1A) and are detailed in Table 1. Conversely, GO analysis of the downregulated genes

highlighted a cellular response to glucose starvation (Fig. S1B). Building upon the insights from the gene expression profile analyses, we hypothesized that, upon HG treatment, cancer cells undergo direct changes in transcription, potentially propelling them towards DNA synthesis to facilitate cell cycle progressions and subsequent proliferation.

We further investigate the impact of HG on cell cycle by gauging the proportion of cells engaged in DNA synthesis, utilizing the 5-ethynyl-2′-deoxyuridine (EdU) incorporation assay. The results show a discernible increase in the percentage of HCT116 cells in the S phase, both at the 6 h and 24 h time points following HG treatment, in contrast to the 5mM glucose control (Mock) condition (Fig. 1D). Additionally, through a cell proliferation analysis, it is evident that cells subjected to HG exhibit a growth advantage when compared to their counterparts in the control conditions (Fig. 1E). In our pursuit of direct evidence indicating enhanced DNA synthesis activity in HG-treated cells, we utilized the DNA fiber assay to determine the speed of replication forks during the replication process. The results show an accelerated replication fork speed during active replication under HG treatment (Fig. 1E). To reinforce the notion that HG-induced phenotype is not exclusive to HCT116 cells, we extended our investigation to another cell line, H460, derived from lung cancer. The results substantiate that HG confers similar enhancing effects on DNA synthesis and cell proliferation in H460 cells as observed in HCT116 cells (Supplementary Fig. 1C-E). This strongly implies that the effects of HG are consistent across different tissue types. Together, these findings provide conclusive

evidence supporting the role of hyperglycemia in driving cell cycle progression and promoting cell proliferation.

2.3b E2F plays a crucial role in high glucose-induced DNA synthesis and cell growth in cancer cells

Subsequently, we performed GSEA analysis to uncover the pivotal transcription factors accountable for the cellular adaption induced by HG. Our findings showed a notable enrichment of E2F gene sets among the top hits (Fig. 2A, Table 2). The E2F family, encompassing eight distinct members designated as E2F1-8, with E2F1 being extensively investigated, was prominently featured. This prompted our hypothesis that E2F1 is implicated in the transcriptional program regulated by HG. To validate the role of E2F1 in facilitating HG-induced DNA synthesis and cell proliferation, we employed lentivirus-mediated RNAi strategy to silence E2F1 expression. Our results unequivocally demonstrated a significant reduction in HG-induced cells progressing into the S phase following E2F1 inhibition (Fig. 2B). This result was also replicated in E2F1-depleted HCT116 cells (Fig. S2A). Importantly, the increased DNA replication fork speed and cellular growth spurred by HG were significantly curtailed upon E2F1 knockdown in H460 cells (Fig. 2C, 2D). Noteworthy, E2F1 knockdown in isolation, when compared to controls, also led to a higher proportion of cells with EdU incorporation in the S phase (Fig. 2B), alongside an escalated pace of DNA replication fork movement (Fig. 2C). Considering that the activating E2F family members (E2F1-3) have been recognized to possess extensive functional overlap and redundancy, it is conceivable that other

members of the E2F family might counterbalance the effects of E2F1 knockdown, resulting in increased cells in the S phase and augmented DNA synthesis. To produce a broad inhibitory impact across the E2F family, we employed a pan-E2F inhibitor named HLM006474, known to impede the chromatin accessibility of E2F family members in cells (Y. Ma et al., 2008). Strikingly, HLM006474 abrogated the entry of HCT116 and H460 cells entering into the S phase, both in the presence and absence of HG (Fig. 2E, Fig. S2B, S2C). Likewise, a remarkable arrest in DNA replication fork progression was evident in cells treated with HLM006474 (Fig. 2F). Taken together, these results collectively underscore the pivotal role of E2F in driving DNA synthesis and cellular proliferation in response to HG treatment.

2.3c Elevate glucose levels induce E2F1-dependent transactivation through Rb1 phosphorylation

To further validate E2F1-mediated transcriptomic modifications in genes associated with DNA synthesis and replication, we selected seven identified DNA replication-associated genes identified from the GSEA data (Table 1, Fig. 1A). Illustrated in Figure 3A, the mRNA levels of RRM2, CHAF1A, CHAF1B, PCNA, CCNE2, CLSPN and RBM14 were significantly elevated in response to HG, in contrast to control conditions. Strikingly, the knockdown of E2F1, effectively attenuated these HG-induced enhancements. Importantly, E2F1 silencing also curbed the increased protein levels of RRM2 and CHAF1A (chromatin assembly factor 1 subunit A) protein levels mediated by HG (Fig. 3B), implying a functional link in this regulation. Moreover, our investigations

revealed that treatment with the pan-E2F inhibitor HLM006474 led to blockade in the upregulation of mRNA and protein levels of DNA replication genes induced by HG (Fig. 3C-D & Fig. S3A). Correspondingly, the overexpression of E2F1 consistently upregulated the mRNA and protein levels of the DNA replication genes and counteracted the HG-mediated upregulation in cells (Fig. S3B-C). These findings collectively indicate that E2F1 operates as a pivotal transcription factor, orchestrating the upregulation of DNA replication genes following exposure to HG.

Several groups have documented E2F1's binding on the RRM2 promoter, resulting in the activation of its transcription (Fang et al., 2015; Mazzu et al., 2018; Rasmussen et al., 2016). In light of these findings, we carried out ChIP analysis to probe whether elevated glucose levels influence E2F1's capacity to bind to promoter DNA segments. Our assay verified E2F1's presence on both the RRM2 and PCNA promoters (Fig. 3E-F). Significantly, exposure of cells to HG substantially amplified the binding affinity of E2F1 to these promoters (Fig. 3E-F). Together, these results imply that elevated glucose levels regulate genes that facilitate DNA replication through E2F1-mediated transactivation.

Interestingly, a previous study has proposed exposure of cells to HG triggers hyper-phosphorylation of Rb1 by CKD4 in murine pancreatic cells (Annicotte et al., 2009). Rb1 is a substrate for phosphorylation by CDKs during the G1 phase of the cell cycle. Once hyper-phosphorylated, Rb1 alleviates the suppression of E2F1, resulting in the activation of E2F1-dependent transcription (Dyson, 2016). To investigate the role of Rb1 phosphorylation in HG-mediated E2F1 transactivation within cancer cells, our initial

approach involved treating the cells with HG and assessing Rb1 phosphorylation levels utilizing a phosphor Ser807/Ser811-specific antibody. As shown in Figure 4A, we distinctly observed escalated Rb1 phosphorylation subsequent to HG treatment in HCT116 cells. Concurrently, this phenomenon was accompanied by the activation of DNA replication genes regulated by E2F1 (Fig. 4A-B, Fig. S4A). However, when we subjected U2OS cells, an osteosarcoma cell line that inherently possess higher basal Rb1 phosphorylation levels, to HG, we did not observe further enhancement of Rb1 phosphorylation (Fig. 4A). Importantly, compared to HG-treated HCT116 cells, the application of HG to U2OS cells also failed to induce the upregulation of DNA replication genes. As a result, the cells lacked the ability to stimulate DNA synthesis and promote cell growth (Fig. 4A-D, Fig. S4A). To affirm the crucial role of Rb1 phosphorylation in HG condition, we treated HCT116 cells with the CDK2/4/6 inhibitor PF-3600 and convincingly demonstrated that inhibition of Rb1 phosphorylation also blocked HG-induced elevation of DNA replication genes (Fig. 4E-F, Fig. S4B) (Freeman-Cook et al., 2021). Collectively, these results strongly suggest that elevated glucose levels upregulate DNA replication genes through the Rb1-E2F signaling pathway.

2.3d Regulation of intracellular dNTP levels by HG is dependent on the E2F1-RRM2 axis

The role of RRM2 as a proto-oncogene has been widely recognized recently. RRM2 serves as a vital component in the holoenzyme RNR, playing a critical role in the reduction of the 2’ carbon of NDP to synthesize dNDP, a pivotal and rate-limiting step in

the DNA *de novo* pathway. Building on our prior finding that HG induces an elevation in both RRM2 mRNA and protein levels, we were motivated to investigate its involvement in regulating intracellular dNTPs following HG treatment. Employing a previously established PCR-based methodology, HG treatment remarkably resulted in a rapid and pronounced increase of all four dNTP levels in the cells (Fig. 5A). In order to elucidate the role of RRM2 in the HG-induced increase of dNTP levels, we subjected the cells to treatment with the RNR inhibitor Triapine at two different concentrations, 250 nM or 500 nM. This intervention led to diminished intracellular dATP and dGTP levels under both conditions. While the Triapine treatment also exerted a diminished effect on intracellular dCTP and dTTP levels, the impact was relatively milder (Fig. 5A), consistent with findings from a previous study (Z. P. Lin et al., 2011). Significantly, inhibition of RNR unequivocally impeded HG-triggered DNA replication fork progression (Fig. 5B). Finally, we confirmed the involvement of E2F1 in HG-induced upregulation of dNTPs. As shown in Fig. 5C, administration of the pan-E2F inhibitor HLM006474 distinctly hindered the increase of dATP and dGTP levels following HG treatment (Fig. 5C). Together, these results strongly support the notion that elevated glucose levels enhanced dNTP levels through the activation of E2F1-RRM2 axis.

2.3e Inhibitions of E2F1-RRM2 axis alleviates HG-induced tumor 3D spheroid growth

We further investigated the contribution of the E2F1-RRM2 axis to cancer cell growth in response to HG treatment. To better replicate the *in vivo* environment, we

established a short-term three-dimensional (3D) tumor spheroid culture, allowing cells to assemble into spheroid-like round or spherical structures for observation (Zoetemelk et al., 2019). Notably, upon HG treatment, a discernible enlargement in the spheroid size was observed, indicative of enhanced cell growth in comparison to non-HG-treated spheroids (Fig. 6A, 6C & 6E, Table S2-4). In further validation of cell growth potential, we assessed overall cell viability of the entire spheroids in the 3D culture following HG treatment. These results provide additional reinforcement to the discovery that elevated glucose steer cells towards faster proliferation.

To probe the role of E2F in HG-induced spheroid growth, we unitized the pan-E2F inhibitor HLM006474. Remarkably, its application effectively suppressed 3D cell viability and restrained spheroid growth size in the presence of HG treatment (Fig. 6A-B). Subsequently, we employed a lentivirus-mediated RNAi approach to knock down E2F1. The result revealed that, compared to scramble controls, the HG-induced increase in spheroid growth was effectively hindered upon E2F1 inhibition (Fig. 6C). Moreover, the elevated cell viability of total spheroids within the 3D cultures, triggered by HG treatment, was notably diminished in E2F1 knockdown cells (Fig. 6D).

Turning our attention to the role of RRM2 in HG-induced spheroid growth, we employed the RNR inhibitor Triapine to treat cells. As depicted in Fig. 6E, the promotion of spheroid growth induced by HG was indeed blocked upon RNR inhibition. As anticipated, the escalated cell viability of total spheroids in the 3D cultures, incited by HG, was also effectively blocked by inhibiting RRM2 (Fig. 6F). Taken together, these

findings distinctly established that the elevated glucose levels promote cancer cell growth through the activation of E2F1-RRM2 pathway.

2.4 Discussion

Diabetes mellitus and cancer exert substantial impacts on global human health (Giovannucci et al., 2010). Epidemiological investigations reveal that T1DM displays a modest association, and T2DM exhibits a comparatively stronger link with cancer risks (Gordon-Dseagu et al., 2013; Wang et al., 2020). Within this context, hyperglycemia has emerged as a key biological bridge connecting these two conditions. Nonetheless, despite its significance, no comprehensive study has explored the direct effects of hyperglycemia on cancer cells. In this study, we have identified E2F family as the core transcriptional regulator involved in guiding cells towards DNA replication and cell proliferation under elevated glucose conditions. Notably, among the E2F1 target genes induced by elevated glucose levels, our findings highlight the activation of RRM2, which in turn drives upregulation of intracellular dNTP levels. This elevation plays a pivotal role in DNA synthesis and consequent cancer cell growth. Taken together, our findings cast light upon the molecular mechanism through which hyperglycemia fosters cancer cell proliferation.

E2F transcription factor family serves as downstream effectors of the tumor suppressor Rb1, playing a pivotal role in governing the progression of cell cycle. E2F1, an extensively studied E2F family member, participates in cellular processes extending beyond the cell cycle, encompassing apoptosis, differentiation and development. Nonetheless, the involvement of E2F1 in guiding cancer cells towards proliferation under

the influence of HG remains relatively unexplored. By the analysis of transcriptomic profiling of cells treated with HG, a significant signature linked to DNA synthesis emerges, directly associated with metabolic process (Fig. 1B, 1C). Furthermore, the result of GSEA analysis suggest that hyperglycemia potentially redirects cancer cells towards DNA replication via E2F1-mediated transcription. Interestingly, this notion finds support in the observation of altered levels of DNA replication genes in fin tissues of a diabetic zebrafish model (Leontovich et al., 2016). Furthermore, the inhibition of GLUT1, a key rate-limiting factor for glucose uptake, has been shown to impede the growth of Rb1-postivie triple-negative breast cancer (TNBC) (Q. Wu et al., 2020). Notably, pathway enrichment analysis of gene expression data also points to the contribution of E2F1 pathway in this process. Together, these results highly imply a HG-regulated Rb1-E2F1 axis in cancer cells. It is indeed intriguing to further assess its significance in Rb1-positive cancer patients.

Emerging evidence has underscored that RRM2, the small subunit of RNR, holds considerable significance as a proto-oncogene and a potential target for cancer therapy (Aye et al., 2015). Its relevance is deeply rooted in its role within DNA replication, tied to its central function in governing dNTP levels. Across various cancer types, RRM2 expression exhibits elevation, with its levels intricately correlated with tumor grades (Aird et al., 2014; Aye et al., 2015). Interestingly, RRM2 has been established as a direct transcriptional target of several transcription factors, including E2F1 (Fang et al., 2015; Rasmussen et al., 2016). Herein, our results, demonstrating the transcriptional activation of RRM2 by E2F1 following HG treatment, forge a fresh connection between diabetes

and cancer. This potentially unveils a novel avenue for targeted cancer therapy tailored to diabetic patients. It is pertinent to mention that the RNR inhibitor Triapine, employed in our study, is currently undergoing clinical trials. Triapine has exhibited the capacity to enhance the sensitivity of cervical cancer to chemotherapy and radiation therapy (Kunos et al., 2010, 2013). Our data, showing the inhibition of HG-induced DNA replication fork through Triapine treatment, further bolsters its potential application in targeted cancer therapy for diabetic patients.

Together, our data put forth a model elucidating how cancer cells adapt to hyperglycemia, shedding light on the molecular mechanism wherein E2F1 assumes the central role for transcriptional regulation, orchestrating the transcriptional levels of downstream DNA replication genes. This orchestration effectively promotes DNA synthesis and drives cellular proliferation (Fig. 7).

2.5 Materials and Methods

Cell culture, reagents, and treatments

HCT116 and U2OS cells were cultured in Dulbecco's Modified Eagle Medium (DMEM) normal glucose (1g/L) supplemented with 10% FBS and 100X penicillin-streptomycin solution. H460 cells were cultured in RPMI 1640 supplemented with 10% FBS and 100X penicillin-streptomycin solution. HEK293T cells were cultured in DMEM high glucose (4.5g/L) supplemented with 10% heat inactivated FBS and 100X penicillin-streptomycin solution. For HG treatments, 25mM glucose (#BM-675, Boston BioProducts) was added into the complete medium for HCT116 and U2OS cells for 6 hrs

or as indicated. H460 cells were cultured in glucose (-) RPMI 1640 supplemented with 10% FBS and 100X penicillin-streptomycin solution and 5 mM (Mock) or 25 mM (HG) glucose. To inhibit E2F activity, cells were treated with 40 μM pan-E2F inhibitor HLM006474 (#SML1260, Sigma-Aldrich) for 9 hrs (Y. Ma et al., 2008). To inhibit RRM2 activity, HCT116 cells were treated with Triapine (#57470, Selleck Chemicals) as the indicated time points and concentrations (Gandhi et al., 2020; Lin et al., 2011). PF-3600 (#35502, Cayman Chemical) was employed to inhibit the phosphorylation of Rb1_S807/S811 at the dose of 1μM and the indicated time points in HCT116 cells (Freeman-Cook et al., 2021). Cell transfection was performed with Lipofectamine 3000 (#L3000008, Thermo Fisher Scientific) according to the manufacturer's instructions.

SDS-PAGE and western blot

Whole cell protein lysate was separated on 10% SDS-polyacrylamide gels and then transferred to nitrocellulose membrane (#10600011, GE Healthcare). The membranes were blocked with 5% nonfat dry milk in TBS with 0.1% Tween-20 (#BP337-500, Fisher Scientific) (TBST), followed by being incubated overnight at 4 °C with primary antibody diluted 1:1,000- 10,000 in 1% non-fat dry milk in TBST. The following antibodies were used for IB: anti-Vinculin (V9131, Sigma-Aldrich), anti-RRM2 (sc-398294, Santa Cruz), anti-E2F1 (sc-251, Santa Cruz), anti-CHAF1A (sc-133105, Santa Cruz), anti-Rb1 (#9309, Cell Signaling Technology), anti-phospho Rb1 (S807/S811) (#8516, Cell Signaling Technology) and anti-β-actin (A3854, Millipore Sigma).

RNA isolation and RT-qPCR

RNA was extracted with the TRIzol reagent (#15596018, Invitrogen) and then reverse-transcribed with the reverse transcription supermix (#1708841, Bio-Rad) according to the manufactures' protocols. qPCR was performed using the SYBR supermix (#1708882, Bio-Rad) in the Bio-Rad CFX cycler with CFX Maestro software. Primers for qPCR are listed in Supplementary Table 1. Results of mRNA relative levels were calculated by $2^{-\Delta\Delta Ct}$ in normalization to the GAPDH or 18S and relative to the control samples. All PCR reactions were performed in technical triplicates.

shRNA-mediated knock down

E2F1-targeting and scramble shRNA (Supplementary Table 1) were cloned into pLKO.1 vector with puromycin selection marker. Lentivirus were produced by transfection of HEK 293T cells with the transfer plasmid and lentiviral packaging and VSVG plasmids. The virus was harvested 48 h post-transfection. Cells were transduced with the lentivirus in the presence of 10 ug/ml polybrene (Millipore). After 48 h, transduced cells were selected with 1 μg/ml puromycin for 7 days.

RNA-seq and data analysis

Total RNA was isolated and purified from HCT116 cells in biological triplicates using Direct-zol RNA Miniprep Plus Kit (#R2070. Zymo Research) according to the supplier's instruction. RNA-seq libraries were then prepared following the manufacturer's protocol of NEBNext Ultra II Directional RNA Library Prep Kit for Illumina (#E7760S,

New England BioLabs). The sequencing was performed on Illumina NextSeq using single end 75bp read length. Sequencing reads were mapped to the human reference genome (GENCODE v34) using Salmon (Patro et al., 2017), followed by differential expression analysis using DESeq2 (Love et al., 2014). Gene set enrichment analysis (GSEA) (v4.2) was used to analyze the enrichment of REACTOME pathways and transcription factor targets among differentially expressed genes (Subramanian et al., 2005). Volcano plot was generated using ggplot2 (v3.4.0). GeneOntology biological process analysis was performed in ShinyGO (v0.75) (Ge et al., 2020).

Cell cycle analysis

Cell cycle analysis was performed by using the Click-iT Plus Edu Kit (#C10632, Thermo Fisher Scientific) according to the manufacturer's protocol. In brief, 2 million cells post-treatment were harvested and fixed in the fixation buffer. EdU was then labeled with Alexa Fluor 488 picolyl azide for 30 min at room temperature. After labeling, total DNA content was stained with 20 ng/ml PI (#P3566, Invitrogen) for 1 h at room temperature. Samples were then analyzed by flow cytometry on the NovoCyte platform (ACEA).

DNA fiber assay

Cells were pulse-labeled with 25 μM CIdU (#C6891, Sigma-Aldrich) for 20 min, followed by a second pulse of 250 μM IdU (#AC122350010, Fisher Scientific) for another 20 min. Cells were harvested, lysed and DNA spread on slides as previously

described (Halliwell et al., 2020). DNA fibers were further denatured in 2.5M HCl and blocked with 1% BSA in PBS with 0.1% Tween-20 (PBST) to reduce background. The labeled CIdU and IdU fibers were immunoblotted with the following primary antibodies (1:500 dilution) for 1 h at room temperature: rat monoclonal anti-BrdU antibody [BU1/75 (ICR1)] (#ab6326, Abcam) and mouse monoclonal anti-BrdU antibody (clone B44) (#BDB347580, Fisher Scientific). Secondary antibodies of Alexa Fluor 555 goat anti-rat IgG (#A21434, Thermo Fisher Scientific) and Alexa Fluor 488 F (ab′)2 goat anti−mouse IgG (#A-11017, Thermo Fisher Scientific) were used to at 1:500 dilution for 2 h at room temperature. Images of well spread DNA fibers were taken using Leica microscope with X 40 oil immersion objective. 100-150 well spread DNA fibers were collected for each condition. Double-labeled DNA fiber lengths were measured in Image J (v1.53k). The rate for DNA replication fork was estimated using the conversion of 2.59 kb/μm as described (Jackson & Pombo, 1998).

ChIP-qPCR

Cells were cross-linked in 1% formaldehyde (#F1635, Sigma-Aldrich) for 10 min at room temperature and followed by attenuation of 125 mM glycine. Nuclei were isolated in NP-40 cell lysis buffer (50 mM Tris pH 8, 150 mM NaCl, 1% NP40, 15 mM EDTA) for 20 min on ice and spun down 5000 rpm for 5 min at 4°C. Nuclei were then lysed in nuclear lysis buffer (50 mM Tris pH 8, 150 mM NaCl, 10 mM EDTA, 1% SDS) for 10 min on ice. Lysed nuclei were then subjected to sonication to generate ~300bp chromatin fragments by confirmation on agarose gel. Immunoprecipitation was continued

by incubating the sheared chromatin with E2F1 antibody (#3742, Cell Signaling) and IgG control (#2729, Cell Signaling) overnight at 4°C. Protein G beads (#10003D, Thermo Fisher Scientific) were added the following day and incubated on a rotator for 4 h at 4°C. Immunoprecipitated beads were then washed twice in low salt wash buffer (0.1% SDS, 1% Triton X-100, 2 mM EDTA, 20 mM Tris pH 8, 150 mM NaCl), high salt wash buffer (0.1% SDS, 1% Triton X-100, 2 mM EDTA, 20 mM Tris pH 8, 500 mM NaCl), LiCl wash buffer (0.25 M LiCl, 1% NP40, 1% deoxycholate, 1 mM EDTA, 10 mM Tris pH 8) and once in TE buffer (1 mM EDTA, 10 mM Tris pH 8) and finally eluted in elution buffer (1% SDS, 0.1 M $NaHCO_3$). The eluted immunoprecipitations and previously saved input samples were reverse cross-linked in a 65°C water bath overnight. Reverse cross-linked DNA was isolated by using PCR purification kit (#28104, Qiangen).

ChIP-qPCR was performed using the SYBR supermix (#1708841, Bio-Rad) in the Bio-Rad CFX cycler with CFX Maestro software. Primers for ChIP-qPCR are listed in Supplementary Table 1. 1% of starting chromatin was used as input and technical triplicates were performed. The ChIP-qPCR data was analyzed with the Percent Input Method including normalization for both IgG levels and input chromatin going into the ChIP.

Cell growth curve

Cell growth curves were performed by counting cell numbers with hemocytometers. Trypan blue was used to stain dead cells. Briefly, cells were seeded at

$2*10^4$ cells per well in a 24-well plate. At each time point, cells were trypsinized and counted on the automated cell counter (Thermo Fisher Scientific).

3D cell growth

Cells were seeded at 2000 cells per well in a 96-well U-bottom plates (#353077, Corning). The 3D cell culture media was a mixture of the complete media for 2D cell culture supplemented with 10% Matrix (#A1413201, Thermo Fisher Scientific). On day 6, sphere colonies were firstly observed under microscope and images were taken using Leica microscope with X 5 bright field objective. The length and width for each spheroid were measured in Image J (v1.53k). The viability for spheroids was determined by CellTiter-Glo® 3D Cell Viability Assay Kit (#G9681, Promega). Briefly, 100 μl CellTiter-Glo® 3D Reagent was added into the wells to be determined, followed by shaking for 5 min. After incubation at room temperature for 25 min, the plate was read on the luminometer plate reader (Promega). The luminescence signals were measured and collected for evaluating the 3D cell growth viability.

Intracellular dNTPs measurement

Intracellular dNTP levels were determined as previously described (Purhonen et al., 2020). Briefly, cell pellets were resuspended in 60% methanol (#A452-4, Fisher Scientific) and then incubated at 95°C for 3 mins. The supernatant was collected after centrifugation and transferred into the Amicon Ultra-0.5ml centrifugal filter (#UFC500396, Millipore) for centrifugation again. After centrifugation, the flow through

was saved and dried using Speed-Vac. The dried pellet was dissolved in 300 µl of sterile water and stored at -80°C. Determination of dNTP levels were performed by following the PCR based assay as previously described (Purhonen et al., 2020).

Statistical analysis

All the data are represented as mean ± SD. All the statistical tests were done by using Graphpad Prism 9 as recommendations based on the imported data types. P values were also generated in Graphpad Prism 9, with *P <0.05, **P <0.01, ***P <0.001, ****P <0.0001, ns represents non-significance.

2.6 References

Aird, K. M., Li, H., Xin, F., Konstantinopoulos, P. A., & Zhang, R. (2014). Identification of ribonucleotide reductase M2 as a potential target for pro-senescence therapy in epithelial ovarian cancer. *Cell Cycle*, *13*(2), 199–207. https://doi.org/10.4161/cc.26953

Annicotte, J.-S., Blanchet, E., Chavey, C., Iankova, I., Costes, S., Assou, S., Teyssier, J., Dalle, S., Sardet, C., & Fajas, L. (2009). The CDK4–pRB–E2F1 pathway controls insulin secretion. *Nature Cell Biology*, *11*(8), 1017–1023. https://doi.org/10.1038/ncb1915

Aye, Y., Li, M., Long, M. J. C., & Weiss, R. S. (2015). Ribonucleotide reductase and cancer: Biological mechanisms and targeted therapies. *Oncogene*, *34*(16), 2011–2021. https://doi.org/10.1038/onc.2014.155

Chang, S.-C., & Yang, W.-C. V. (2016). Hyperglycemia, tumorigenesis, and chronic inflammation. *Critical Reviews in Oncology/Hematology*, *108*, 146–153. https://doi.org/10.1016/j.critrevonc.2016.11.003

Dyson, N. J. (2016). RB1: A prototype tumor suppressor and an enigma. *Genes & Development*, *30*(13), 1492–1502. https://doi.org/10.1101/gad.282145.116

Fang, Z., Gong, C., Liu, H., Zhang, X., Mei, L., Song, M., Qiu, L., Luo, S., Zhu, Z., Zhang, R., Gu, H., & Chen, X. (2015). E2F1 promote the aggressiveness of human colorectal cancer by activating the ribonucleotide reductase small subunit M2. *Biochemical and Biophysical Research Communications*, *464*(2), 407–415. https://doi.org/10.1016/j.bbrc.2015.06.103

Freeman-Cook, K., Hoffman, R. L., Miller, N., Almaden, J., Chionis, J., Zhang, Q., Eisele, K., Liu, C., Zhang, C., Huser, N., Nguyen, L., Costa-Jones, C., Niessen, S., Carelli, J., Lapek, J., Weinrich, S. L., Wei, P., McMillan, E., Wilson, E., … Dann, S. G. (2021). Expanding control of the tumor cell cycle with a CDK2/4/6 inhibitor. *Cancer Cell*, *39*(10), 1404-1421.e11. https://doi.org/10.1016/j.ccell.2021.08.009

Ge, S. X., Jung, D., & Yao, R. (2020). ShinyGO: A graphical gene-set enrichment tool for animals and plants. *Bioinformatics*, *36*(8), 2628–2629. https://doi.org/10.1093/bioinformatics/btz931

Gerards, M. C., van der Velden, D. L., Baars, J. W., Brandjes, D. P. M., Hoekstra, J. B. L., Vriesendorp, T. M., & Gerdes, V. E. A. (2017). Impact of hyperglycemia on the efficacy of chemotherapy—A systematic review of preclinical studies. *Critical Reviews in Oncology/Hematology*, *113*, 235–241. https://doi.org/10.1016/j.critrevonc.2017.03.007

Giovannucci, E., Harlan, D. M., Archer, M. C., Bergenstal, R. M., Gapstur, S. M., Habel, L. A., Pollak, M., Regensteiner, J. G., & Yee, D. (2010). Diabetes and Cancer. *Diabetes Care*, *33*(7), 1674–1685. https://doi.org/10.2337/dc10-0666

Gordon-Dseagu, V. L. Z., Shelton, N., & Mindell, J. S. (2013). Epidemiological evidence of a relationship between type-1 diabetes mellitus and cancer: A review of the existing literature. *International Journal of Cancer*, *132*(3), 501–508. https://doi.org/10.1002/ijc.27703

Hanahan, D. (2022). Hallmarks of Cancer: New Dimensions. *Cancer Discovery*, *12*(1), 31–46. https://doi.org/10.1158/2159-8290.CD-21-1059

Hanahan, D., & Weinberg, R. A. (2000). The Hallmarks of Cancer. *Cell*, *100*(1), 57–70. https://doi.org/10.1016/S0092-8674(00)81683-9

Hanahan, D., & Weinberg, R. A. (2011). Hallmarks of Cancer: The Next Generation. *Cell*, *144*(5), 646–674. https://doi.org/10.1016/j.cell.2011.02.013

Jackson, D. A., & Pombo, A. (1998). Replicon clusters are stable units of chromosome structure: Evidence that nuclear organization contributes to the efficient activation and propagation of S phase in human cells. *The Journal of Cell Biology*, *140*(6), 1285–1295. https://doi.org/10.1083/jcb.140.6.1285

Kunos, C. A., Radivoyevitch, T., Waggoner, S., Debernardo, R., Zanotti, K., Resnick, K., Fusco, N., Adams, R., Redline, R., Faulhaber, P., & Dowlati, A. (2013). Radiochemotherapy plus 3-aminopyridine-2-carboxaldehyde thiosemicarbazone (3-AP, NSC #663249) in advanced-stage cervical and vaginal cancers. *Gynecologic Oncology*, *130*(1), 75–80. https://doi.org/10.1016/j.ygyno.2013.04.019

Kunos, C. A., Waggoner, S., von Gruenigen, V., Eldermire, E., Pink, J., Dowlati, A., & Kinsella, T. J. (2010). Phase I trial of pelvic radiation, weekly cisplatin, and 3-aminopyridine-2-carboxaldehyde thiosemicarbazone (3-AP, NSC #663249) for locally advanced cervical cancer. *Clinical Cancer Research : An Official Journal of the American Association for Cancer Research*, *16*(4), 1298. https://doi.org/10.1158/1078-0432.CCR-09-2469

Leontovich, A. A., Intine, R. V., & Sarras, M. P. (2016). Epigenetic Studies Point to DNA Replication/Repair Genes as a Basis for the Heritable Nature of Long Term Complications in Diabetes. *Journal of Diabetes Research*, *2016*, e2860780. https://doi.org/10.1155/2016/2860780

Lin, Z. P., Lee, Y., Lin, F., Belcourt, M. F., Li, P., Cory, J. G., Glazer, P. M., & Sartorelli, A. C. (2011). Reduced Level of Ribonucleotide Reductase R2 Subunits Increases Dependence on Homologous Recombination Repair of Cisplatin-Induced DNA Damage. *Molecular Pharmacology*, *80*(6), 1000–1012. https://doi.org/10.1124/mol.111.074708

Love, M. I., Huber, W., & Anders, S. (2014). Moderated estimation of fold change and dispersion for RNA-seq data with DESeq2. *Genome Biology*, *15*(12), 550. https://doi.org/10.1186/s13059-014-0550-8

Mazzu, Y. Z., Armenia, J., Chakraborty, G., Yoshikawa, Y., Gerke, T. A., Atiq, M. O., Stopsack, K. H., Komura, K., Lee, G.-S. M., Mucci, L. A., & Kantoff, P. W. (2018). Transcriptional and post-transcriptional regulation of ribonucleotide reductase (RRM2) control its oncogenic role in prostate cancer progression. *Journal of Clinical Oncology*, *36*(15_suppl), 5044–5044. https://doi.org/10.1200/JCO.2018.36.15_suppl.5044

Palm, W., & Thompson, C. B. (2017). Nutrient acquisition strategies of mammalian cells. *Nature*, *546*(7657), Article 7657. https://doi.org/10.1038/nature22379

Patro, R., Duggal, G., Love, M. I., Irizarry, R. A., & Kingsford, C. (2017). Salmon provides fast and bias-aware quantification of transcript expression. *Nature Methods*, *14*(4), Article 4. https://doi.org/10.1038/nmeth.4197

Purhonen, J., Banerjee, R., McDonald, A. E., Fellman, V., & Kallijärvi, J. (2020). A sensitive assay for dNTPs based on long synthetic oligonucleotides, EvaGreen dye and inhibitor-resistant high-fidelity DNA polymerase. *Nucleic Acids Research*, *48*(15), e87. https://doi.org/10.1093/nar/gkaa516

Rasmussen, R. D., Gajjar, M. K., Tuckova, L., Jensen, K. E., Maya-Mendoza, A., Holst, C. B., Møllgaard, K., Rasmussen, J. S., Brennum, J., Bartek, J., Syrucek, M., Sedlakova, E., Andersen, K. K., Frederiksen, M. H., Bartek, J., & Hamerlik, P. (2016). BRCA1-regulated RRM2 expression protects glioblastoma cells from endogenous replication stress and promotes tumorigenicity. *Nature Communications*, *7*(1), 13398. https://doi.org/10.1038/ncomms13398

Sanchez-Vega, F., Mina, M., Armenia, J., Chatila, W. K., Luna, A., La, K. C., Dimitriadoy, S., Liu, D. L., Kantheti, H. S., Saghafinia, S., Chakravarty, D., Daian, F., Gao, Q., Bailey, M. H., Liang, W.-W., Foltz, S. M., Shmulevich, I., Ding, L., Heins, Z., … Schultz, N. (2018). Oncogenic Signaling Pathways in The Cancer Genome Atlas. *Cell*, *173*(2), 321-337.e10. https://doi.org/10.1016/j.cell.2018.03.035

Subramanian, A., Tamayo, P., Mootha, V. K., Mukherjee, S., Ebert, B. L., Gillette, M. A., Paulovich, A., Pomeroy, S. L., Golub, T. R., Lander, E. S., & Mesirov, J. P. (2005). Gene set enrichment analysis: A knowledge-based approach for interpreting genome-wide expression profiles. *Proceedings of the National Academy of Sciences*, *102*(43), 15545–15550. https://doi.org/10.1073/pnas.0506580102

Szablewski, L. (2014). Diabetes mellitus: Influences on cancer risk. *Diabetes/Metabolism Research and Reviews*, *30*(7), 543–553. https://doi.org/10.1002/dmrr.2573

Tran, K. B., Lang, J. J., Compton, K., Xu, R., Acheson, A. R., Henrikson, H. J., Kocarnik, J. M., Penberthy, L., Aali, A., Abbas, Q., Abbasi, B., Abbasi-Kangevari, M., Abbasi-Kangevari, Z., Abbastabar, H., Abdelmasseh, M., Abd-Elsalam, S., Abdelwahab, A. A., Abdoli, G., Abdulkadir, H. A., … Murray, C. J. L. (2022). The global burden of cancer attributable to risk factors, 2010–19: A systematic analysis for the Global Burden of Disease Study 2019. *The Lancet*, *400*(10352), 563–591. https://doi.org/10.1016/S0140-6736(22)01438-6

Wang, M., Yang, Y., & Liao, Z. (2020). Diabetes and cancer: Epidemiological and biological links. *World Journal of Diabetes*, *11*(6), 227–238. https://doi.org/10.4239/wjd.v11.i6.227

Warburg, O. (1956). On the Origin of Cancer Cells. *Science*, *123*(3191), 309–314. JSTOR.

Wu, Q., Ba-Alawi, W., Deblois, G., Cruickshank, J., Duan, S., Lima-Fernandes, E., Haight, J., Tonekaboni, S. A. M., Fortier, A.-M., Kuasne, H., McKee, T. D., Mahmoud, H., Kushida, M., Cameron, S., Dogan-Artun, N., Chen, W., Nie, Y., Zhang, L. X., Vellanki, R. N., … Arrowsmith, C. H. (2020). GLUT1 inhibition blocks growth of RB1-positive triple negative breast cancer. *Nature Communications*, *11*(1), Article 1. https://doi.org/10.1038/s41467-020-18020-8

Zoetemelk, M., Rausch, M., Colin, D. J., Dormond, O., & Nowak-Sliwinska, P. (2019). Short-term 3D culture systems of various complexity for treatment optimization of colorectal carcinoma. *Scientific Reports*, *9*(1), Article 1. https://doi.org/10.1038/s41598-019-42836-0

2.7 Figures and Tables

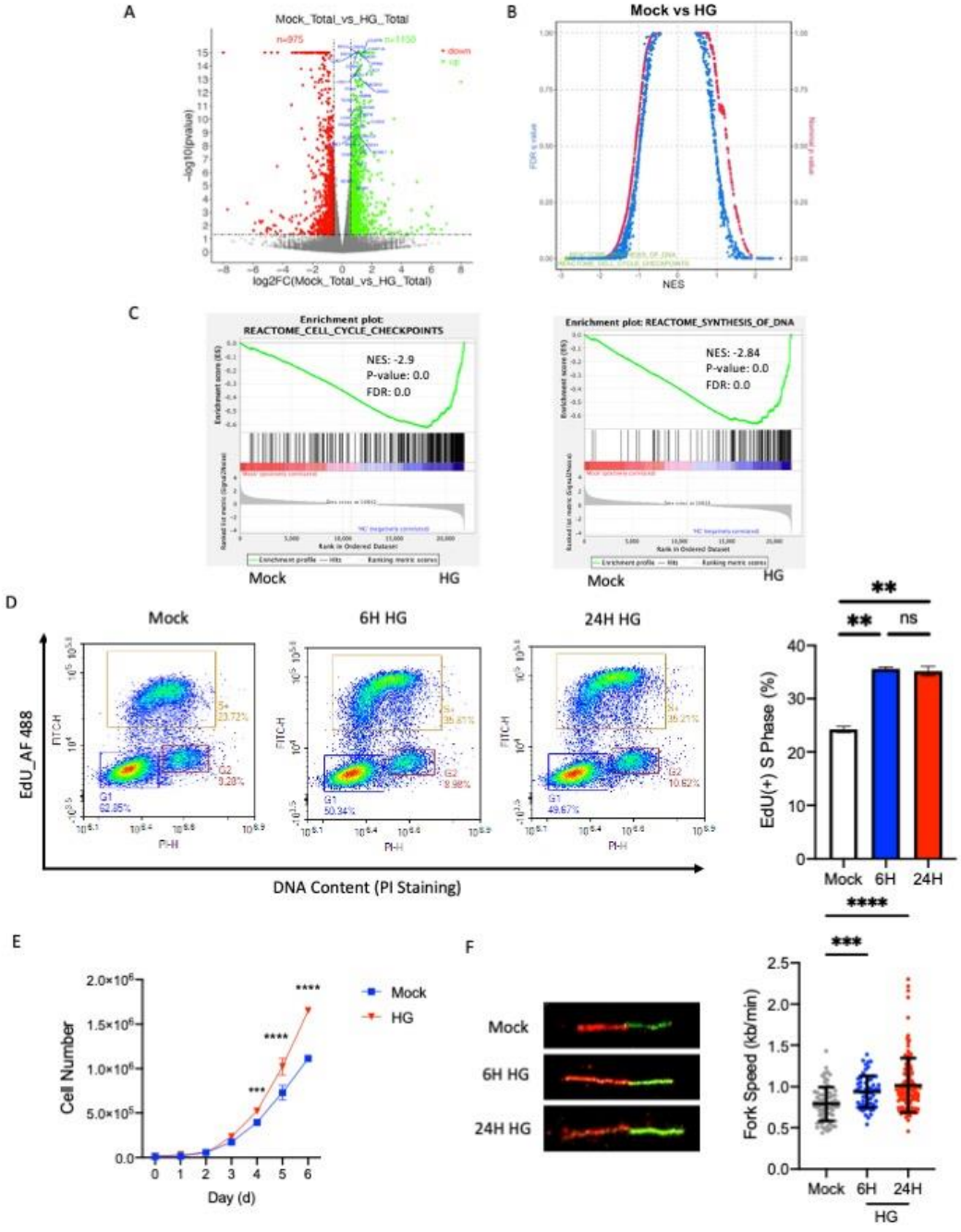

Figure 2.1 Elevated glucose levels prompt DNA synthesis and cell growth. (A) Volcano plot depicting differential gene expression in HCT116 cells following HG exposure (up = fluorescent green; down = red). Dashed lines demarcate fold change (FC) and *p* value cutoffs for differentially expressed genes. The cutoffs for log2(FC) and -log10(*p* value) are ±0.58 and 1.3, respectively. −log10(*p* value) and log2(FC) values have been capped at 15 and ±8, respectively. Triangles (Δ) represent data points exceeding the cap. The DNA synthesis relevant genes are denoted in blue. (B) Comparative analysis of REACTOME pathway gene sets from the MSigDB using GSEA for increased (left) and reduced (right) expression of global genes caused by HG treatment. The data is displayed as a scatterplot, with the normalized p value (right y-axis) and false discovery q value (left y-axis), along with the normalized enrichment score (NES) (x-axis) for each assessed gene set. The gene sets highlighted in fluorescent green indicated cell cycle checkpoints and synthesis of DNA. (C) The top 2 most significantly enriched gene set of REACTOME pathways from GSEA were shown with calculated NES. (D) Cell cycle profiles of EdU incorporation and DNA content staining in HCT116 treated with HG at the indicated time. The left panel is the representative dots analysis of flow cytometry. G1, S+ and G2 of the cell cycle were gated as indicated. The right panel indicates the percentage of EdU-incorporated cells in the S phase (S+) from the left panel. (E) Cell growth curve of HCT116 cells under 5 mM (Mock) and 25 mM (HG) conditions for a consecutive of 6 days. (F) DNA replication fork progression of HG-treated HCT116 cells was determined by DNA fiber assay at the indicated time. The right panel summarizes measuring 100-150 spread DNA fibers in HCT116 cells for each condition. Results are displayed in mean ± SD for n=3 replicates.

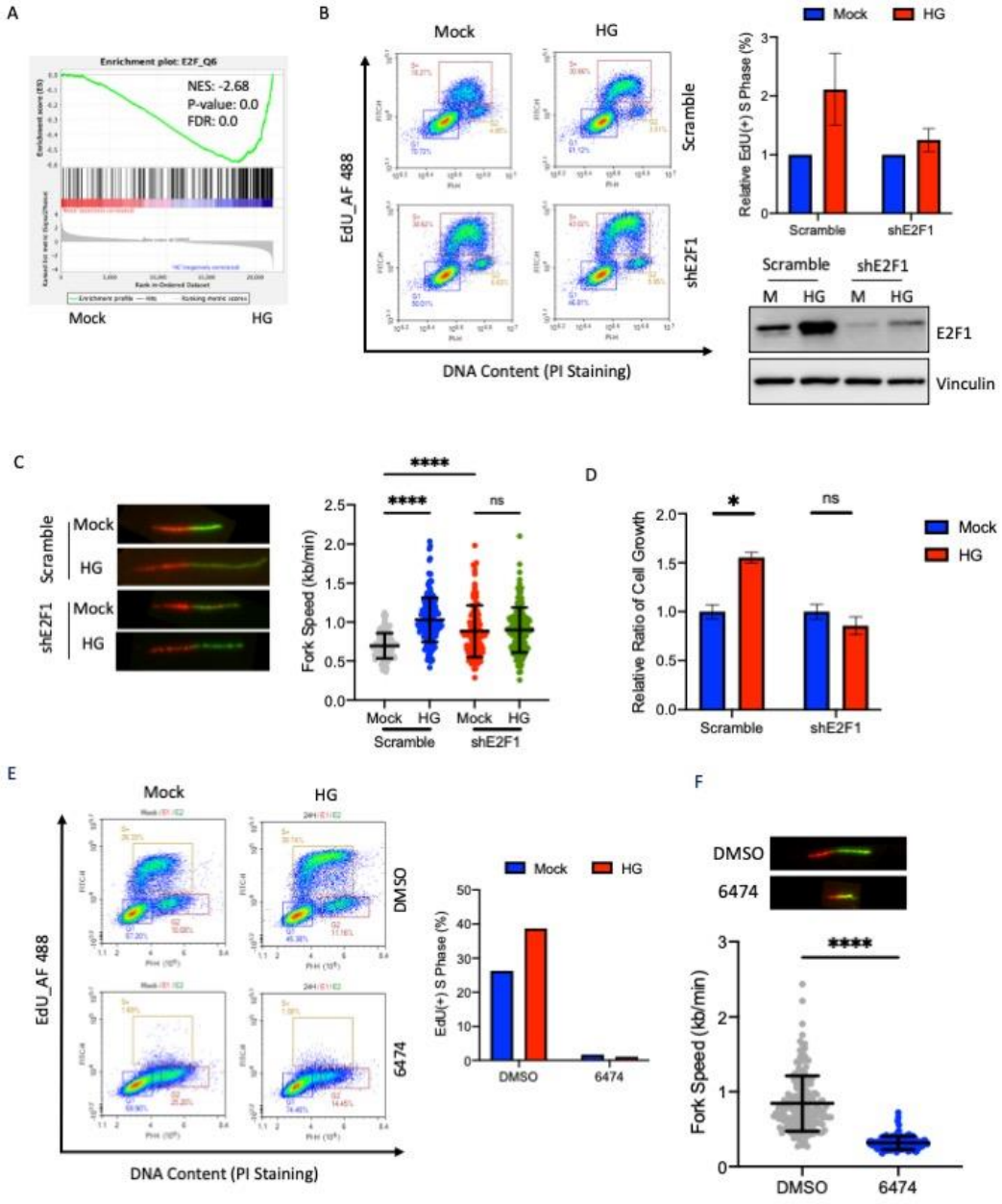
A
Enrichment plot: E2F_Q6
NES: -2.68
P-value: 0.0
FDR: 0.0
Mock
HG
B
Mock
HG
Scramble
shE2F1
EdU_AF 488
DNA Content (PI Staining)
Mock
HG
Relative EdU(+) S Phase (%)
Scramble
shE2F1
Scramble
shE2F1
M
HG
M
HG
E2F1
Vinculin
C
Scramble
shE2F1
Mock
HG
Mock
HG
****
****
ns
Fork Speed (kb/min)
Mock
HG
Mock
HG
Scramble
shE2F1
D
*
ns
Relative Ratio of Cell Growth
Mock
HG
Scramble
shE2F1
E
Mock
HG
DMSO
6474
EdU_AF 488
DNA Content (PI Staining)
Mock
HG
EdU(+) S Phase (%)
DMSO
6474
F
DMSO
6474
****
Fork Speed (kb/min)
DMSO
6474

Figure 2.2 E2F plays a crucial role in HG-induced DNA synthesis and cell growth. (A) The most significant enriched transcription factor revealed by GSEA. (B) EdU incorporation and DNA content staining in HG-treated H460 cells transduced with scramble virus or E2F1-targeting shRNA (shE2F1). The left panel is the dots analysis with gates of G1, S+ and G2 of the cell cycle. The right panel indicates the relevant percentage change of EdU-labeled cells. The E2F1 levels were verified by Western analysis. (C) DNA replication progression of HG-treated H460 cells with or without E2F1 knock down. (D) Cell growth assay of scramble or E2F1 knock down H460 cells following HG treatment. (E) HCT116 cells were treated with DMSO or the pan-E2F inhibitor HLM006474. EdU incorporation and DNA content staining were analyzed by flow cytometry following HG exposure. The left panel is the dots analysis with gates of G1, S+ and G2 of the cell cycle. The right panel indicates the percentage of EdU-positive cells in the S phase. (F) DNA replication fork progression of HCT116 cells treated with HLM006474 was determined by DNA fiber assay. The bottom panel summarizes the measurement of 100-150 spread DNA fibers for each condition.

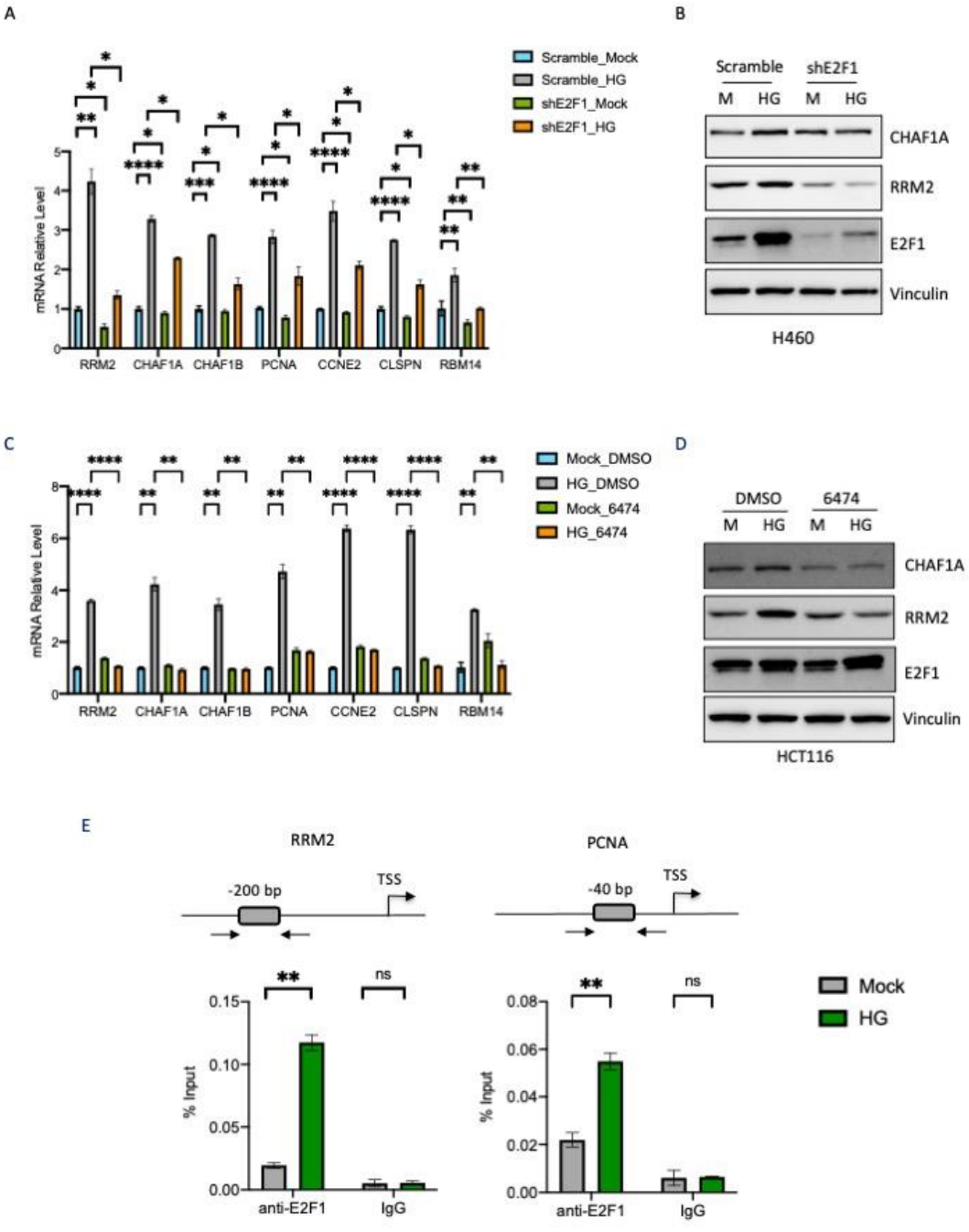
A
Scramble_Mock
Scramble_HG
shE2F1_Mock
shE2F1_HG
mRNA Relative Level
RRM2
CHAF1A
CHAF1B
PCNA
CCNE2
CLSPN
RBM14
B
Scramble
shE2F1
M
HG
M
HG
CHAF1A
RRM2
E2F1
Vinculin
H460
C
Mock_DMSO
HG_DMSO
Mock_6474
HG_6474
mRNA Relative Level
RRM2
CHAF1A
CHAF1B
PCNA
CCNE2
CLSPN
RBM14
D
DMSO
6474
M
HG
M
HG
CHAF1A
RRM2
E2F1
Vinculin
HCT116
E
RRM2
-200 bp
TSS
PCNA
-40 bp
TSS
ns
% Input
anti-E2F1
IgG
Mock
HG

Figure 2.3 E2F1 regulates transcription of DNA replication genes in response to elevated glucose levels. (A) RT-qPCR of top DNA replication genes in control (scramble) or E2F1 knock down H460 cells following HG exposure. (B) Western analysis of CHAF1A, RRM2 and E2F1 protein levels from the same treatment as indicated in 3A. Vinculin was used as a loading control. (C) RT-qPCR of top DNA replication genes in control or HLM006474 treated HCT 116 cells following HG exposure. (D) Immunoblot analysis of RRM2, CHAF1A and E2F1 from the same treatment as indicated in 3C. (E) Top: schematic representations of the RRM2 and PCNA promoters. The putative binding sites for E2F1 are identified as grey rectangles and labeled with the positions ahead of the transcription start site (TSS). Bottom: ChIP-qPCR analysis of E2F1 binding to the RRM2 and PCNA promoters in the HCT116 cells following HG exposure. Results are displayed in mean ± SD for n=3 replicates.

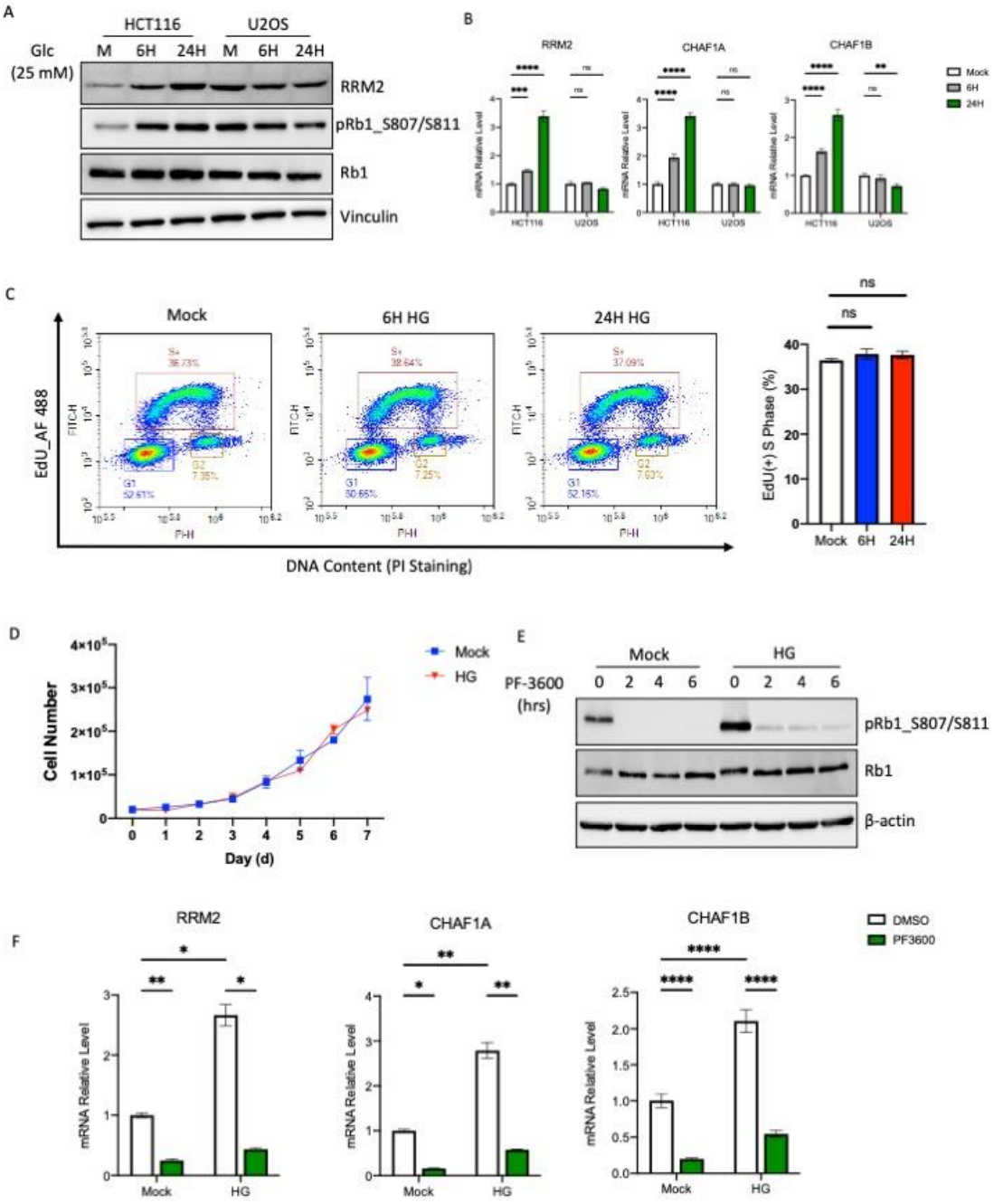
A
HCT116
U2OS
Glc
(25 mM)
M
6H
24H
M
6H
24H
RRM2
pRb1_S807/S811
Rb1
Vinculin
B
RRM2
CHAF1A
CHAF1B
mRNA Relative Level
HCT116
U2OS
Mock
6H
24H
C
Mock
6H HG
24H HG
EdU_AF 488
DNA Content (PI Staining)
G1
S
G2
EdU(+) S Phase (%)
ns
Mock
6H
24H
D
Cell Number
Day (d)
Mock
HG
E
Mock
HG
PF-3600
(hrs)
0
2
4
6
pRb1_S807/S811
Rb1
β-actin
F
RRM2
CHAF1A
CHAF1B
mRNA Relative Level
Mock
HG
DMSO
PF3600

Figure 2.4 HG-induced Rb1 phosphorylation is requited for activation of DNA replication genes. (A) Western blot analysis of total Rb1, Ser807/Ser811-phosphorylated Rb1 and RRM2 in HCT116 and U2OS cells following HG exposure. (B) RT-qPCR of RRM2, CHAF1A and CHAF1B genes in HCT116 and U2OS cells following HG treatment. (C) Cell cycle profiles of EdU incorporation and DNA content in U2OS cells following HG treatment at the indicated time. The right panel indicates the percentage of EdU-labled cells in the S phase. (D) Cell growth curve of U2OS cells under 5 mM (Mock) and 25 mM (HG) conditions for a consecutive of 7 days. (E) HCT116 cells were treated with the CDK2/4/6 inhibitor PF-3600 at the indicated time. Total Rb1 and Ser807/Ser811-phosphorylated Rb1 were determined by western blot analysis. (F) RT-qPCR of RRM2, CHAF1A and CHAF1B was performed in HCT116 cells following 6hrs of HG and PF-3600 treatment. Results are displayed in mean ± SD for n=3 replicates.

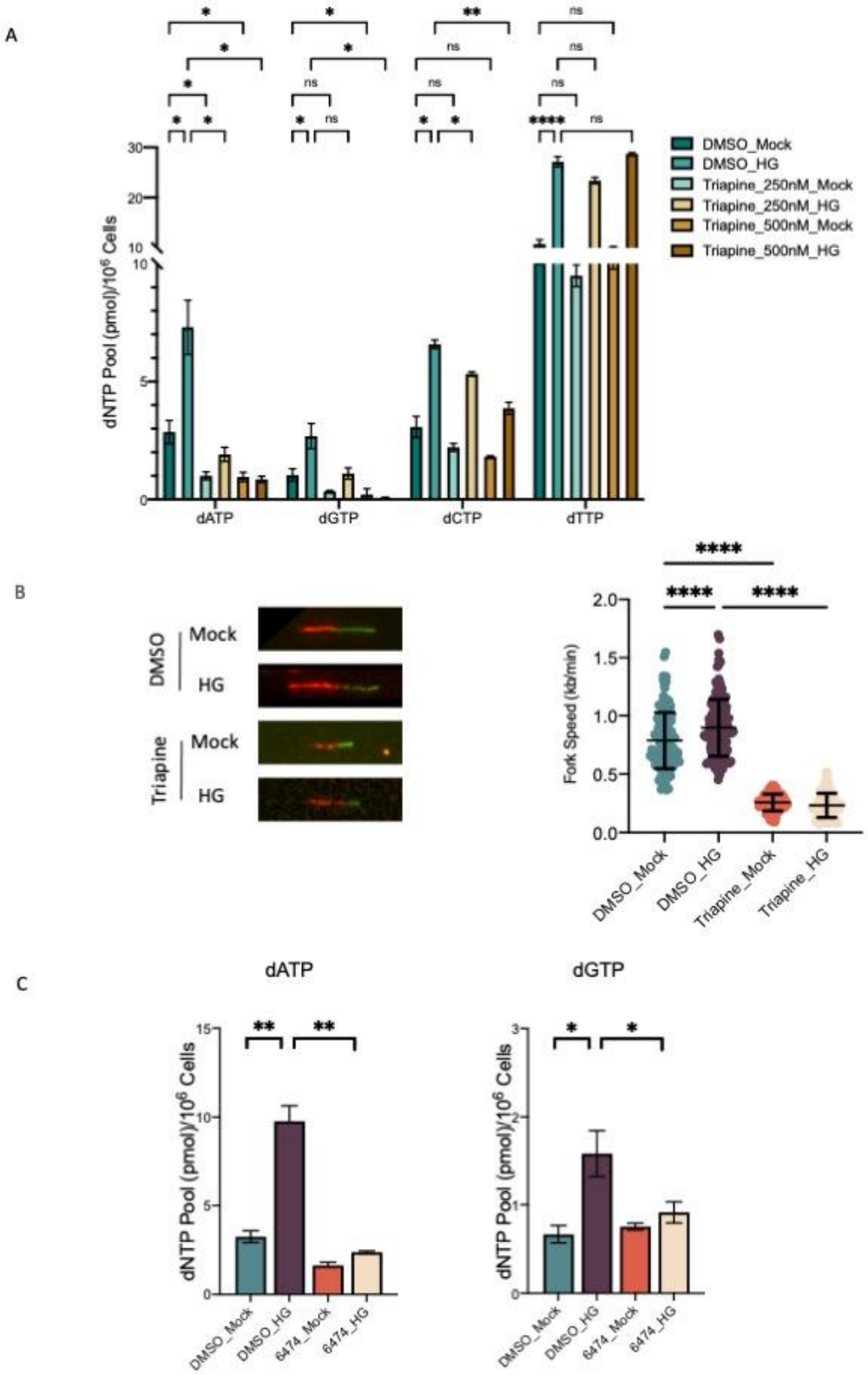
A
dNTP Pool (pmol)/10^6 Cells
dATP
dGTP
dCTP
dTTP
DMSO_Mock
DMSO_HG
Triapine_250nM_Mock
Triapine_250nM_HG
Triapine_500nM_Mock
Triapine_500nM_HG
B
DMSO
Mock
HG
Triapine
Mock
HG
Fork Speed (kb/min)
DMSO_Mock
DMSO_HG
Triapine_Mock
Triapine_HG
C
dATP
dGTP
dNTP Pool (pmol)/10^6 Cells
DMSO_Mock
DMSO_HG
6474_Mock
6474_HG

Figure 2.5 Regulation of intracellular dNTP levels by HG is dependent on the E2F1-RRM2 axis. (A) Intracellular dNTP levels in HCT116 cells treated with or without Triapine and HG as indicated. (B) DNA replication fork progression of Triapine-treated HCT116 cells following HG exposure. The right panel summarizes measuring of 100-150 spread DNA fibers for each condition. (C) HCT116 cells were treated with the pan-E2F inhibitor HLM006474. Intracellular dATP and dGTP levels were determined in cells following HG treatment. Results are displayed in mean ± SD for n=3 replicates.

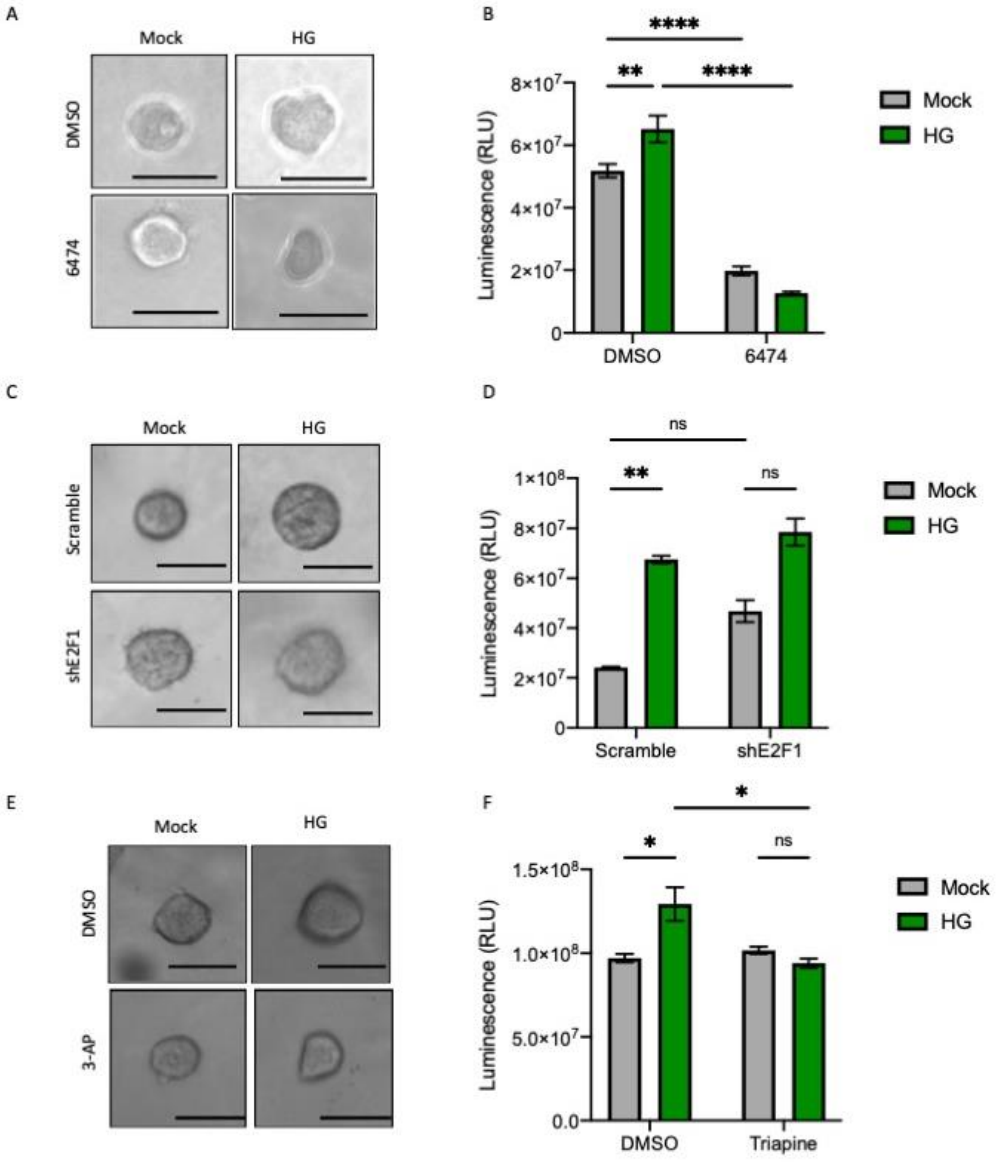

Figure 2.6 Inhibition of the E2F1-RRM2 axis alleviates HG-induced 3D cancer cell growth. (A) Representative bright field images of HCT116-derived spheroids in the presence of HG and/or pan-E2F inhibitor HLM006474 as indicated for 6 days. Scale bar: 100 μm. (B) ATP luminescence signals represented for the spheroid's viability. (C) Representative bright field images of H460 derived spheroids in the presence of scramble control or shE2F1 for 6 days following HG exposure. Scale bar: 100 μm. (D) Luminescence signals represented for the spheroid's viability indicated in 6C. (E) Representative bright field images of HCT116-derived spheroids following HG and/or Triapine as indicated for 6 days. (F) ATP luminescence signals represented for the spheroid's viability. Results are displayed in mean ± SD of three separate experiments.

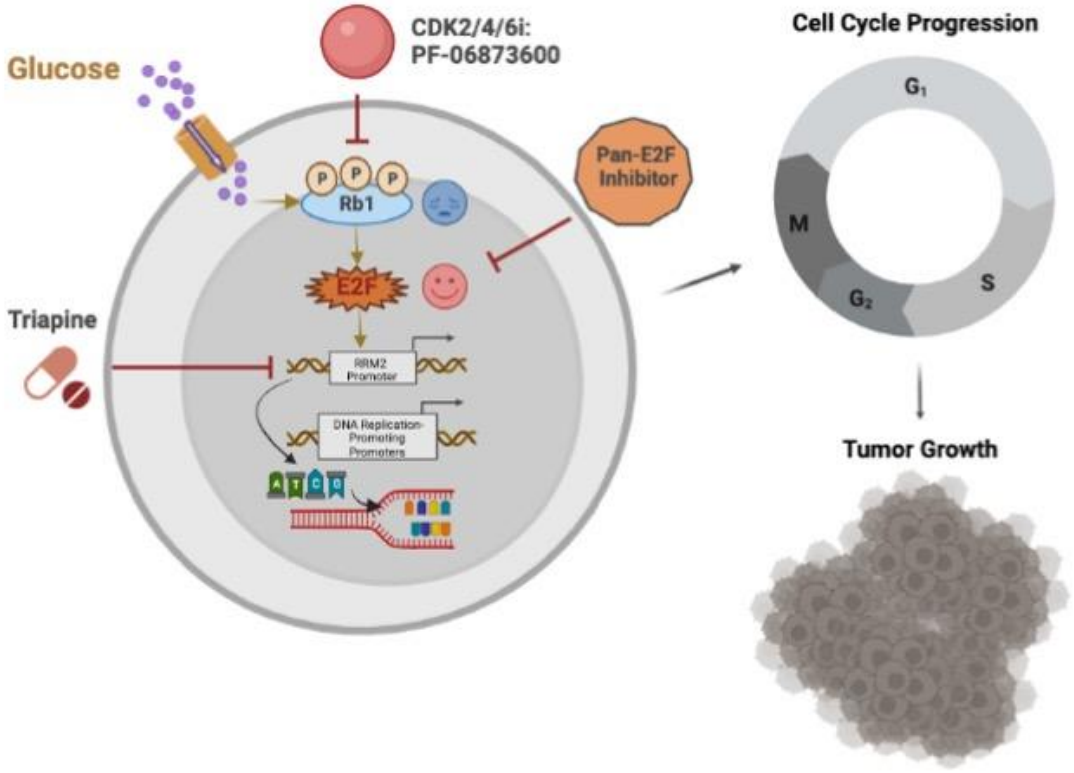

Figure 2.7 Schematic of biological process of cancer cells in response to hyperglycemia. Glucose enters the cells through the glucose transporter (orange cylinder) located on the cellular membrane. It then de-actives Rb1 via phosphorylation, followed by activating the transcription factor E2F to bind on the promoters of the DNA replication genes, including RRM2, therefore activating the transcriptions. Once the level of RRM2 is increased in cells, the cells can synthesize more nucleotides, which are essential materials for the DNA replication. As a result, the cells undergo proliferation out of control. During the whole process, there are three potential targets available for growth inhibition: 1) CDK2/4/6i PF-3600 for inhibiting Rb1 phosphorylation; 2) pan-E2F inhibitor HLM006474 for inhibiting E2F activity; 3) Triapine for inhibiting RRM2 function.

Table 2.1 Hallmark genes with 2-FC differentially expressed enriched in DNA replication

Gene Symbol	Gene Name
BLM	BLM RecQ like helicase
CCNA2	cyclin A2
CCNE1	cyclin E1
CCNE2	cyclin E2
CDK1	cyclin dependent kinase 1
CDK2	cyclin dependent kinase 2
CHAF1A	chromatin assembly factor 1 subunit A
CHAF1B	chromatin assembly factor 1 subunit B
CLSPN	claspin
DSCC1	DNA replication and sister chromatid cohesion 1
DTL	denticleless E3 ubiquitin protein ligase homolog
E2F7	E2F transcription factor 7
E2F8	E2F transcription factor 8
ESCO2	establishment of sister chromatid cohesion N-acetyltransferase 2
EXO1	exonuclease 1
FEN1	flap structure-specific endonuclease 1
GINS1	GINS complex subunit 1
GINS2	GINS complex subunit 2
GMNN	geminin, DNA replication inhibitor
MCM10	minichromosome maintenance 10 replication initiation factor
MCM2	minichromosome maintenance complex component 2
MCM4	minichromosome maintenance complex component 4
MCM6	minichromosome maintenance complex component 6
MSH6	mutS homolog 6
ORC1	origin recognition complex subunit 1
ORC6	origin recognition complex subunit 6
PCNA	proliferating cell nuclear antigen
PRIM2	DNA primase subunit 2
RAD51	RAD51 recombinase
RFC4	replication factor C subunit 4
RRM2	ribonucleotide reductase regulatory subunit M2
SLBP	stem-loop binding protein
TICRR	TOPBP1 interacting checkpoint and replication regulator
TONSL	tonsoku like, DNA repair protein
TREX1	three prime repair exonuclease 1

Table 2.2 List of top 20 gene sets of transcription factors identified in GSEA

NAME	NES	NOM p-val	FDR q-val
E2F_Q6	-2.675365	0	0
E2F_Q4	-2.6746166	0	0
SGCGSSAAA_E2F1DP2_01	-2.6326556	0	0
E2F1DP1RB_01	-2.6103704	0	0
E2F4DP1_01	-2.573035	0	0
E2F1_Q6	-2.5444624	0	0
E2F_02	-2.5388935	0	0
E2F1DP1_01	-2.5196557	0	0
E2F1_Q6_01	-2.516277	0	0
E2F1DP2_01	-2.5162504	0	0
E2F1_Q3	-2.511075	0	0
E2F4DP2_01	-2.5015657	0	0
E2F_Q3_01	-2.489931	0	0
E2F_03	-2.4838407	0	0
E2F_Q4_01	-2.4393415	0	0
E2F_Q3	-2.3998244	0	0
E2F_Q6_01	-2.3758159	0	0
E2F1_Q4_01	-2.361822	0	0
PPARGC1A_TARGET_GENES	-2.0692632	0	2.42E-04
HSF2_TARGET_GENES	-2.051176	0	2.86E-04

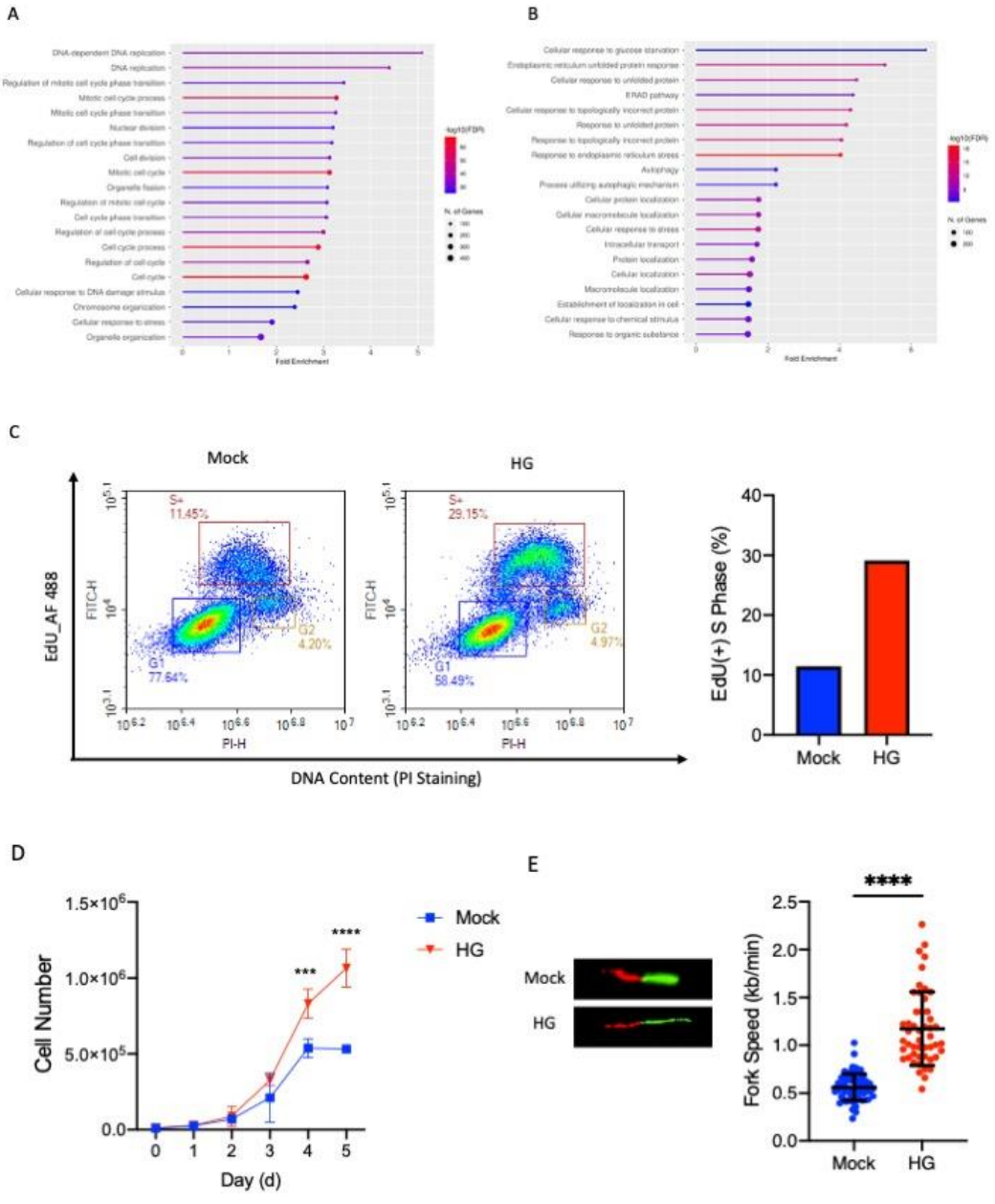
A
B
C
Mock
HG
S+
11.45%
G1
77.64%
G2
4.20%
S+
29.15%
G1
58.49%
G2
4.97%
FITC-H
PI-H
EdU_AF 488
DNA Content (PI Staining)
EdU(+) S Phase (%)
Mock
HG
D
Cell Number
Day (d)
Mock
HG
***
****
E
Mock
HG
Fork Speed (kb/min)
****
Mock
HG

Supplementary Figure 2.1 Elevated glucose levels prompt DNA synthesis and cell growth. (A) GO_BP analysis (ShinyGO v0.75) of enriched pathways of all up-regulated genes in HCT116 cells following HG treatment. The FDR cut-off is 0.05 and the top 20 enriched pathways are displayed here. (B) GO_BP analysis (ShinyGO v0.75) of enriched pathways of all down-regulated genes in HCT116 cells following HG treatment. The FDR cut-off is 0.05 and the top 20 enriched pathways are displayed here. (C) EdU incorporation and DNA content staining in HG-treated H460 cells. The left panel is the dots analysis of flow cytometry. G1, S+ and G2 of the cell cycle were gated. The right panel indicates the percentage of cells labeled with EdU from the left panel. (D) Cell growth curve of H460 cells treated with or without HG for 5 days. (E) DNA replication fork progression of H460 cells following HG treatment.

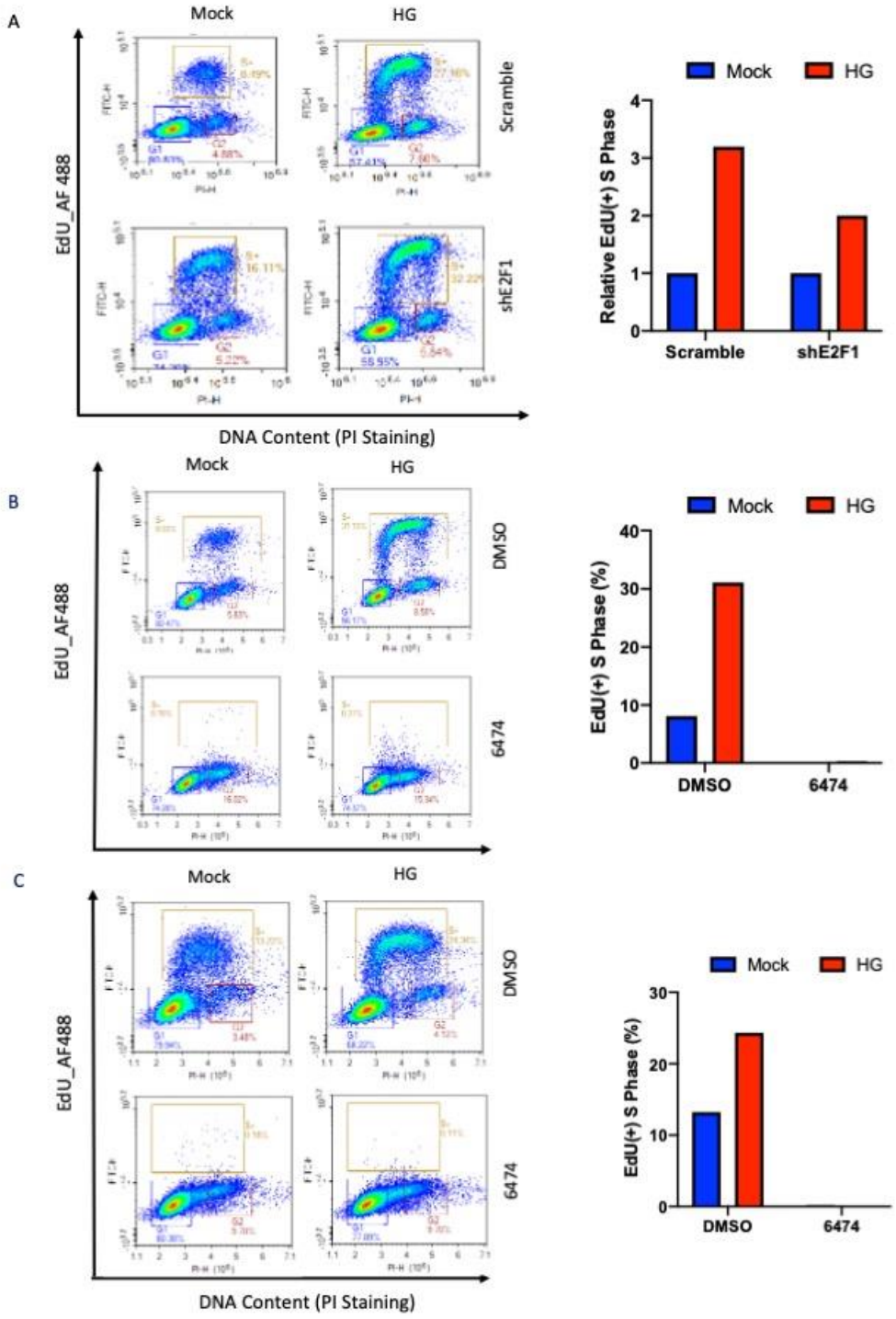
A
Mock
HG
Scramble
shE2F1
EdU_AF 488
DNA Content (PI Staining)
Mock
HG
Relative EdU(+) S Phase
Scramble
shE2F1
B
Mock
HG
DMSO
6474
EdU_AF488
Mock
HG
EdU(+) S Phase (%)
DMSO
6474
C
Mock
HG
DMSO
6474
EdU_AF488
DNA Content (PI Staining)
Mock
HG
EdU(+) S Phase (%)
DMSO
6474

Supplementary Figure 2.2 E2F plays a crucial role in HG-induced DNA synthesis and cell growth. (A) Cell cycle analysis of the EdU incorporation and DNA content in either control (scramble) or E2F1-depleted HCT116 cells upon HG exposure. The left panel is the dots analysis with gates of G1, S+ and G2 of the cell cycle. The right panel indicates the percentage of EdU-labeled cells. (B) HCT116 cells were treated with HG and pan-E2F inhibitor HLM006474. EdU incorporation and DNA content staining was analyzed by flow cytometry. The left panel is the dots analysis with gates of G1, S+ and G2 of the cell cycle. The right panel indicates the percentage of EdU-labeled cells. (C) H460 cells were treated with HG and pan-E2F inhibitor HLM006474. EdU incorporation and DNA content staining was analyzed by flow cytometry. The left panel is the dots analysis with gates of G1, S+ and G2 of the cell cycle. The right panel indicates the percentage of EdU-labeled cells.

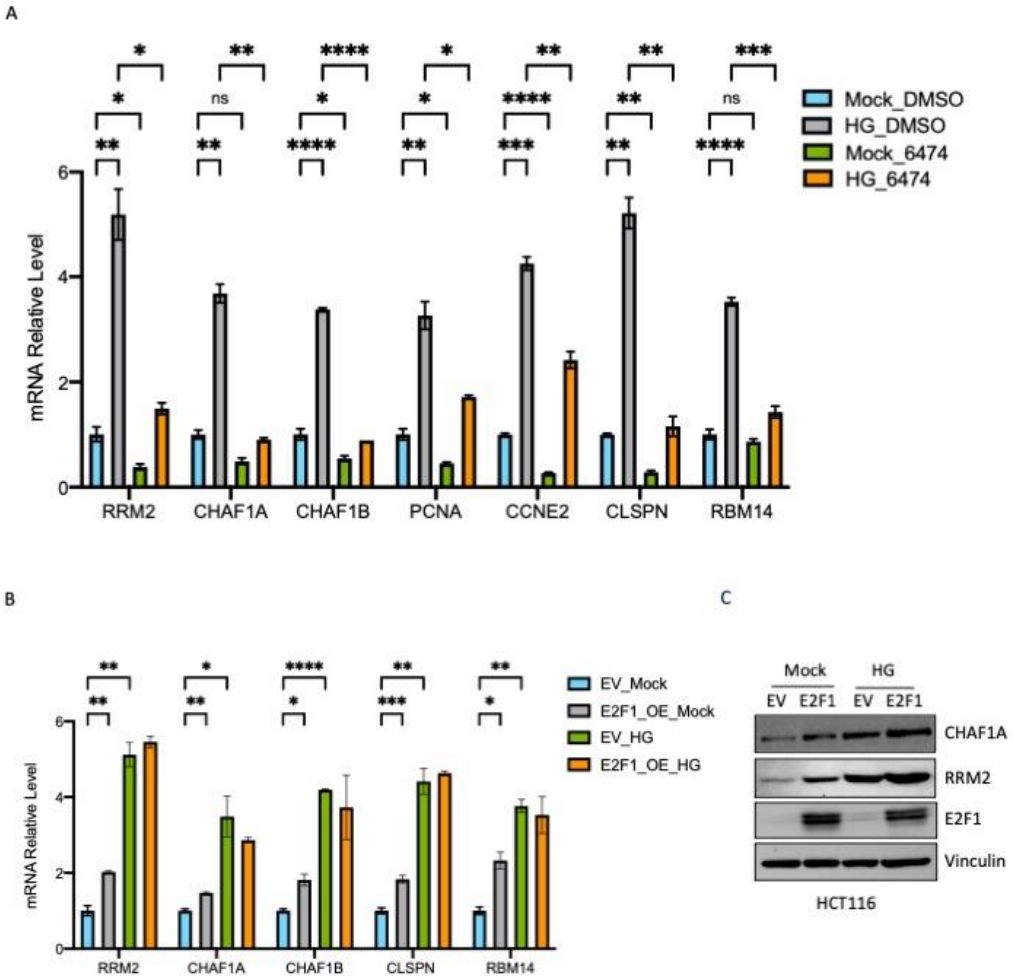

Supplementary Figure 2.3 E2F1 regulates transcription of DNA replication genes in response to elevated glucose levels. (A) RT-qPCR of 7 top DNA replication genes in H460 cells treated with either HG or HLM006474 as indicated. (B) HCT116 cells were transiently overexpressed with flag tagged E2F1, followed by HG treatment. The top DNA replication genes were determined by RT-qPCR. (C) Protein levels of RRM2, CHAF1A and E2F1 were determined by western blot in the cells from S3B. Vinculin was used as a loading control. Results are displayed in mean ± SD for n=3 replicates.

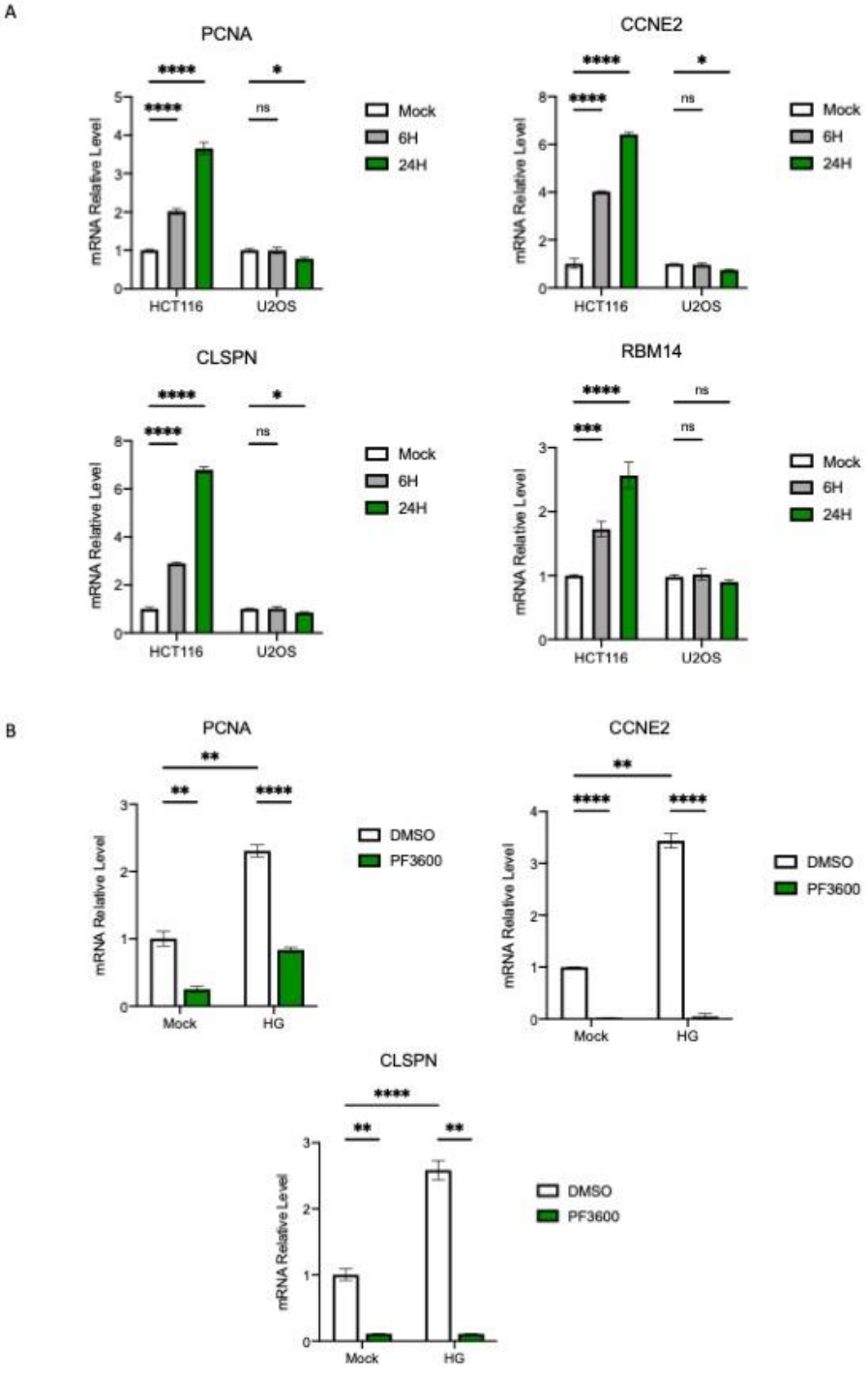
A
PCNA
CCNE2
CLSPN
RBM14
mRNA Relative Level
HCT116
U2OS
Mock
6H
24H
ns
B
DMSO
PF3600
Mock
HG

Supplementary Figure 2.4 HG-induced Rb1 phosphorylation is requited for activation of DNA replication genes. (A) RT-qPCR of DNA replication genes in HCT116 and U2OS cells following HG treatment. (B) RT-qPCR of DNA replication genes were detected in HCT116 cells treated with CDK2/4/6i PF-3600 and HG for 6hrs. Results are displayed in mean ± SD for n=3 replicates.

Supplementary Table 2.1 List of oligonucleotide sequences

Type	Name	Sequence (5'->3')
qPCR Primers	GAPDH_F	ACAACTTTGGTATCGTGGAAGG
	GAPDH_R	GCCATCACGCCACAGTTTC
	RRM2_F	GTGGAGCGATTTAGCCAAGAA
	RRM2_R	CACAAGGCATCGTTTCAATGG
	CHAF1A_F	TTAGACCGAAACTTGTCAACGG
	CHAF1A_R	GTCTGGCTGCTCATTCGAGT
	CHAF1B_F	AGAGGCAAGAAGCTACCGGAT
	CHAF1B_R	CTGGCGTGAGAAGCAAAGA
	PCNA_F	CCTGCTGGGATATTAGCTCCA
	PCNA_R	CAGCGGTAGGTGTCGAAGC
	CCNE2_F	GGAACCACAGATGAGGTCCAT
	CCNE2_R	CCATCAGTGACGTAAGCAAACT
	CLSPN_F	TGGAGAGTGGGGTCCATTCAT
	CLSPN_R	CCGGGGTTTACGTTTGAAGAAA
	RBM14_F	CTACCAGCAGGCTTTTGGCA
	RBM14_R	GTCATGGGCTGAGTCCGATAG
	18S rRNA_F	CTCAACACGGGAAACCTCAC
	18S rRNA_R	CGCTCCACCAACTAAGAACG
shRNA	Scramble	GCGTACATCACTCGTTAATAT
	shE2F1	CGCTATGAGACCTCACTGAAT
ChIP-qPCR Primers	RRM2_E2F1_F	ACGGGGGTGTCCCCGGGGGT
	RRM2_E2F1_R	CTTCCCATTGGCTGCGCCTT
	PCNA_E2F1_F	GCGACGTCACCACGCTGTC
	PCNA_E2F1_R	TGCGGCCGGGTTCAGGAG

Supplementary Table 2.2 Sizes of the spheres in HCT116 cells treated with HG and/or panE2F inhibitor HLM006474

HCT116	Mock		HG	
	Length (μm)	Width (μm)	Length (μm)	Width (μm)
DMSO	68.84±23.79	56.43±18.69	90.05±34.76	68.31±34
6474	62.96±25.15	52.2±21.78	44.78±13.56	37.14±8.9

Supplementary Table 2.3 Sizes of the spheres in HCT116 cells treated with HG and/or RNR inhibitor Triapine

HCT116	Mock		HG	
	Length (μm)	Width (μm)	Length (μm)	Width (μm)
DMSO	72.1±12.17	64±11.49	86.44±19.41	68.5±14.41
3-AP	81.61±13.29	69.26±11.26	70.23±10.81	59.32±8.17

Supplementary Table 2.4 Sizes of the spheres in E2F1-depleted H460 cells with HG treatment

H460	Mock		HG	
	Length (μm)	Width (μm)	Length (μm)	Width (μm)
Scramble	68.03±13.88	57.42±10.15	78.27±11.27	69.39±10.95
shE2F1	90.34±17.77	77.40±14.63	82.64±10.87	72.14±11.71

Chapter 3

Untargeted metabolomic analysis in cancer cells upon high glucose exposure

3.1 Introduction

The Warburg effect, initially observed by Otto Warburg in 1965, reveals a distinct metabolic behavior in cancer cells. These cells exhibit a preference for glycolysis over oxidative phosphorylation even in the presence of oxygen, due to compromised mitochondrial respiration (Alfarouk et al., 2014; Warburg, 1956). This shift leads to the generation of lactic acid and an acidic tumor microenvironment, promoting tumor aggressiveness and resistance to treatment (Böhme & Bosserhoff, 2016; Justus et al., 2013). During the glycolysis, various metabolic pathways branch out from glycolytic intermediates, with a more emphasize on pathways like pentose phosphate pathway, hexosamine synthesis pathway and serine biosynthesis in cancer cells (Hay, 2016). These pathways contribute to the biomass synthesis, including essential components like nucleotides and amino acids, crucial for sustaining cell growth and proliferation.

An elevated fasting blood glucose level serves as a shared characteristic and diagnostic criterion for both Type 1 and Type 2 diabetes. Diabetes exhibits a positive association with the incidence of various cancer types, with a more pronounced association observed in Type 2 diabetes (Harding et al., 2015). A most recent study further highlighted the increased cancer risk associated with high fasting plasma glucose levels over the past decade (Tran et al., 2022). These epidemiological studies strongly suggest the role of hyperglycemia in promoting cancer development and progression. While extensive studies have been conducted on the metabolic reprogramming of glucose molecules in cancer cells, there remains a significant gap in understating the metabolic alterations occurring in cancer cells under the hyperglycemic condition. In Chapter 2, we

unveiled a finding that high glucose levels could elevate the levels of all four intracellular dNTP in cancer cells. However, it is important to note that these data, with the inspiration derived from RNA-seq analysis, provides only a partial picture. Therefore, we sought to carry out a dedicated study to directly investigate how the hyperglycemia mediates changes in metabolite levels within cancer cells.

In this chapter, we described an untargeted analysis of metabolites, using chromatography/mass spectrometry techniques, in cancer cells upon high glucose (HG) treatment in HCT116 cells. From the metabolomic profiling, a total of 150 metabolites were identified spanning glucose metabolism, amino acid metabolism and nucleotide metabolism. The metabolite set enrichment analysis (MSEA) revealed several significantly enriched metabolic pathways, primarily driven by an elevated level of fructose. Notably, HG-treated cells exhibited concurrent increases in fructose, sorbitol and glucose concentrations, strongly suggesting the activation of polyol pathway mediated by hyperglycemia. To further validate the observed increase in nucleotide synthesis activity obtained from Chapter 2, we also examined these metabolites in nucleotide synthesis, and several of them exhibited increased levels in cancer cells under HG condition. Lastly, our analysis indicated an elevation in the level of lactic acid, an end-product of anerobic glycolysis, in HG-treated cells. While this metabolic profiling does not cover certain vital metabolites of interest due to the technical limitation, it does illuminate activated metabolic pathways that remained beyond the scope of the RNA-seq data. Thus, these findings provide us with some insights into the metabolic alterations in cancer cells in response to HG, shedding light on previously unexplored facets.

3.2 Results

3.2a Analysis of differential metabolic pathways in cancer cells upon HG treatment

To comprehensively investigate the metabolic changes induced by hyperglycemia in cancer cells, we carried out an untargeted metabolomic profiling in HCT116 post 6h HG treatment. The metabolomic profiling identified a total of 150 distinct metabolites. These encompass various aspects of metabolites, arising from glucose metabolism, amino acid metabolism, as well as purine and pyrimidine metabolism (Table 1). Specifically, the MSEA revealed four significantly enriched metabolic pathways in HG-treated cells: amino sugar and nucleotide sugar metabolism, starch and sucrose metabolism, fructose and mannose metabolism, and neomycin, kanamycin and gentamicin biosynthesis (Fig. 1A & Table 1). However, no evident crosstalk or interconnections were observed among these pathways (Fig. 1B).

In the context of amino sugar and nucleotide sugar metabolic pathway, we noted upregulated levels of fructose, N-actylmannosamine, and uridine diphosphate glucuronic acid in the HG condition (Supplementary Fig. 1). The increased levels of both fructose and glucose contributed to the enrichment of starch and sucrose metabolism following HG treatment (Supplementary Fig. 2). With respect to fructose and mannose metabolism, we identified elevated levels of fructose and sorbitol in cells subjected to HG condition (Supplementary Fig. 3). Additionally, an augmented level of glucose was observed in the neomycin, kanamycin and gentamicin biosynthesis (Supplementary Fig. 4). Notably, fructose appears to play a role in the enrichment of all four metabolic pathways based on our data.

3.2b Hyperglycemia induces the activation of the polyol pathway in cancer cells

Upon analyzing our metabolomic profiling data, a notable finding emerged: the fructose molecule displayed the most substantial fold change of 5.8 among all the upregulated metabolites following HG treatment (Fig. 2B, Supplementary Table 1). Similarly, sorbitol exhibited a 3.4-fold change, while glucose demonstrated a 2.2-fold change in HG-treated cells (Fig. 2B & 2C, Supplementary Table 1). Interestingly, these three molecules are recognized as participating in the polyol pathway, which contains a two-step sequence. The first step involves the reduction of glucose into sorbitol, concomitant with the conversion of NADPH into $NADP^+$. Subsequently, the sorbitol is further oxidized to fructose, with NAD^+ being converted into NADH (Fig. 2A). The concurrent elevation of these three molecules highly suggests that the hyperglycemia is able to activate the polyol pathway in cancer cells. The pathway has been implicated in diabetic complications, especially in microvascular damage to retina, kidney, and nerves.

The polyol pathway involves the participation of two enzymes: aldose reductase, responsible for the first step, and sorbitol dehydrogenase, governing the second step. The gene AKR1B1 encodes aldose reductase while the SORD gene encodes the sorbitol dehydrogenase. We thus searched expressions of those two genes in our RNA-seq data described in Chapter 2. However, when comparing the normalized read counts from the HG-treated cells with that from the mock cells, we did not observe any significant differences in mRNA levels for these two genes (Fig. 2E & 2F). Nevertheless, the significant metabolic shifts observed in glucose, sorbitol and fructose strongly indicate

that the activation of the polyol pathway in HG-treated HCT116 cells is primarily dependent on metabolites rather than enzymes.

3.2c Hyperglycemia triggers the changes in the levels of metabolites associated with nucleotide metabolism in cancer cells

Given the insights gained from Chapter 2, we observed an elevated levels of all dNTP species in HCT116 cells following the exposure to HG. Although we did not observe any significant enrichment of the pathways related to nucleotide metabolism revealed by MSEA, we speculate that this absence is due to the limited coverage of these metabolites in our metabolomic profiling. Therefore, we extracted the detectable metabolites associated with nucleotide metabolism from the metabolomic profiling data and categorize them into pyrimidine metabolism and purine metabolism, with the aim of looking at the metabolite's level change individually. Among these selected metabolites, glutamine is involved in *de novo* nucleotide synthesis for both pyrimidine and purine. However, we did not observe any significant change of its level post HG treatment (Fig. 3A & Fig. 4A). In pyrimidine metabolism, we identified six detectable metabolites in cells: cytidine monophosphate, thymine, ureidosuccinic acid, orotic acid, uracil and beta alanine (Fig. 3B-G). Among these, cytidine monophosphate experienced a decreased level while orotic acid exhibited an increase of abundance following HG treatment (Fig. 3B & 3E). In purine metabolism, a total of seven detectable metabolites emerged. These included xanthine, D-ribose-5-phosphate, adenosine monophosphate, adenosine, hypoxanthine, inosine and adenine (Fig. 4). Notably, there was a slight, yet significant

rise in normalized abundance for xanthine and adenosine monophosphate (Fig. 4B & 4D). Collectively, these findings provide partial insight into our previous speculation that HG treatment enhances the activity of nucleotide synthesis.

3.2d High glucose levels lead to an elevated level of lactic acid in cancer cells

The Warburg effect underscores the heighted reliance of tumor cells on glycolysis for a continuous production of ATP energy molecules (Fiehn et al., 2008). Within this context, we aimed to explore the potential alterations in intermediates in the glycolytic pathway in the HG-treated cells. In our non-targeted metabolomic profiling, we identified a total of six metabolites associated with glycolysis: glucose-1-phosphate, glucose-6-phosphate, 3-phosphoglyceric acid, 2,3-diphosphoglyceric acid, pyruvic acid and lactic acid (Fig. 5). Interestingly, a significant increase in lactic acid (Fig. 5F) was observed under HG condition, while no significant differences were revealed for other metabolites (Fig. 5A-E).

Furthermore, we sought to see whether ATP levels were influenced by HG environment. Unfortunately, the metabolic profiling data did not contain the result for ATP levels. Nonetheless, precursors for ATP, such as adenosine monophosphate, adenosine and adenine, were detectable. Surprisingly, our analysis revealed a slight but significant increase in adenosine monophosphate, potentially indicating increased ratios of AMP/ATP, whereas no significant changes were observed for adenosine and adenine (Fig. 4D-E, 4H). These findings potentially suggest that elevated glucose levels give rise

in the increase of lactic acid, as a consequence of enhanced glycolysis. However, it is important to note that we did not obtain direct evidence of increased ATP levels.

3.3 Discussion

The reprogramming of glucose metabolism in cancer cells gained significant attention in cancer research (Allen & Locasale, 2018; Ediriweera & Jayasena, 2023; Hay, 2016; Hirata et al., 2016; Lin et al., 2020). Elevated blood glucose levels are recognized as an important risk factor for cancer incidence (Tran et al., 2022), motivating an exploration into having a deep understanding of the hyperglycemia-mediated metabolic alteration in cancer cells. Given the limited investigations carried out in this field, we conducted an untargeted metabolomic analysis in cancer cells subjected to HG treatment. The results of our analysis, as revealed by MSEA, have showcased several pathways associated with monosaccharide metabolism, all arising from the significant increase in fructose levels in HG-treated cells. Moreover, the activation of polyol pathway is strongly indicated, as evidenced by the concurrent elevation in concentrations of glucose, sorbitol and fructose. Additionally, our study identified heightened levels of three metabolites associated with nucleotide metabolism under hyperglycemic condition, suggesting a potential role of hyperglycemia involved in the nucleotide synthesis. Notably, the Warburg effect was confirmed by elevated lactic acid levels in HG-treated cells. This observation underscores the increased reliance of cancer cells on glycolysis to fulfill their demands for growth and proliferation. While the scope of detectable metabolites within

our metabolomic profiling remains limited, it does expand our understanding in the metabolic alterations occurring in cancer cells under the hyperglycemic condition.

Of note, we have observed an activation of polyol pathway under HG condition in cancer cells. The polyol pathway constitutes a metabolic route that converts glucose into fructose (Srikanth & Orrick, 2023). Traditionally, this pathway has been implicated in the pathogenesis of complications seen in patients with end-stage diabetes, such as lens swelling, osmotic imbalance, and peripheral neuropathy (Srikanth & Orrick, 2023). However, our study has shed new light on its involvement in cancer, particularly in the context of hyperglycemia. In a previous investigation, it was found that the polyol pathway plays a pivotal role in the metabolic reprogramming in cancer cells, potentially leading to enhanced glycolysis and increased cell proliferation (Han et al., 2020). Another study highlights the pathway's significance as a link between glucose metabolism and cancer cell differentiation and aggressiveness (Schwab et al., 2018). This connection is mediated through the enzymes of aldose reductase and sorbitol dehydrogenase, which appear to drive the epithelial-to-mesenchymal transition (EMT) and contribute to the acquisition of a cancer stem cell (CSC) state (Schwab et al., 2018). Although no significant changes were observed in the RNA levels of these two enzymes, the increased levels of both sorbitol and fructose provide solid evidence of the activation of this pathway in cancer cells post HG treatment. Furthermore, fructose, as the end product of this pathway, has also been implicated as an increased risk of cancer, particularly pancreatic and intestinal cancers (Goncalves et al., 2019; Port et al., 2012). It has been reported that fructose exerts its indirect effect on cell proliferation through the stimulation

of protein synthesis (Port et al., 2012). Our lab has previously demonstrated that high glucose levels promote the activation of the mTOR/S6K pathway. When combined with the elevated fructose levels observed in this study, it strongly indicates that the activation of this pathway is a direct result caused by increased fructose levels, which is induced by HG in the cancer cells.

In this study, we also extend our focus on the metabolites associated with nucleotide metabolism inspired by the data derived from Chapter 2 that showed hyperglycemia-mediated increases in intracellular dNTP levels in cancer cells. However, we yielded a limited coverage of metabolites from the nontargeted metabolomic profiling. Specifically, six metabolites are involved in pyrimidine metabolism, and seven associated with purine metabolism and glutamine for both pathways. Among these identified metabolites, only three (orotic acid, xanthine and adenosine monophosphate) exhibited a slight increase in levels, while the remaining metabolites in HG-treated cells showed no discernible differences. Among the metabolites within the pyrimidine metabolism, ureidosuccinic acid, orotic acid and beta alanine are metabolic intermediates involved in early stage of pyrimidine synthesis. Conversely, thymine and uracil primarily play roles in the salvage pathway of pyrimidine synthesis. This also applies to adenine and adenosine in purine metabolism. However, it is evident that the cancer cells lean more heavily towards *de novo* nucleotide synthesis to meet the increased demands of cellular growth and proliferation (Villa et al., 2019). Additionally, certain metabolites, such as xanthine, hypoxanthine and inosine, are involved in the purine degradation

pathway, rendering them unsuitable for our objective of assessing nucleotide synthesis activity.

Last, it is important to acknowledge the limitations associated with untargeted metabolomic analysis platform utilized in our study. Firstly, our primary goal was to achieve a global and unbiased metabolomic profiling within our HG model. While we obtained a dataset containing 553 detectable metabolites, only 150 of them could ultimately and unequivocally be characterized for subsequent analysis. These 150 well-defined metabolites encompass several different categories, including amino acids metabolism, glucose metabolism and nucleotide metabolism. However, it is crucial to note that we did not obtain complete information for every metabolite within each pathway. For most of the pathways, critical metabolites were not included in our dataset, potentially interfering the fidelity of the following analysis and lowering down the confidence in the data quality. In our endeavor to assess the RRM2 function in our samples, we anticipated identifying a cluster of metabolites, including NDP, dNDP and dNTP. Unfortunately, we were unable to detect any of these crucial metabolites, and the ones we did identify did not play a central role in the dNTP synthesis pathway. These incomplete results have hindered us to form any substantive and dependable conclusions. Additionally, it is worth noting that the untargeted metabolomic analysis excels in detecting small molecules but may be less effective in identifying larger ones, such as complex oligosaccharides (Liu et al., 2021). In our study, it is highly possible that glucose molecules were converted into complex oligosaccharides. Consequently, we may have

overlooked this transformation, potentially introducing bias into our analysis data, which could lead us in a misleading direction for future research.

While the method employed in this study possesses certain limitation, the data offers valuable insights into the metabolic changes that occur in the cancer cells following HG treatment. According to the current metabolomic profiling data, glucose is predominantly transformed into fructose via the polyol pathway, ultimately influencing cell metabolism and proliferation. Future research study can prioritize investigating this pathway to elucidate its intricate mechanisms in cancer cells under hyperglycemic condition.

3.4 Materials and Methods

Cell culture, reagents, and treatments

HCT116 cells were cultured in Dulbecco's Modified Eagle Medium (DMEM) normal glucose (1g/L) supplemented with 10% FBS and 100X penicillin-streptomycin solution. For HG treatments, 25 mM glucose (#BM-675, Boston BioProducts) was added into the complete medium for HCT116 cells for 6 hrs.

Sample collection and metabolite extraction

Cell pellets were harvested and stored in -80 °C before being shipped on dry ice to West Coast Metabolomics Center at UC Davis. The extraction of metabolites was conducted following the procedures described in the previous study (Fiehn et al., 2008).

Gas chromatography time-of-flight mass spectrometry (GC-TOF-MS) (Provided by West Coast Metabolomics Center at UC Davis)

Purified metabolites were resuspended in the volume of 50 µl and 0.5 µl samples were injected into ALEX-CIS GCT-OF. Data are acquired using the following chromatographic parameters, with more details to be found in the previous paper (Fiehn et al., 2008). Column: Restek corporation Rtx-5Sil MS (30 m length x 0.25 mm internal diameter with 0.25 µm film made of 95% dimethyl/5%diphenylpolysiloxane). Mobile phase: Helium. Column temperature: 50-330°C. Flow-rate: 1 mL min^{-1}. Injection volume: 0.5 µL. Injection: 25 splitless time into a multi-baffled glass liner. Injection temperature: 50°C ramped to 250°C by 12°C s^{-1}. Oven temperature program: 50°C for 1 min, then ramped at 20°C min^{-1} to 330°C, held constant for 5 min. Mass spectrometry parameters are used as follows: a Leco Pegasus IV mass spectrometer is used with unit mass resolution at 17 spectra s^{-1} from 80-500 Da at -70 eV ionization energy and 1800 V detector voltage with a 230°C transfer line and a 250°C ion source. Untargeted analyses screen was employed in our samples.

Data processing (Provided by West Coast Metabolomics Center at UC Davis)

Raw data files are preprocessed directly after data acquisition and stored as ChromaTOF-specific *.peg files, as generic *.txt result files and additionally as generic ANDI MS *.cdf files. ChromaTOF vs. 2.32 is used for data preprocessing without smoothing, 3 s peak width, baseline subtraction just above the noise level, and automatic mass spectral deconvolution and peak detection at signal/noise levels of 5:1 throughout

the chromatogram. Apex masses are reported for use in the BinBase algorithm. Result *.txt files are exported to a data server with absolute spectra intensities and further processed by a filtering algorithm implemented in the metabolomics BinBase database.

The BinBase algorithm (rtx5) used the settings: validity of chromatogram (<10 peaks with intensity >10^7 counts s-1), unbiased retention index marker detection (MS similarity>800, validity of intensity range for high m/z marker ions), retention index calculation by 5th order polynomial regression. Spectra are cut to 5% base peak abundance and matched to database entries from most to least abundant spectra using the following matching filters: retention index window ±2,000 units (equivalent to about ±2 s retention time), validation of unique ions and apex masses (unique ion must be included in apexing masses and present at >3% of base peak abundance), mass spectrum similarity must fit criteria dependent on peak purity and signal/noise ratios and a final isomer filter. Failed spectra are automatically entered as new database entries if s/n >25, purity <1.0 and presence in the biological study design class was >80%. All thresholds reflect settings for ChromaTOF v. 2.32. Quantification is reported as peak height using the unique ion as default, unless a different quantification ion is manually set in the BinBase administration software BinView. A quantification report table is produced for all database entries that are positively detected in more than 10% of the samples of a study design class (as defined in the miniX database) for unidentified metabolites. A subsequent post-processing module is employed to automatically replace missing values from the *.cdf files. Replaced values are labeled as ‘low confidence’ by color coding, and for each metabolite, the number of high-confidence peak detections is recorded as well as the ratio

of the average height of replaced values to high-confidence peak detections. These ratios and numbers are used for manual curation of automatic report data sets to data sets released for submission. Metabolite set enrichment analysis (v5.0) was used to analyze the enrichment metabolic pathways in the metabolite set library KEGG for human metabolic pathways (Pang et al., 2021).

Statistical analysis

All the data are represented as mean ± SD. All the statistical tests were done by using Graphpad Prism 9 as recommendations based on the imported data types. P values were also generated in Graphpad Prism 9, with *P <0.05, **P <0.01, ***P <0.001, ****P <0.0001, ns represents non-significance.

3.5 References

Alfarouk, K. O., Verduzco, D., Rauch, C., Muddathir, A. K., Adil, H. H. B., Elhassan, G. O., Ibrahim, M. E., David Polo Orozco, J., Cardone, R. A., Reshkin, S. J., & Harguindey, S. (2014). Glycolysis, tumor metabolism, cancer growth and dissemination. A new pH-based etiopathogenic perspective and therapeutic approach to an old cancer question. *Oncoscience*, *1*(12), 777–802.

Allen, A. E., & Locasale, J. W. (2018). Glucose metabolism in cancer—The saga of pyruvate kinase continues. *Cancer Cell*, *33*(3), 337–339. https://doi.org/10.1016/j.ccell.2018.02.008

Böhme, I., & Bosserhoff, A. K. (2016). Acidic tumor microenvironment in human melanoma. *Pigment Cell & Melanoma Research*, *29*(5), 508–523. https://doi.org/10.1111/pcmr.12495

Ediriweera, M. K., & Jayasena, S. (2023). The Role of Reprogrammed Glucose Metabolism in Cancer. *Metabolites*, *13*(3), Article 3. https://doi.org/10.3390/metabo13030345

Fiehn, O., Wohlgemuth, G., Scholz, M., Kind, T., Lee, D. Y., Lu, Y., Moon, S., & Nikolau, B. (2008). Quality control for plant metabolomics: Reporting MSI-compliant studies. *The Plant Journal*, *53*(4), 691–704. https://doi.org/10.1111/j.1365-313X.2007.03387.x

Giovannucci, E., Harlan, D. M., Archer, M. C., Bergenstal, R. M., Gapstur, S. M., Habel, L. A., Pollak, M., Regensteiner, J. G., & Yee, D. (2010). Diabetes and Cancer. *Diabetes Care*, *33*(7), 1674–1685. https://doi.org/10.2337/dc10-0666

Goncalves, M. D., Lu, C., Tutnauer, J., Hartman, T. E., Hwang, S.-K., Murphy, C. J., Pauli, C., Morris, R., Taylor, S., Bosch, K., Yang, S., Wang, Y., Riper, J. V., Lekaye, H. C., Roper, J., Kim, Y., Chen, Q., Gross, S. S., Rhee, K. Y., … Yun, J. (2019). High-fructose corn syrup enhances intestinal tumor growth in mice. *Science*, *363*(6433), 1345–1349. https://doi.org/10.1126/science.aat8515

Han, B., Wang, L., Wei, M., Rajani, C., Yang, H., Xie, G., & Jia, W. (2020). *Fructose fuels tumor growth through the polyol pathway and GLUT 8 transporter* (p. 2020.06.04.132902). bioRxiv. https://doi.org/10.1101/2020.06.04.132902

Harding, J. L., Shaw, J. E., Peeters, A., Cartensen, B., & Magliano, D. J. (2015). Cancer risk among people with type 1 and type 2 diabetes: Disentangling true associations, detection bias, and reverse causation. *Diabetes Care*, *38*(2), 264–270. https://doi.org/10.2337/dc14-1996

Hay, N. (2016). Reprogramming glucose metabolism in cancer: Can it be exploited for cancer therapy? *Nature Reviews Cancer*, *16*(10), 635–649. https://doi.org/10.1038/nrc.2016.77

Hirata, H., Sugimachi, K., Komatsu, H., Ueda, M., Masuda, T., Uchi, R., Sakimura, S., Nambara, S., Saito, T., Shinden, Y., Iguchi, T., Eguchi, H., Ito, S., Terashima, K., Sakamoto, K., Hirakawa, M., Honda, H., & Mimori, K. (2016). Decreased Expression of Fructose-1,6-bisphosphatase Associates with Glucose Metabolism and Tumor Progression in Hepatocellular Carcinoma. *Cancer Research*, *76*(11), 3265–3276. https://doi.org/10.1158/0008-5472.CAN-15-2601

Justus, C. R., Dong, L., & Yang, L. V. (2013). Acidic tumor microenvironment and pH-sensing G protein-coupled receptors. *Frontiers in Physiology*, *4*. https://doi.org/10.3389/fphys.2013.00354

Lin, X., Xiao, Z., Chen, T., Liang, S. H., & Guo, H. (2020). Glucose Metabolism on Tumor Plasticity, Diagnosis, and Treatment. *Frontiers in Oncology*, *10*, 317. https://doi.org/10.3389/fonc.2020.00317

Liu, N., Xiao, J., Gijavanekar, C., Pappan, K. L., Glinton, K. E., Shayota, B. J., Kennedy, A. D., Sun, Q., Sutton, V. R., & Elsea, S. H. (2021). Comparison of Untargeted Metabolomic Profiling vs Traditional Metabolic Screening to Identify Inborn Errors of Metabolism. *JAMA Network Open*, *4*(7), e2114155. https://doi.org/10.1001/jamanetworkopen.2021.14155

Pang, Z., Chong, J., Zhou, G., de Lima Morais, D. A., Chang, L., Barrette, M., Gauthier, C., Jacques, P.-É., Li, S., & Xia, J. (2021). MetaboAnalyst 5.0: Narrowing the gap between raw spectra and functional insights. *Nucleic Acids Research*, *49*(W1), W388–W396. https://doi.org/10.1093/nar/gkab382

Port, A. M., Ruth, M. R., & Istfan, N. W. (2012). Fructose consumption and cancer: Is there a connection? *Current Opinion in Endocrinology, Diabetes, and Obesity*, *19*(5), 367–374. https://doi.org/10.1097/MED.0b013e328357f0cb

Schwab, A., Siddiqui, A., Vazakidou, M. E., Napoli, F., Böttcher, M., Menchicchi, B., Raza, U., Saatci, Ö., Krebs, A. M., Ferrazzi, F., Rapa, I., Dettmer-Wilde, K., Waldner, M. J., Ekici, A. B., Rasheed, S. A. K., Mougiakakos, D., Oefner, P. J., Sahin, O., Volante, M., … Ceppi, P. (2018). Polyol Pathway Links Glucose Metabolism to the Aggressiveness of Cancer Cells. *Cancer Research*, *78*(7), 1604–1618. https://doi.org/10.1158/0008-5472.CAN-17-2834

Srikanth, K. K., & Orrick, J. A. (2023). Biochemistry, Polyol Or Sorbitol Pathways. In *StatPearls*. StatPearls Publishing. http://www.ncbi.nlm.nih.gov/books/NBK576381/

Szablewski, L. (2014). Diabetes mellitus: Influences on cancer risk. *Diabetes/Metabolism Research and Reviews*, *30*(7), 543–553. https://doi.org/10.1002/dmrr.2573

Tran, K. B., Lang, J. J., Compton, K., Xu, R., Acheson, A. R., Henrikson, H. J., Kocarnik, J. M., Penberthy, L., Aali, A., Abbas, Q., Abbasi, B., Abbasi-Kangevari, M., Abbasi-Kangevari, Z., Abbastabar, H., Abdelmasseh, M., Abd-Elsalam, S., Abdelwahab, A. A., Abdoli, G., Abdulkadir, H. A., … Murray, C. J. L. (2022). The global burden of cancer attributable to risk factors, 2010–19: A systematic analysis for the Global Burden of Disease Study 2019. *The Lancet*, *400*(10352), 563–591. https://doi.org/10.1016/S0140-6736(22)01438-6

Villa, E., Ali, E. S., Sahu, U., & Ben-Sahra, I. (2019). Cancer Cells Tune the Signaling Pathways to Empower de Novo Synthesis of Nucleotides. *Cancers*, *11*(5), 688. https://doi.org/10.3390/cancers11050688

Warburg, O. (1956). On the Origin of Cancer Cells. *Science*, *123*(3191), 309–314. JSTOR.

3.6 Figures and Tables

A

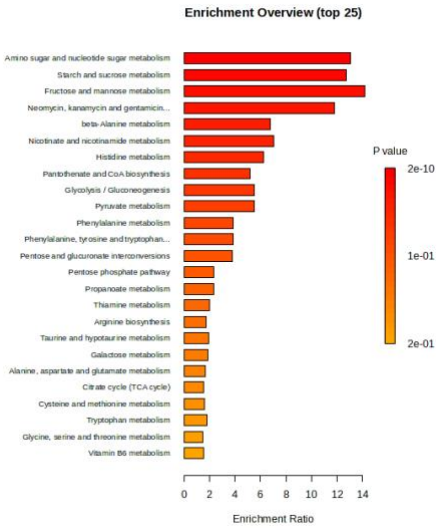

B

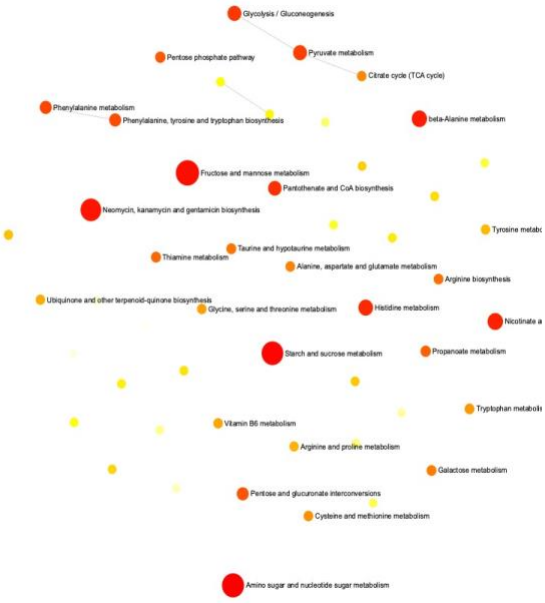

Figure 3.1 Overview of metabolite set enrichment analysis (MSEA) in HCT116 cells following HG treatment. (A) Metabolic pathway analysis using the untargeted metabolic profiling in HCT116 cells under HG condition. Bar colors indicate difference in significance and lengths indicate different fold enrichment. The top 25 perturbed pathways are shown. (B) Scatter plot of the metabolic pathway analysis. A smaller p value is encoded by the intensity of red color of circles and size of the circles represents the strength of fold enrichment. Connecting lines indicate relationships of inter-metabolic pathways.

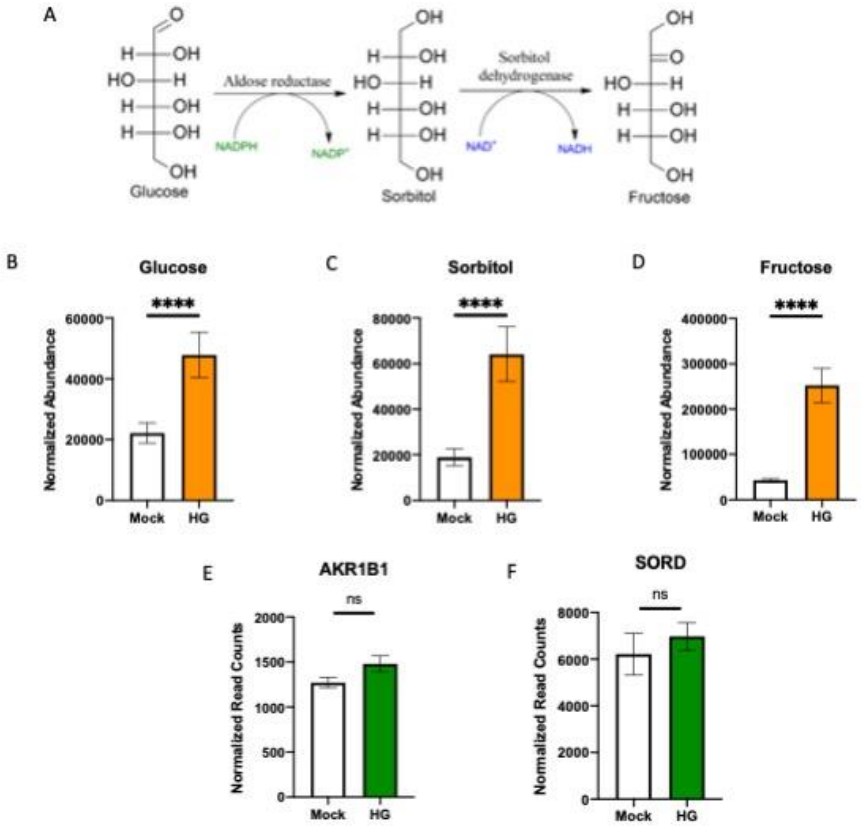

Figure 3.2 Hyperglycemia induces the activation of the polyol pathway in cancer cells. (A) The schematic of polyol pathway. (B-D) Normalized abundances of glucose (B), sorbitol (C) and fructose (D) in HCT116 cells treated with and without HG. E-F. Normalized RNA read counts of AKR1B1 (E) and SORD (F) in HCT116 cells following HG treatment. Results are displayed in mean ± SD for n=8 replicates.

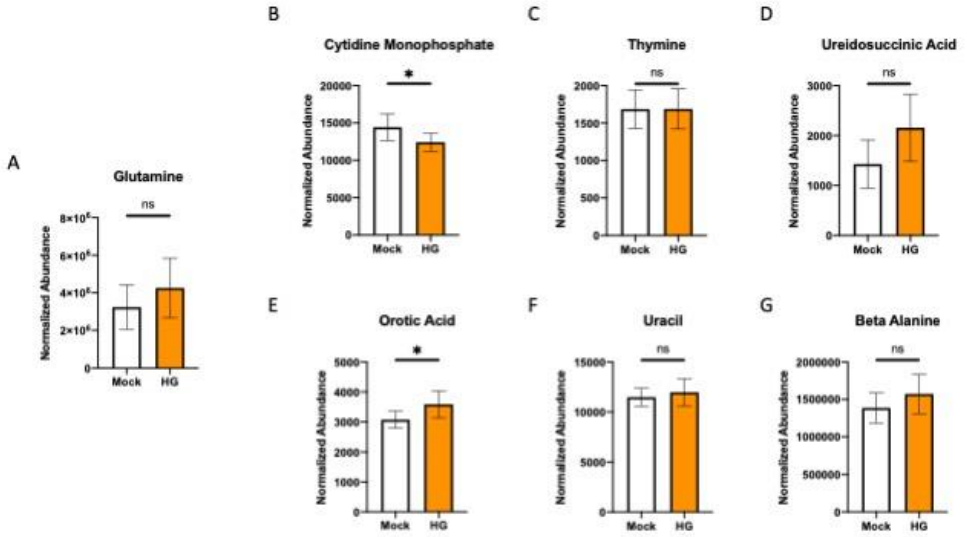

Figure 3.3 The normalized abundances of metabolic intermediates involved in pyrimidine metabolism in HCT116 cells following HG treatment. The associated metabolites determined from untargeted metabolomic profiling include glutamine (A), cytidine monophosphate (B), thymine (C), ureidosuccinic acid (D), orotic acid (E), uracil (F) and beta alanine (G). Results are displayed in mean ± SD for n=8 replicates.

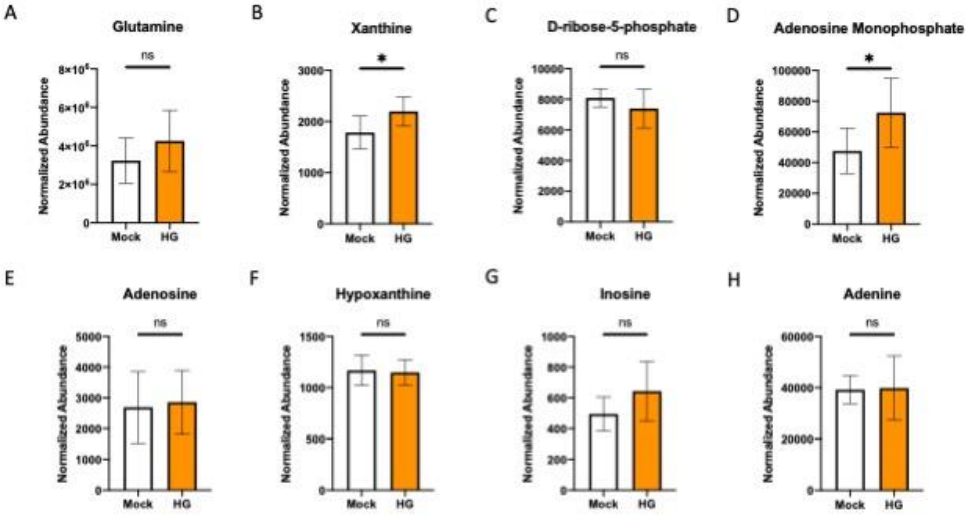

Figure 3.4 The normalized abundances of metabolic intermediates involved in purine metabolism in HCT116 cells following HG treatment. The associated metabolites determined from untargeted metabolomic profiling include glutamine (A), xanthine (B), D-ribose-5-phosphate (C), adenosine monophosphate (D), adenosine (E), hypoxanthine (F), inosine (G) and adenine (H).

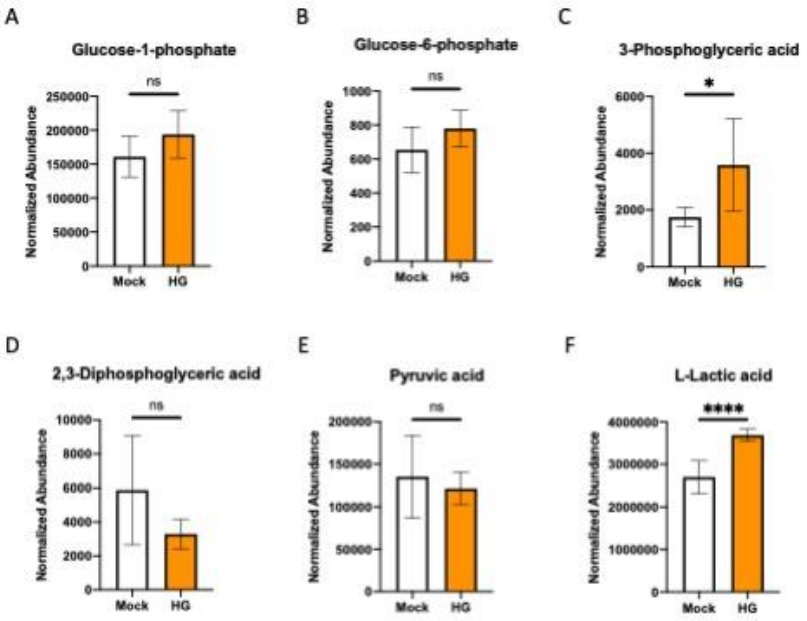

Figure 3.5 High glucose levels lead to an elevated level of lactic acid in cancer cells. Normalized abundances of glucose-1-phosphate (A), glucose-6-phosphate (B), 3-phosphoglyceric acid (C), 2,3-diphospheglyceric acid (D), pyruvic acid (E) and L-lactic acid (F) in HCT116 cells following HG treatment.

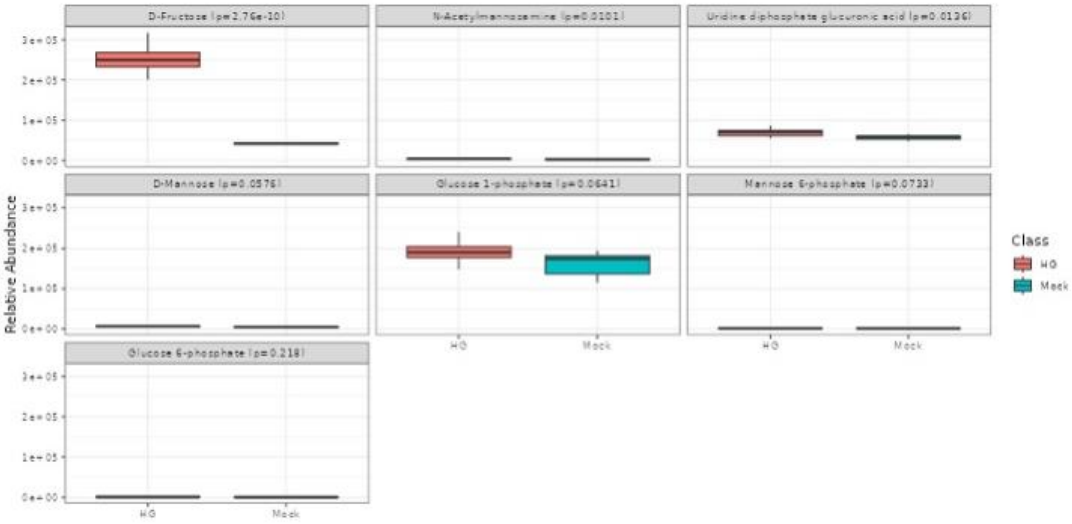

Supplementary Figure 3.1 The normalized abundances of metabolites hit within the pathway of amino sugar and nucleotide sugar metabolism in untargeted metabolomic profiling. The associated metabolites include fructose, N-acetylmannosamine, uridine diphosphate glucuronic acid, mannose, glucose-1-phoaphate, mannose 6-phosphate and glucose-6-phosphate.

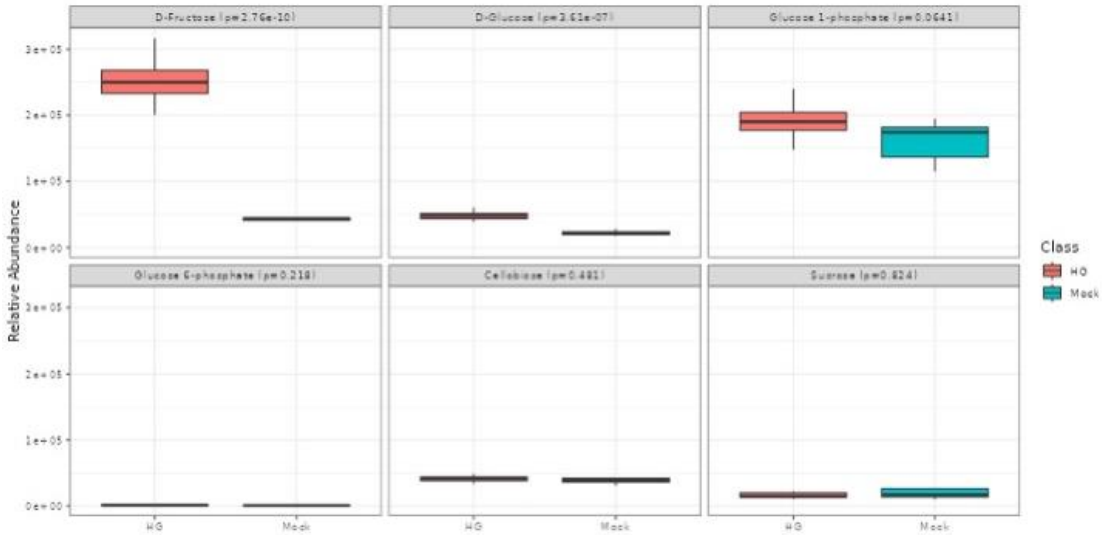

Supplementary Figure 3.2 The normalized abundances of metabolites hit within the pathway of starch and sucrose metabolism in untargeted metabolomic profiling. The associated metabolites include fructose, glucose, glucose-1-phosphate, glucose-6-phosphate, cellobiose and sucrose.

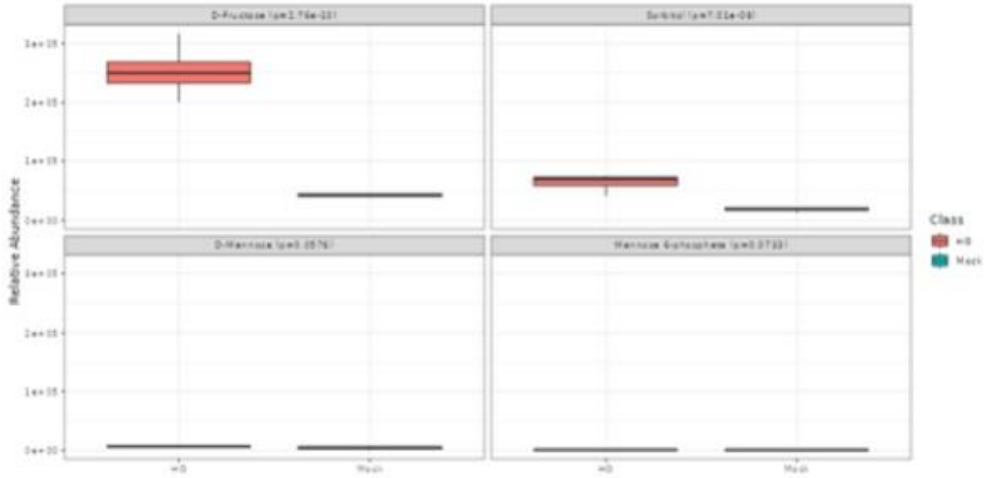

Supplementary Figure 3.3 The normalized abundances of metabolites hit within the pathway of fructose and mannose metabolism in untargeted metabolomic profiling. The associated metabolites include fructose, sorbitol, mannose and mannose-6-phosphate.

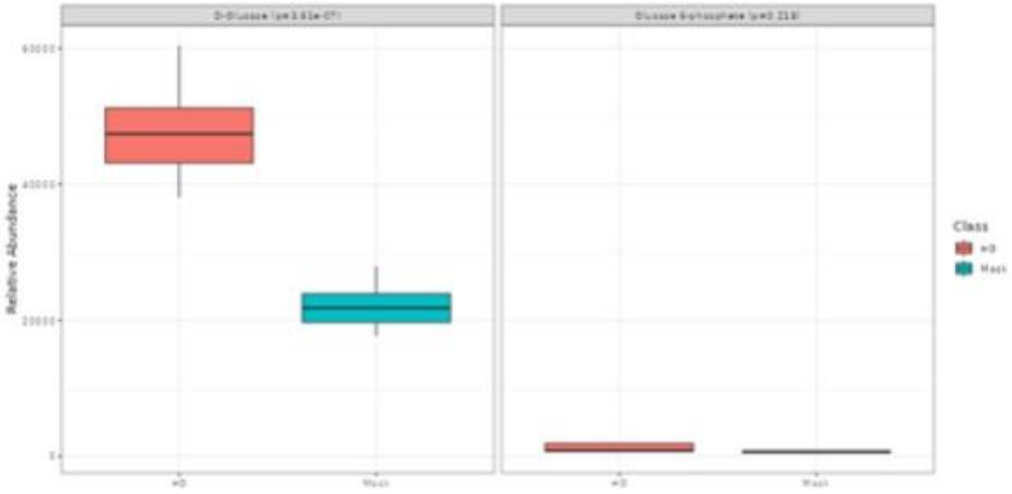

Supplementary Figure 3.4 The normalized abundances of metabolites hit within the pathway of neomycin, kanamycin and gentamicin biosynthesis in untargeted metabolomic profiling. The associated metabolites include glucose and glucose-6-phosphate.

Table 3.1 Detected metabolites in untargeted metabolomic profiling

xylitol	orotic acid	glycerol-alpha-phosphate	arabitol
xanthine	O-phosphoserine	glycerol-3-galactoside	aminomalonate
valine	oleic acid	glyceric acid	alpha-ketoglutarate
urea	octadecylglycerol	glutathione	alpha-aminoadipic acid
uracil	octadecanol	glutamine	alanine
UDP-N-acetylglucosamine	N-methylglutamic acid	glutamate	adipic acid
UDP-glucuronic acid	nicotinamide	glucuronic acid	adenosine-5-monophosphate
tyrosine	N-carbamoylaspartate	glucose-6-phosphate	adenosine
tryptophan	N-acetylputrescine	glucose-1-phosphate	adenine
trans-4-hydroxyproline	N-acetylmannosamine	glucose	aconitic acid
tocopherol alpha	N-acetylglutamate	gluconic acid	5-methoxytryptamine
thymine	N-acetylaspartic acid	glucoheptulose	5-hydroxy-3-indoleacetic acid
threose	myristic acid	galacturonic acid	5'-deoxy-5'-methylthioadenosine
threonine	myo-inositol	galactose-6-phosphate	5-aminovaleric acid
threonic acid	methionine sulfoxide	galactitol	3-phosphoglycerate
threitol	methionine	fumaric acid	3-hydroxy-3-methylglutaric acid
taurine	methanolphosphate	fructose	2-picolinic acid
sucrose	mannose-6-phosphate	ethanolamine	2-monoolein
succinic acid	mannose	erythrose	2-ketoisocaproic acid
sorbitol	maltose	erythritol	2-ketobutyric acid
sophorose	malic acid	docosahexaenoic acid	2-hydroxyvaleric acid
serotonin	maleic acid	dihydroxyacetone	2-hydroxyglutaric acid
serine	lyxitol	D-erythro-sphingosine	2-aminobutyric acid
saccharic acid	lysine	cytidine-5-monophosphate	2,5-dihydroxypyrazine
ribose-5-phosphate	levoinositol	cysteine-glycine	2,3-bisphosphoglyceric acid
ribitol	levoglucosan	cysteine	1-monostearin
pyruvic acid	leucine	cyanoalanine	1-monopalmitin
pyrophosphate	lactic acid	creatinine	1-methylgalactose
pyridoxine	isothreonic acid	citric acid	1,3-dihydroxypyridine
putrescine	isoleucine	cis-gondoic acid	1,2-anhydro-myo-inositol
pseudo uridine	isocitric acid	cholesterone	
proline	inositol-4-monophosphate	cholesterol	
pipecolinic acid	inosine	cellobiose	
phosphoethanolamine	hypoxanthine	capric acid	
phosphate	hydroquinone	butyrolactam	
phenylalanine	homoserine	beta-alanine	
pelargonic acid	histidine	beta sitosterol	
pantothenic acid	hexadecylglycerol	azelaic acid	
palmitoleic acid	guanidinosuccinate	aspartic acid	
oxoproline	glycine	asparagine	

Table 3.2 Four significantly enriched metabolic pathways in HG-treated HCT116 cells

	Total Cmpd	Hits	Statistic Q	Expected Q	Raw p	Holm p	FDR
Amino sugar and nucleotide sugar metabolism	37	7	87.16	6.6667	1.83E-10	9.87E-09	5.27E-09
Starch and sucrose metabolism	18	6	84.754	6.6667	2.21E-10	1.17E-08	5.27E-09
Fructose and mannose metabolism	20	4	94.293	6.6667	2.93E-10	1.52E-08	5.27E-09
Neomycin, kanamycin and gentamicin biosynthesis	2	2	78.71	6.6667	7.80E-07	3.98E-05	1.05E-05

Chapter 4

Conclusion

4.1 Summary

Epidemiological studies have unveiled a heightened occurrence of cancer and diabetes mellitus diagnosis within the same individual (Giovannucci et al., 2010). Initially identified in population-based studies during the 1960s, the association between these two conditions has gained substantial attention. Recent accumulating evidence has underscored this significant correlation, particularly within specific cancer type such as breast, liver, pancreas, colon, kidney and bladder (Giovannucci et al., 2010; Simon et al., 2018; Yuan et al., 2020). The exploration of the intricate interplay between cancer and diabetes mellitus has been a focal point in scientific research for numerous years. While the association is complicated and multifactorial, our study focuses on the hyperglycemia, a hallmark of diabetes for both type 1 and type 2 that transcends gender and body mass. Noteworthy previous research has shown that a high-glucose diet can induce tumorigenesis and significantly expedite tumor growth in mouse models (Goncalves et al., 2019; Su et al., 2023). Nonetheless, the precise mechanism linking the hyperglycemia and cancer remains largely unexplored in these studies. Given the tumor-promoting role of hyperglycemia evident in animal models and epidemiological data, coupled with the inconclusive insights into the underlying molecular mechanism, we carried out this project to comprehensively investigate how hyperglycemia exerts its influence in promoting cancer cell growth.

In Chapter 2, our genome-wide RNA sequencing data unequivocally demonstrates that HG condition robustly promotes DNA synthesis, subsequently facilitating cell cycle progression and ultimately conferring a distinct growth advantage to cells. Notably, all

the genes that experience up-regulation in cells treated with HG exhibit a pronounced enrichment in DNA synthesis and cell cycle activities. Meanwhile, E2F transcription factor family is identified as the pivotal orchestrator governing this HG-mediated promotion of cell growth. Remarkably, E2F1, a well-studied E2F family member, emerges as the upstream regulator responsible for enhancing mRNA expression levels of the DNA replication genes following exposure to HG. While prior research has indicated this shifts in DNA replication and DNA metabolism gene expression levels in diabetic animal tissues (Leontovich et al., 2016), our study further elucidates the exclusive contribution of E2F1 in propelling the growth of HG-responsive cancer cells. This is achieved through the transcriptional activation of genes related to DNA replication.

We further expanded our research on exploring the functional implications of oncogenic CDKs-Rb1-E2F pathway in the HG-treated cancer cells. In investigating the phosphorylation status of Rb1 across different cell lines, an unexpected finding emerged: instead of a uniform response, cells exhibited different reactions to HG treatment based on the baseline Rb1 phosphorylation levels. Specifically, in the case of HCT116, characterized by relatively lower Rb1 phosphorylation, HG treatment led to Rb1 deactivation through phosphorylation, subsequently triggering a substantial activation of DNA replication and cellular growth. Conversely, the U2OS cell line, which possessed a higher basal level of Rb1 phosphorylation, demonstrated insensitivity to HG stimuli, failing to confer a direct growth advantage comparable to the HCT116 cell line. While earlier studies have noted variable accumulation of underphosphorylated Rb1 levels in

cancer cells (Broceño et al., 2002), our research uniquely underscores that this variability can culminate in distinct cell growth phenotypes following HG treatment.

Our study also illuminates the functional role of RRM2 in the metabolic alteration in a hyperglycemic environment. RRM2 assumes an essential role in nucleotide metabolism by catalyzing the conversion of NDP into dNDP. Emerging studies have positioned RRM2 as a proto-oncogene in cancer, with implications as a negative predictor for chemotherapeutic response (Aye et al., 2015; Ferrandina et al., 2010; Zhan et al., 2021). Our findings reveal elevated RRM2 levels result in increased intracellular dNTP concentrations and enhanced DNA synthesis activity. Significantly, this metabolic alteration in response to hyperglycemia can be efficiently counteracted by Triapine, an RNR inhibitor currently undergoing clinical trials and showing promise as a small molecule compound. Collectively, this segment of our research unveils a metabolic alteration within cancer cells upon exposure to hyperglycemia.

In Chapter 3, we conducted untargeted metabolomic profiling analysis to gain a comprehensive understanding of the metabolic alterations induced by hyperglycemia. It is widely recognized that cancer cells have a preference on the glycolysis, known as Warburg effect. Our data demonstrated that hyperglycemia could intensify the glycolytic activity, as revealed by elevated levels of lactic acid in HG-treated cells. Furthermore, our findings provided a novel perspective: under the influence of hyperglycemia, cancer cells are more motivated to shift the glucose metabolism towards the polyol pathway, resulting in an elevated production of fructose. Considering the established role of hyperglycemia in promoting cell proliferation and the previously reported contributions of fructose to

cancer progression and development (Han et al., 2020; Port et al., 2012), we speculate that the fructose serves as a more pivotal role in influencing cellular growth and proliferation at the metabolic level. In a hyperglycemic environment, cancer cells may experience a dual stimulus from both glucose and fructose, further enhancing their capacity for cellular proliferation.

4.2 Potential Limitations of the Study

It is essential to highlight that the three chemical compounds (CDK2/4/6i PF-3600, E2F inhibitor HLM006474 and RRM2 inhibitor Triapine) employed in Chapter 2 effectively inhibit the DNA synthesis and impede cell cycle progression in both Mock and HG conditions. While Rb1/E2F signaling is pivotal in regulating these processes, it is crucial to acknowledge that these compounds may exert non-specific effects on the rapidly dividing cells, including hair cells, cells lining the digestive system and bone marrow cells. Moreover, delayed wound healing is a prevalent complication in diabetic patients (Dasari et al., 2021). E2F1 is essential for skin wound healing and the lack of E2F1 in keratinocytes impairs the wound repair (D'Souza et al., 2002; Li et al., 2019). Given the skin cells exposed to wounds undergo accelerated cell division, it raised up a concern that the use of these three compounds could interfere with the wound healing process in tumor-bearing diabetic patients. This limitation potentially restricts the application of them in patients undergoing the complication of slower wound healing.

The untargeted metabolomic profiling, due to its limited detection capacity, provides a constrained scope of metabolites for our study. While it has yielded a

noteworthy and novel finding that glucose is primarily converted into fructose via the polyol pathway, the confidence of this finding remains somewhat limited. Given that this approach does not comprehensively analyze all cellular metabolites, it is plausible that metabolites with significant roles may remain undetected, potentially masking their importance. Consequently, there is a possibility that the current available data may overemphasize the significance of the polyol pathway in our study. Future investigations should focus on confirming and validating the role of polyol pathway in the HG-treated cells.

The primary objective of conducting both RNA-seq and untargeted metabolomic profiling was to cross-validate the data in each dataset. However, we encountered challenges in corroborating the results obtained from RNA-seq with those from metabolomic profiling and vice versa. For example, we aimed to examine NDP, dNDP and dNTP levels in the metabolomic profiling data to confirm the function of RRM2 as indicated from the RNA-seq data. Unfortunately, due to the limited coverage of detected metabolites, none of them were identified. Moreover, we had anticipated that the enzymes aldose reductase and sorbitol dehydrogenase would show increase based on elevated levels of sorbitol and fructose observed in metabolomic profiling. However, the RNA-seq data did not reveal any changes in RNA levels of these two genes. As a result, we are limited to drawing conclusions separately from each dataset, and unable to integrate them to form a definitive conclusion.

4.3 Future studies

DNA replication in eukaryotic cells unfolds within a careful orchestrated temporal program during the S phase, recognized as the replication timing (RT) program (Dileep et al., 2015). Given our revelation concerning HG-mediated alteration of DNA replication and cell cycle, the significance of further exploring the RT profiles in both HG-treated and untreated cells become even more pronounced. Employing the Next-Generation Sequencing (NGS) technique of Repli-Seq emerges as an instrumental approach to elucidate the temporal choreography of RT, particularly within mammalian cells (Marchal et al., 2018; Zhao et al., 2020). The high-throughput methodology not only furnishes insights into individual replication unit but also unveils the intricate 3D landscape of spatiotemporally segregated subnuclear compartments. It strengthens our insight into the chromosome architecture and functional dynamics of cancer cells in hyperglycemic milieu.

Our result reveals distinct and significant patterns of hyperglycemic response in the HCT116 and U2OS cell lines. Notably, hyperglycemia fails to further activate Rb1/E2F oncogenic signaling in U2OS cells, which inherently exhibit a higher level of Rb1 phosphorylation. Interestingly, a previous study reported the absence of underphosphorylated Rb1 production upon G1 entry in U2OS cells, though the precise mechanism remains inconclusive (Broceño et al., 2002). Further investigation is warranted to comprehensively address the molecular basis underlying the divergence in HG-induced effects between these two cell lines. Such studies will undoubtedly gain deeper insights into the impact of hyperglycemia on cancer cells.

To mimic an *in vivo* environment, we conducted a spheroid formation assay in a 3D cell culture medium, yielding the anticipated results. This data holds greater significance in the pursuit of establishing a feasible diabetic animal model to further in-depth examination of the role of Rb1/E2F signaling *in vivo*. While researchers have extensively explored tumor growth within diabetic mouse models, the published outcomes exhibit notable variability (Goncalves et al., 2019; K et al., 2019; Su et al., 2023; Wu et al., 2018). The variation is likely attributed to differences in the injected tumor cell types and mouse strains employed for the studies. To faithfully mirror human tumor development, the utilization of genetically engineered mouse models is advocated in our future study. Specifically, adenomatous polyposis coli (APC) mutant mice can be considered, given that a substantial portion of our *in vitro* data originated from the colon cancer cell line HCT116. Furthermore, in establishing diabetic models, researchers often adopt two main approaches: drug-induced disruption of pancreatic β cells and dietary-based oral glucose intake. Both methods ultimately elevate blood glucose levels. The drug-based approach directly causes the insulin deprivation *in vivo*, mirroring the T1DM. However, our future study should predominantly consider the oral glucose intake route. This aligns with the fact that many cancer cells heavily rely on the insulin/insulin-like growth factor (IGF) axis. In summary, our ongoing research is poised to explore these avenues with an aim to enhance our understanding of the intricate relationship between hyperglycemia and cancer progression *in vivo*.

Future studies can encompass an exploration of additional pivotal HG-responsive transcription factors and potential crosstalk between these factors and Rb1/E2F signaling

pathway. Interestingly, recent findings highlight p53 as a glucose-responsive transcription regulator in cancer cells (Su et al., 2023). Our lab has previously showed that hyperglycemia promotes cancer progression via p53-Thr55 phosphorylation-mediated degradation of the p53 protein. In this context, p21 represents a transcriptional activity of p53 and is primarily associated with CDK2 kinase inhibition. It is reasonable to suspect that the function of p21 becomes impeded due to HG-induced p53 protein degradation. Consequently, the release of p21's inhibition on CDK2 kinase activity may further stimulate the Rb1/E2F signaling pathway in cancer cells. These insights underline the potential complexity of interactions that require exploration for a comprehensive understanding of hyperglycemia-driven oncogenic mechanisms.

It has been reported that the chromatin accessibility of E2F1 is associated with the histone demethylase KDM4A and KDM6B in different contexts (D'Oto et al., 2021; Wang et al., 2016; Zhang et al., 2021). This prompts us to consider, beyond the scope of transcription, exploring alterations occurred at the epigenetic level in HG-treated cells. By employing NGS-based epigenetic sequencing methods, such as ATAC-seq, CUT&Tag etc., we can gain a comprehensive understanding of the chromatin accessibility and the interactions between E2F1 and DNA in cancer cells under hyperglycemic condition. Furthermore, these approaches can help us to identify coactivators and enhancers that associate with E2F1's transcriptional activity, as defined in Chapter 2. Moreover, investigating how long the HG-induced epigenetic changes persist when cells are returned to normal glucose levels could provide valuable insights into the plasticity of cancer cells in different glucose environment. This exploration of the duration of

epigenetic memory gained from HG treatment holds significant promise for understanding cancer cell behavior.

4.4 Conclusion and Implication

Collectively, our study validates the role of hyperglycemia in fueling cancer cell proliferation and provides detailed insights into its mechanisms from both molecular and metabolic aspects. Leveraging our genome-wide RNA-seq data, we pinpoint E2F as the primary player among HG-responsive transcriptional factors. E2F1 orchestrates the transcriptional activation of a cluster of DNA replication genes. Furthermore, we delineate the function significance of Rb1/E2F oncogenic signaling pathway in mediating cell growth under HG conditions. Additionally, our study uncovers a metabolic shift in nucleotide metabolism in HG-treated cells. This alteration arises from the transcriptional activation of RRM2, a key player in *de novo* nucleotide synthesis and a direct transcriptional target of E2F1. From another perspective, our untargeted metabolomic profiling data demonstrates the activations of glycolysis and polyol pathway, offering an alternative viewpoint on HG-mediated cell growth and proliferation. In the polyol pathway, the elevated levels of fructose, mainly derived from glucose, may exert a more substantial influence on cell proliferation under hyperglycemic condition, challenging the conventional view that glucose plays the pivotal role. In conclusion, although our study may appear straightforward, it deciphers significant biological and metabolic alterations in cancer cells, conferring them with heightened self-proliferative capacity under hyperglycemic conditions. Our findings contribute to a broader understanding of cancer

biology and offer more insights for oncologist when treating tumor-bearing diabetic patients.

4.5 References

Aye, Y., Li, M., Long, M. J. C., & Weiss, R. S. (2015). Ribonucleotide reductase and cancer: Biological mechanisms and targeted therapies. *Oncogene*, *34*(16), 2011–2021. https://doi.org/10.1038/onc.2014.155

Broceño, C., Wilkie, S., & Mittnacht, S. (2002). RB activation defect in tumor cell lines. *Proceedings of the National Academy of Sciences of the United States of America*, *99*(22), 14200–14205. https://doi.org/10.1073/pnas.212519499

Dasari, N., Jiang, A., Skochdopole, A., Chung, J., Reece, E. M., Vorstenbosch, J., & Winocour, S. (2021). Updates in Diabetic Wound Healing, Inflammation, and Scarring. *Seminars in Plastic Surgery*, *35*(3), 153–158. https://doi.org/10.1055/s-0041-1731460

Dileep, V., Rivera-Mulia, J. C., Sima, J., & Gilbert, D. M. (2015). Large-Scale Chromatin Structure–Function Relationships during the Cell Cycle and Development: Insights from Replication Timing. *Cold Spring Harbor Symposia on Quantitative Biology*, *80*, 53–63. https://doi.org/10.1101/sqb.2015.80.027284

D'Oto, A., Fang, J., Jin, H., Xu, B., Singh, S., Mullasseril, A., Jones, V., Abu-Zaid, A., von Buttlar, X., Cooke, B., Hu, D., Shohet, J., Murphy, A. J., Davidoff, A. M., & Yang, J. (2021). KDM6B promotes activation of the oncogenic CDK4/6-pRB-E2F pathway by maintaining enhancer activity in MYCN-amplified neuroblastoma. *Nature Communications*, *12*(1), 7204. https://doi.org/10.1038/s41467-021-27502-2

D'Souza, S. J. A., Vespa, A., Murkherjee, S., Maher, A., Pajak, A., & Dagnino, L. (2002). E2F-1 is essential for normal epidermal wound repair. *The Journal of Biological Chemistry*, *277*(12), 10626–10632. https://doi.org/10.1074/jbc.M111956200

Ferrandina, G., Mey, V., Nannizzi, S., Ricciardi, S., Petrillo, M., Ferlini, C., Danesi, R., Scambia, G., & Del Tacca, M. (2010). Expression of nucleoside transporters, deoxycitidine kinase, ribonucleotide reductase regulatory subunits, and gemcitabine catabolic enzymes in primary ovarian cancer. *Cancer Chemotherapy and Pharmacology*, *65*(4), 679–686. https://doi.org/10.1007/s00280-009-1073-y

Giovannucci, E., Harlan, D. M., Archer, M. C., Bergenstal, R. M., Gapstur, S. M., Habel, L. A., Pollak, M., Regensteiner, J. G., & Yee, D. (2010). Diabetes and Cancer. *Diabetes Care*, *33*(7), 1674–1685. https://doi.org/10.2337/dc10-0666

Goncalves, M. D., Lu, C., Tutnauer, J., Hartman, T. E., Hwang, S.-K., Murphy, C. J., Pauli, C., Morris, R., Taylor, S., Bosch, K., Yang, S., Wang, Y., Riper, J. V., Lekaye, H. C., Roper, J., Kim, Y., Chen, Q., Gross, S. S., Rhee, K. Y., … Yun, J. (2019). High-fructose corn syrup enhances intestinal tumor growth in mice. *Science*, *363*(6433), 1345–1349. https://doi.org/10.1126/science.aat8515

Han, B., Wang, L., Wei, M., Rajani, C., Yang, H., Xie, G., & Jia, W. (2020). *Fructose fuels tumor growth through the polyol pathway and GLUT 8 transporter* (p. 2020.06.04.132902). bioRxiv. https://doi.org/10.1101/2020.06.04.132902

K, W., X, Y., Z, H., D, Z., X, Y., Yl, W., Q, H., Kt, K., Y, E., R, I., Kt, N., S, Z., G, C., Qh, C., G, W., Jv, V., & Y, W. (2019). Targeting of PP2Cδ By a Small Molecule C23 Inhibits High Glucose-Induced Breast Cancer Progression In Vivo. *Antioxidants & Redox Signaling*, *30*(17). https://doi.org/10.1089/ars.2017.7486

Leontovich, A. A., Intine, R. V., & Sarras, M. P. (2016). Epigenetic Studies Point to DNA Replication/Repair Genes as a Basis for the Heritable Nature of Long Term Complications in Diabetes. *Journal of Diabetes Research*, *2016*, e2860780. https://doi.org/10.1155/2016/2860780

Li, D., Kular, L., Vij, M., Herter, E. K., Li, X., Wang, A., Chu, T., Toma, M.-A., Zhang, L., Liapi, E., Mota, A., Blomqvist, L., Sérézal, I. G., Rollman, O., Wikstrom, J. D., Bienko, M., Berglund, D., Ståhle, M., Sommar, P., … Landén, N. X. (2019). Human skin long noncoding RNA WAKMAR1 regulates wound healing by enhancing keratinocyte migration. *Proceedings of the National Academy of Sciences*, *116*(19), 9443–9452. https://doi.org/10.1073/pnas.1814097116

Marchal, C., Sasaki, T., Vera, D., Wilson, K., Sima, J., Rivera-Mulia, J. C., Trevilla-García, C., Nogues, C., Nafie, E., & Gilbert, D. M. (2018). Genome-wide analysis of replication timing by next-generation sequencing with E/L Repli-seq. *Nature Protocols*, *13*(5), 819–839. https://doi.org/10.1038/nprot.2017.148

Port, A. M., Ruth, M. R., & Istfan, N. W. (2012). Fructose consumption and cancer: Is there a connection? *Current Opinion in Endocrinology, Diabetes, and Obesity*, *19*(5), 367–374. https://doi.org/10.1097/MED.0b013e328357f0cb

Simon, T. G., King, L. Y., Chong, D. Q., Nguyen, L. H., Ma, Y., VoPham, T., Giovannucci, E. L., Fuchs, C. S., Meyerhardt, J. A., Corey, K. E., Khalili, H., Chung, R. T., Zhang, X., & Chan, A. T. (2018). Diabetes, metabolic comorbidities, and risk of hepatocellular carcinoma: Results from two prospective cohort studies. *Hepatology*, *67*(5), 1797–1806. https://doi.org/10.1002/hep.29660

Su, Y., Luo, Y., Zhang, P., Lin, H., Pu, W., Zhang, H., Wang, H., Hao, Y., Xiao, Y., Zhang, X., Wei, X., Nie, S., Zhang, K., Fu, Q., Chen, H., Huang, N., Ren, Y., Wu, M., Chow, B. K. C., … Rao, F. (2023). Glucose-induced CRL4COP1-p53 axis amplifies glycometabolism to drive tumorigenesis. *Molecular Cell*, *83*(13), 2316-2331.e7. https://doi.org/10.1016/j.molcel.2023.06.010

Wang, L.-Y., Hung, C.-L., Chen, Y.-R., Yang, J. C., Wang, J., Campbell, M., Izumiya, Y., Chen, H.-W., Wang, W.-C., Ann, D. K., & Kung, H.-J. (2016). KDM4A Coactivates E2F1 to Regulate the PDK-Dependent Metabolic Switch between Mitochondrial Oxidation and Glycolysis. *Cell Reports*, *16*(11), 3016–3027. https://doi.org/10.1016/j.celrep.2016.08.018

Wu, D., Hu, D., Chen, H., Shi, G., Fetahu, I. S., Wu, F., Rabidou, K., Fang, R., Tan, L., Xu, S., Liu, H., Argueta, C., Zhang, L., Mao, F., Yan, G., Chen, J., Dong, Z., Lv, R., Xu, Y., … Shi, Y. G. (2018). Glucose-regulated phosphorylation of TET2 by AMPK reveals a pathway linking diabetes to cancer. *Nature*, *559*(7715), 637–641. https://doi.org/10.1038/s41586-018-0350-5

Yuan, C., Babic, A., Khalaf, N., Nowak, J. A., Brais, L. K., Rubinson, D. A., Ng, K., Aguirre, A. J., Pandharipande, P. V., Fuchs, C. S., Giovannucci, E. L., Stampfer, M. J., Rosenthal, M. H., Sander, C., Kraft, P., & Wolpin, B. M. (2020). Diabetes, Weight Change, and Pancreatic Cancer Risk. *JAMA Oncology*, *6*(10), e202948. https://doi.org/10.1001/jamaoncol.2020.2948

Zhan, Y., Jiang, L., Jin, X., Ying, S., Wu, Z., Wang, L., Yu, W., Tong, J., Zhang, L., Lou, Y., & Qiu, Y. (2021). Inhibiting RRM2 to enhance the anticancer activity of chemotherapy. *Biomedicine & Pharmacotherapy*, *133*, 110996. https://doi.org/10.1016/j.biopha.2020.110996

Zhang, W., Liu, W., Jia, L., Chen, D., Chang, I., Lake, M., Bentolila, L. A., & Wang, C.-Y. (2021). Targeting KDM4A epigenetically activates tumor-cell-intrinsic immunity by inducing DNA replication stress. *Molecular Cell*, *81*(10), 2148-2165.e9. https://doi.org/10.1016/j.molcel.2021.02.038

Zhao, P. A., Sasaki, T., & Gilbert, D. M. (2020). High-resolution Repli-Seq defines the temporal choreography of initiation, elongation and termination of replication in mammalian cells. *Genome Biology*, *21*(1), 76. https://doi.org/10.1186/s13059-020-01983-8